ETHYLATION OF BENZENE OVER DIFFERENT ZEOLITE CATALYSTS

BY

TAIWO AYODEJI ODEDAIRO

A Thesis Presented to the
DEANSHIP OF GRADUATE STUDIES

KING FAHD UNIVERSITY OF PETROLEUM & MINERALS
DHAHRAN, SAUDI ARABIA

In Partial Fulfillment of the
Requirements for the Degree of

MASTER OF SCIENCE
In
CHEMICAL ENGINEERING

APRIL 2010

KING FAHD UNIVERSITY OR PETROLEUM & MINERALS
DHAHRAN 31261, SAUDI ARABIA
DEANSHIP OF GRADUATE STUDIES

This thesis, written by Taiwo Ayodeji Odedairo under the direction of his thesis advisor and approved by his thesis committee, has been presented to the Dean of Graduate Studies, in partial fulfillment of the requirement for the degree of **MASTER OF CHEMICAL ENGINEERING.**

Thesis Committee

Dr Sulaiman Al-Khattaf
(Thesis Advisor)

Dr. Mohammed Al-Daous
(Member)

Dr. Mohammed Ba-Shammakh
(Member)

A. Al Amer
Dr. Adnan Al- Amer
(Department Chairman)

Dr. Salam A. Zummo
(Dean of Graduate Studies)

21/6/10
Date

DEDICATION

This work is dedicated to my father, Abiodun Odedairo and to my mother; Funmilola Odedairo for their immeasurable love, affection, moral and financial support.

ACKNOWLEDGEMENT

All praise is to Allah (SWT) the lord of the worlds. And may the peace and blessings of Allah be upon the Holy Prophet Muhammed, the leader of mankind (SAW).

First, I thank Allah (SWT) for sparing my life and guiding me to this point in my career. I thank him for His divine guidance and His uncountable favors which He has bestowed on me. To Him belongs all praise in the Heavens and on Earth.

I would also like to express my profound appreciation to my thesis advisor, Dr Sulaiman Al-Khattaf who in spite of his very tight schedule has found ample time to follow every step of this work making useful suggestions, corrections and directing the whole course of the work. It was really a great pleasure working under him and I remain highly indebted to him. My appreciation also goes to my other thesis committee members; Dr. Mohammed Al-Daous and Dr. Mohammed Ba-Shammakh for their immense assistance throughout this work. Never would I forget also the contributions of Dr. Saudi Waziri particularly in the area of modeling and Mr. Mariano Gica for always and patiently been around to assist in the experimental part of this work.

To my parents, brothers (Seun and Tunde), sister (Kehinde) and friends (Tajudeen, Lateef and Moshood), I say words alone cannot express my deep appreciation to you for all that you have done for me. I only pray Allah (SWT) reward you abundantly. To all my brothers in the Nigerian Community here in KFUPM, I say a very big thank you brotherly assistance and prayers. Finally, I would like to thank the chairman, all the faculty members, and the staff and graduate students of the department. It's been really great having you around.

TABLE OF CONTENT

LIST OF TABLES

LIST OF FIGURES

THESIS ABSTRACT

Name: **TAIWO AYODEJI ODEDAIRO**

Title of Study: **ETHYLATION OF BENZENE OVER DIFFERENT ZEOLITE CATALYSTS**

Degree: **MASTER OF SCIENCE**

Major Field: **CHEMICAL ENGINEERING**

Date of Degree: **April, 2010**

A novel fluidized bed process for the production of ethylbenzene from benzene ethylation over zeolite based catalysts was studied. Experimental runs were carried out in a riser simulator at 250, 275, 300, 325, 350 and 400^0C for reaction times of 3, 5, 7, 10, 13, 15 and 20 sec. Five different catalysts based on ZSM-5, Y, SSZ-33, TNU-9 and mordenite zeolites were used. Over all the catalysts, benzene conversion was found to increase with reaction time and temperature. Partial deactivation of the external acid sites of ZSM-5 based catalyst with coke deposit from 1,3,5-triisopropylbenzene was found to have a significant positive effect on the P/O ratio. The conversion of benzene in the ethylation reaction of benzene with ethanol over the different zeolite catalysts follows the order: SSZ-33 > TNU-9 > ZSM-5 > mordenite. TNU-9 catalyst behaves like the 10-ring ZSM-5 with respect to ethylbenzene selectivity, while the behavior of SSZ-33 is close to that of a large pore zeolite with potential cage effects. EB selectivity follows the order: ZSM-5 > TNU-9 > SSZ-33 > mordenite, which implies that this order is not directly related to the benzene conversion. The experimental results were also modeled based on both time-on-stream (TOS) and reactant conversion model (RC).

تجريد

الاسم : تايو ابو ديجي أوديدايرو

عنوان الرسالة : أثيلة البنزين بواسطة حفازات الزيولايت المختلفة .

الدرجة العلمة : ماجستير .

التخصص : الهندسة الكيميائية .

التاريخ : ابرايل 2010

تمت دراسة عملية الطبقة المتميعة لانتاج إيثيل البنزين من البنزين بواسطة حفازات الزيولايت . ثم إجراء التجارب علي مفاعل المحاكاة الرافع عند درجات حرارة 250 , 275, 300,350 و 400 درجة مئوية لمدة 3, 5 , 7 ,10 , 13, 15 و 20 ثانية .ثم استخدام خمسة انواع مختلفة من حفازات الزيولايت وهي : ZSM-5, Y , SSZ-33 ,TNU-9 و الموردنايت . من خلال كل الحفازات تبين ان تحويل البنزين يزيد بزيادة زمن التفاعل ودرجة الحرارة , ووجد ان التثبيط الجزئي للمواقع الحمضية الخارجية ل ZSM-5 بواسطة الكربون المتراكم من 1, 2, 3- بنزين ثلاثي الايزوبروبين له ثاثير ايجابي علي نسبة P/O. ترتيب تحويل البنزين من تفاعل الاثيلية يتبع للترتيب موردنايت <SSZ-33>TNU-9>ZSM-5> . ال TUN-9 يتشابة مع ال ZSM-5 ذو العشر حلقات بينما سلوك ال SSZ-33 يشبه سلوك الزيولايت كبير الثقوب ذو تاثير التكهف الموضعي . إنتقائية إثيل البنزين تتبع تتبع الترتيب موردنايت <ZSM-5>TNU-9>SSZ-33> مما يدل علي ان هذا الترتيب ليس ذو علاقة كبيرة بتحويل البنزين , تمت نمذجة نتائج التجارب علي اساس نموذج الزمن المساري ونموذج تحول المفاعل .

CHAPTER 1

INTRODUCTION

1.1 Background

Ethylbenzene (EB) is an important raw material in the petrochemical industry for the manufacture of styrene, which is a widely used industrial monomer. Styrene is an important monomer in the production of synthetic rubber, synthetic plastics and resins. Ethylbenzene has a limited use also as a solvent and for the production of dyes [1]. The ethylbenzene production in 2010 is estimated to be about 34 million metric tons [2]. Conventionally, ethylbenzene is produced by benzene alkylation with ethylene using homogeneous mineral acids such as aluminium chloride or phosphoric acid as catalysts that cause a number of problems concerning handling, safety, corrosion and waste disposal [3,4]. Benzene ethylation over zeolite based catalyst to produce ethylbenzene amongst other product is gaining remarkable attention and has been replacing the convectional catalysts. The vapor phase alkylation of benzene with ethanol in the presence of ZSM-5 zeolites is the famous Mobil-Badger process, which is now in commercial practice for production of ethylbenzene [5].

Lately, the direct use of ethanol, instead of ethene, as an alkylating agent with benzene for this reaction has gained more attention [6-8]. A long stable catalyst life is observed when alcohol, rather than ethylene, is used as an alkylating agent [1]. In addition to the academic interest, the direct use of ethanol in manufacture of ethylbenzene is also economical significance to those countries and regions where biomass derived

alcohol is an additional raw material for the manufacture of chemicals. The use of zeolite catalysts offers an environmentally friendly route to ethylbenzene and the possibility of achieving superior product selectivity through pore size control [9-12]. Zeolites are attractive materials for alkylation reactions because of their acid-base properties. The role of the acid-base properties of zeolites catalysts on product distribution of aromatic alkylation reactions has been reviewed by Giordano et al. [13]. The ring-alkylation mechanism over acid catalysts would proceed via the formation of methoxonium ion, which requires Bronsted acid sites [14-18]. Chandawar et al. [19] reported a significant improvement in ethylbenzene selectivity by modification of ZSM-5 by P or B to eliminate the strong acid sites on the surface of the catalyst. Levesque and Dao [20] also studied the alkylation of benzene with ethanol using steamed-treated ZSM-5 zeolite and chryso-zeolite ZSM-5 catalysts. They reported that ethylbenzene selectivity increased at high benzene/ethanol molar ratio. Gao et al. [21] studied the effect of zinc salt on the synthesis of ZSM-5 for alkylation of benzene with ethanol. They observed that the increase in ethylbenzene selectivity was due to higher Lewis/Bronsted acid ratio and the smaller crystal size. Ethylation of benzene with ethanol over MnAPO-5 catalyst was also studied by Raj et al. [22]. Raj et al. [22] used a molar ratio of 1:1 (benzene/ethanol) and obtained a significant amount of ethylbenzene at 400^0C.

In a recent publication, Odedairo and Al-Khattaf [23] investigated the ethylation of benzene with ethanol over ZSM-5 based catalyst, with an acidity of 0.23mmol/g. It was found that, the reaction proceed via two alkylation steps, producing EB and diethylbenzene (DEB), respectively. The apparent activation energy for benzene ethylation was found to be 32.28kJ/mol.

A number of researchers have reported the studies on alkylation reactions over ZSM type zeolites [24-29]. However, only a few researchers have performed alkylation reactions over USY-zeolite. Wang et al. [30] studied the alkylation of benzene over three kinds of faujasite type zeolites from different company with different SiO_2/Al_2O_3 ratios. They found that USH-Y with SiO_2/Al_2O_3 ratio of 80 showed the highest conversion, up to 97.8% conversion for 1-dodecene. Yuan et al. [31] investigated the alkylation of benzene over USY zeolite catalyst. The authors found that the catalytic activity and stability depends closely on the pretreatment temperature of catalyst and reaction conditions. The influence of Si/Al ratio of Y-zeolites on the activity and selectivity of benzene alkylation was studied by Nociar et al. [32]. They obtained the maximum alkylation activity for Y-zeolite at Si/Al ratio of 7. Alkylation of benzene with long chain alcohols over different Y-type zeolite catalysts has also been reported [33]. Deshmukh et al. [33] reported that the Re-Na-Y catalyst was found to be very effective in the alkylation of benzene with other long chain linear alcohols having 8-18 carbons. Namuangruk et al. [34] investigated the alkylation of benzene over faujasite zeolite using the ONIOM3 model. The model was found to be accurate in predicting adsorption energies of the reactants and product compared to experimental estimates. Odedairo and Al-Khattaf [35] also studied the ethylation of benzene over Y-zeolite based catalysts. Toluene was reported to be one of the major products, which was formed as a result of EB cracking.

Zeolite SSZ-33 (CON topology) possesses a channel system complied of intersecting 12-MR (member ring) and 10-MR pores; it is the first synthetic zeolite having 4-4 = 1 SBU (secondary building unit) in the structure [36]. Recently, Corma et

al. [37] studied the alkylation of benzene with ethanol over SSZ-33, in which the selectivity behavior was found to be closer to that of a large pore zeolite with potential cage effects.

TNU-9 represents a new three dimensional zeolites with 10 ring channel systems, being rather similar to the industrially most frequently employed ZSM-5. The size of the channels of TNU-9 is 0.52 X 0.60 and 0.51 X 0.55nm, thus, a slightly larger zeolite compared with ZSM-5 [38].

In addition to catalyst development and study of reaction mechanism, the kinetics of benzene ethylation has been studied over different zeolites types. One of the earliest kinetic models proposed for this reaction was that due to Sridevi et al. [5]. Different models based on Langmuir-Hinshelwood-Hougen-Watson reaction mechanisms were proposed and a mathematical fit for the best model was found. They determined the activation energy of benzene ethylation to be ~60.03kJ/mol over $AlCl_3$-impregnated 13X zeolite catalyst at constant benzene to ethanol molar ratio of 3:1. Similarly, kinetic model for benzene alkylation over cerium exchanged NaX zeolite catalyst was also studied by Barman et al. [1]. They reported an apparent energy of activation of ~56kJ/mol for the alkylation reaction at constant benzene to ethanol molar ratio of 3:1. In most of the kinetic studies mentioned above, ethylbenzene is usually considered to be the only product of the alkylation reaction, while other products like diethylbenzene (DEB) are negligible, whereas, the present study took into consideration the second alkylation step in its kinetic model development. Moreover, virtually all of these studies were carried out in fixed-bed reactors where temperature and concentration gradients may have significant effects on the values of estimated model parameters, as pointed out by Ma and Savage

[39]. Furthermore, in most of the previous kinetic studies on benzene ethylation, the deactivation of catalyst was not adequately accounted for, in the development of the kinetic models used in such studies.

In this work, the problems of benzene ethylation are addressed from a different perspective by attempting to optimize the process variables of the reaction. This can be achieved specifically by minimizing the undesirable secondary reactions on the external acid sites of the catalyst and catalyst deactivation by controlling the contact time. This can offer a superior route to high ethylbenzene yield and high para-diethylbenzene selectivity compared to multiple pre-treatment of the catalyst to eliminate external acid sites. Furthermore, to ensure that significant benzene conversion can be achieved in the proposed short reaction time, a fluidized bed process will be used in contrast to the more commonly used fixed bed process. It is expected that fluidization which enhances the catalyst-reactant contact will lead to high benzene conversion in a short time. The overall results of the process will then be the attainment of high benzene conversion while maintaining high ethylbenzene yield and high para-diethylbenzene selectivity. Another important potential advantage which the fluidized bed process can have over the fixed bed process is better heat distribution resulting in a more uniform product quality in contrast to the fixed bed processes where large temperature gradients in the reactor can negatively affect the quality of the product.

Experimental runs will be carried out in a novel bench riser simulator invented by *de* Lasa [40]. The riser simulator which perfectly mimics the operation of real commercial fluidized bed reactors has found consideration application in the area of catalyst evaluation and kinetic modeling.

1.2 Scope and Objectives of the Thesis

The main objectives of this work are explained in the following sections.

1.2.1. Initiation of a novel fluidized bed process for benzene ethylation

The main objective of this work is to initiate a fluidized bed process for benzene ethylation to produce ethylbenzene over fluidizable zeolite based catalysts using short reaction times. It is expected that the use of short contact times can restrict undesirable secondary reactions like further ethylbenzene ethylation, diethylbenzene ethylation and ethylbenzene cracking. In addition, it is believed that the use of short contact times as a means of increasing the yield of ethylbenzene and the proportion of para-diethylbenzene (measured by P/O and P/M ratios) in the reaction product can serve as a suitable alternative to repeated catalyst modification.

Experiments will be carried out at different reaction conditions (temperature and time) to determine the effects of these reaction conditions on the following important variables

i. Benzene conversion

ii. Ethylbenzene yield

iii. Diethylbenzene yield

iv. Toluene yield

v. P/O and P/M ratios

1.2.2. Studying the effect of catalyst structure on the benzene ethylation process.

Experimental runs will be carried out five fluidizable catalysts based on the ZSM-5, Y, mordenite, SSZ-33 and TNU-9 zeolites to study the effect of the different zeolite structures on the process of benzene ethylation. Zeolite Y was chosen for this study because it is a standard FCC catalyst. On the other hand, ZSM-5 was chosen because of its remarkable shape selective properties which can be used to enhance the proportion of para-diethylbenzene (measured by P/O and P/M ratios) in the reaction product.

1.2.3. Studying the effect of catalyst pre-coking

Catalyst pre-coking is an important catalyst modification technique used to enhance the proportion of para-ethylbenzene in the reaction product of benzene ethylation. It involves treating the fresh catalyst with a highly carbonaceous compound like 1,3,5 tri-isopropyl benzene to deposit coke on the external surface sites where undesirable para-ethylbenzene isomerization occurs. However, depending on the coking procedures, significant fall in benzene conversion is always a major disadvantage of the technique.

Therefore in this work, the effects of pre-coking the ZSM-5 based catalyst on the following variables will be studied;

i. Benzene conversion

ii. Ethylbenzene yield

iii. Diethylbenzene yield

iv. P/O ratio

1.2.4 Kinetic modeling

Key to any process development is the availability of important design parameters such as the activation energy of the reaction, rate constants, e.t.c.

Therefore kinetic modeling of benzene ethylbenzene over the five catalysts used forms a major part of this work. The modeling will be carried out as follows;

i. Proposing different possible reaction models

ii. Fitting experimental data into the proposed models to check the validity of the models

iii. Determination of models parameters; apparent activation energy, apparent reaction rate constants and catalyst decay constants.

CHAPTER 2

2 LITERATURE SURVEY

2.1. Background

Conventionally, ethylbenzene is produced by benzene alkylation with ethylene using homogeneous mineral acids such as aluminium chloride or phosphoric acid as catalysts that cause a number of problems concerning handling, safety, corrosion and waste disposal [3,4]. Benzene ethylation over zeolite based catalyst to produce ethylbenzene amongst other product is gaining remarkable attention and has been replacing the convectional catalysts. The vapor phase alkylation of benzene with ethanol in the presence of ZSM-5 zeolites is the famous Mobil-Badger process, which is now in commercial practice for production of ethylbenzene [5].

. The role of the acid-base properties of zeolites catalysts on product distribution of aromatic alkylation reactions has been reviewed by Giordano et al. [13]. The ring-alkylation mechanism over acid catalysts would proceed via the formation of methoxonium ion, which requires Bronsted acid sites. Hence benzene ethylation with ethanol is seen as a promising alternative for the selective production of ethylbenzene instead of using ethylene or ethane as alkylating agent.

2.2. Some important variables in benzene ethylation

The efficiency of a benzene ethylation process is a function of the following important variables

2.2.1. Benzene conversion

This is the ratio of the amount of benzene transformed into products to the amount originally present in the feedstock. Benzene conversion is usually expressed in percentages and it is given mathematically as:

$$\text{Ben. Conv. (\%)} = \frac{\text{Amt. of ben. in feedstock} - \text{Amt. of ben. left in product}}{\text{Amt. of ben. in feedstock}} \times 100 \quad (2.1)$$

2.2.2. Ethylbenzene selectivity

This is an indicator of how much of the converted benzene goes into ethylbenzene. It is also expressed in percentages. Mathematically ethylbenzene selectivity can be defined as;

$$\text{Ethylbenzene selectivity} = \frac{\text{Total amount of ethylbenzene formed}}{\text{Benzene conversion}} \times 100 \quad (2.2)$$

2.2.3. Para-diethylbenzene selectivity

This indicates the relative proportion of para-diethylbenzene in the mixture of diethylbenzene (formed). Mathematically, para-diethylbenzene selectivity is defined as;

$$\text{Para-diethylbenzene selectivity} = \frac{\text{Total amount of para-DEB formed}}{\text{Total amount of diethylbenzene formed}} \times 100 \quad (2.3)$$

Para-diethylbenzene selectivity is also commonly measured by the following important ratios;

(a) P/O ratio: This is the ratio of the amount of para-diethylbenzene to ortho-diethylbenzene in the reaction product.

(b) P/M ratio: This is the ratio of the amount of para-diethylbenzene to meta-diethylbenzene in the reaction product.

2.3. Catalysts for benzene ethylation

The most widely used catalysts for benzene ethylation at present are based on zeolites; a special class of Microporous crystalline solids which occurs naturally as minerals. Zeolites are also synthesized on a commercial scale for applications like adsorption separation, purification of commercial waste water containing heavy metals, and nuclear effluents containing radioactive isotopes. The following sections give a brief insight into the different forms of zeolites and their applications in benzene ethylation.

2.3.1. Zeolites

Zeolites-based molecular sieves are crystalline aluminosilicates with a three dimensional framework consisting of SiO_4 and AlO_4 tetrahedra, the primary building units, which are connected by bridging oxygen atoms [41-43]. The connection of two AlO_4 tetrahedra is excluded by Lowenstein's rule. Because of the lower valency of Al compared to Si, the number of AlO_4 tetrahedra controls the negative charge on the zeolite framework. This negative charge is usually compensated by organic or inorganic cations or protons. The protons represent Bronsted acid sites and participate in acid-catalyzed transformations of organic molecules. Moreover, dehydroxylation of bridging OH groups

leads to the formation of unsaturated aluminium species, which act as electron-acceptor sites, i.e., Lewis acids. These sites also contribute to the overall reactions of aromatic hydrocarbons. However, their contribution is believed to be less than that of the Bronstein acid sites.

2.3.2. Structure/ Types of zeolites

Depending on the connections between the individual tetrahedra, channels of Microporous dimensions up to 1.0nm and /or cavities can be formed. The diameter of the channel window is governed by the number of tetrahedra forming these windows. In the case of aluminosilicate molecular sieves, zeolites with windows consisting of 6, 7, 8, 9, 10, 12 and 14 member rings have been synthesized and described. It is evident that the size and shape of these windows control the sieving effect of the zeolites that has consequences for their adsorption and catalytic performance. Zeolites possessing windows with odd-membered rings are divided into the following groups;

(i) Medium-pore zeolites (10-membered rings up to 0.55 nm) e.g., ZSM-5, ZSM-11, ZSM-35, MCM-22 (possessing 12-member ring pockets on the crystal surface) and TNU-9. TNU-9 represents new 3D zeolites with 10-ring channels systems, being rather similar to industrially the most frequently employed ZSM-5. The size of the channels of TNU-9 is 0.52 x 0.60 and 0.51 x 0.55nm, thus, a slightly higher compared with ZSM-5.

(ii) Large-pore zeolites (12-membered rings up to 0.75nm) e.g., zeolite X, Y, beta, mordenite, ZSM-12 and SSZ-33. Zeolite SSZ-33 (CON topology) possesses a channel system complied of intersecting 12-MR (member ring) and 10-MR pores; it is the first synthetic zeolite having 4-4 = 1 SBU (secondary building unit) in the structure [44].

(iii) Extra-large-pore zeolites (14-membered rings with pore diameter smaller than 1.0nm); only two zeolites (CIT-5 and UTD-1) with 14-membered rings are known [11].

Zeolites also differ in the dimensionality of their channels, with one-dimensional channels without any intersections up to three-dimensional channels. In some cases, the channel system can consist of channels of different diameters (ferrierite, mordenite) or possesses two independent channel systems (e.g. MCM-22 [45]). The most utilized structural types of zeolites for catalyzing aromatic reactions are shown in Fig. 2.1.

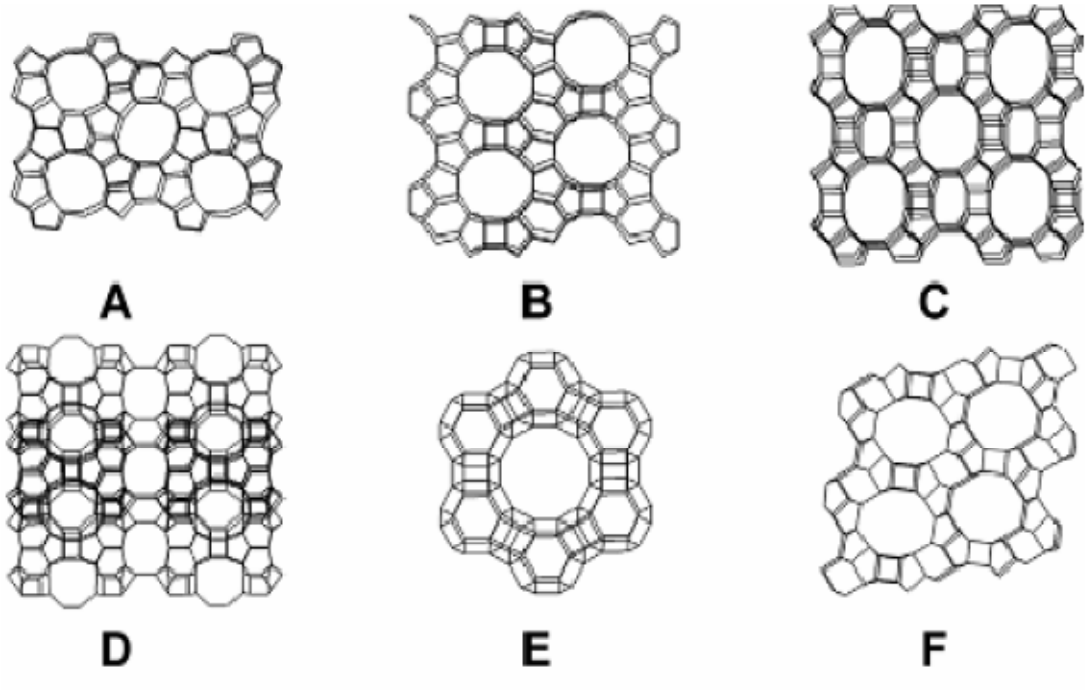

Figure 2.1 Structures of zeolites

ZSM-5 (A), mordenite (B), Beta (C), MCM-22 (D), zeolite Y (E), and zeolite L (F). (Taken from reference [11])

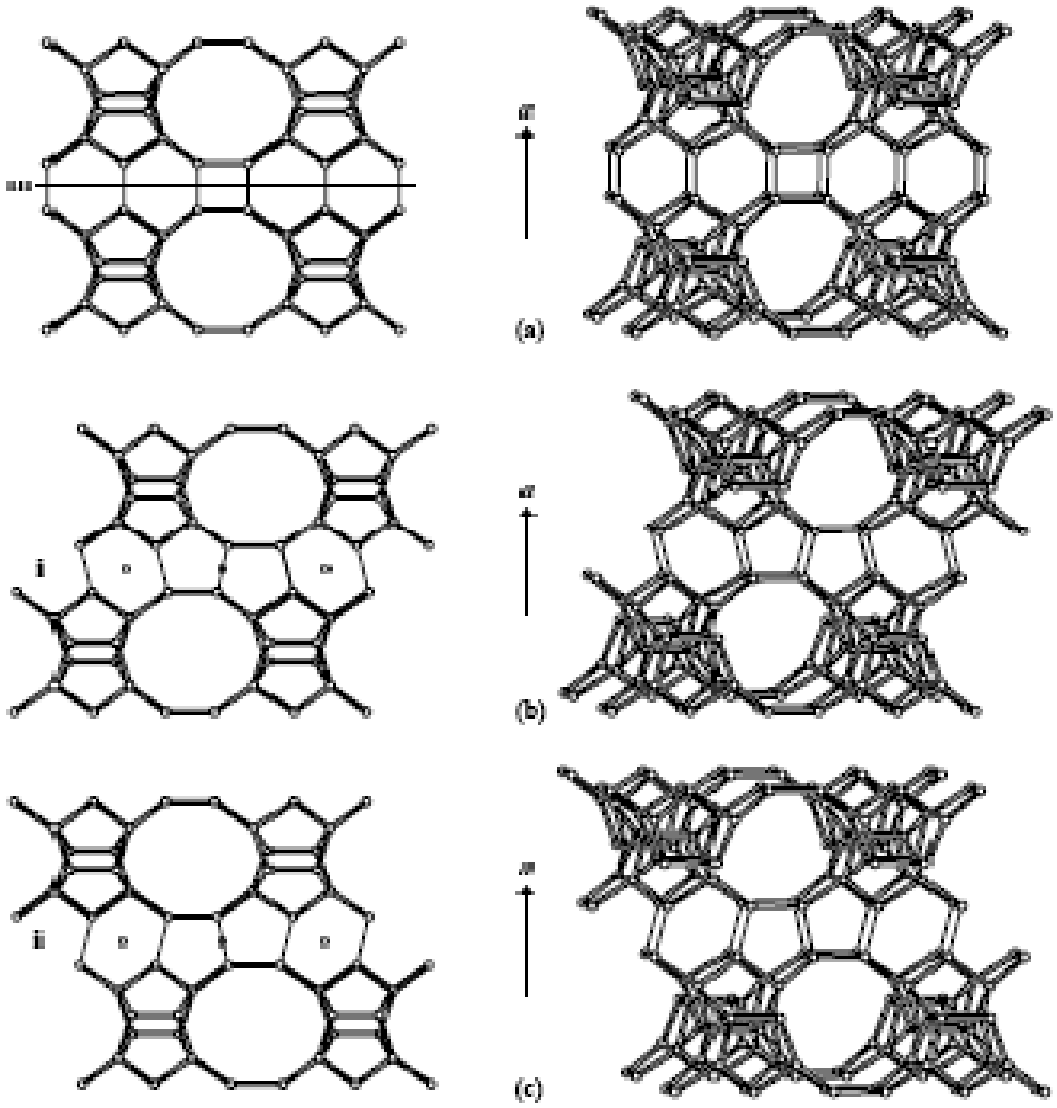

Figure 2.2 Structure of SSZ-33 zeolite

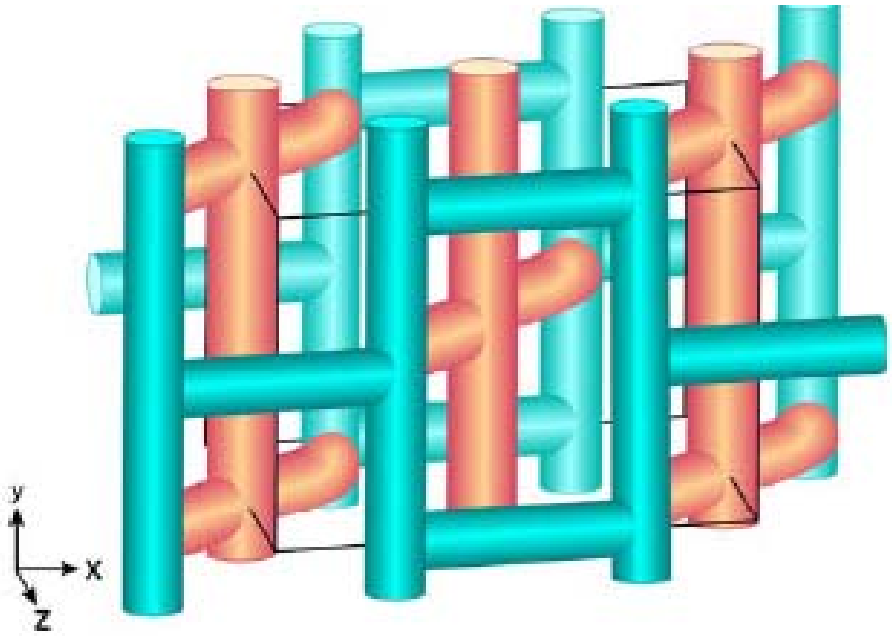

Figure 2.3 Schematic drawing of three-dimensional channel system of TNU-9. Channel A is orange and channels B is green (Taken from reference [46])

2.3.3 Advantages of zeolites over other solid acids as catalysts for aromatic transformations

The main advantages of zeolite and zeotype catalysts compared to convectional solid acids include;

(a) Well-defined inorganic crystalline structures usually based on aluminosilicate (or metallosilicate) and aluminophosphate matrices, with a variety of structures differing in channels diameters, geometry, and dimensionality;

(b) A precisely defined inner void volume providing high surface area up to $1200m^2/g$ for mesoporous molecular sieves;

(c) The ability to absorb and transform molecules in the inner volume;

(d) Isomorphism substitution of some trivalent cations into the silicate framework enabling tuning of the strength and concentration of the acid sites;

(e) Shape selectivity, given by the ratio of the kinetic diameters of the reactants, intermediates, and products to the dimensions of the channels;

(f) Environmental tolerance.

2.3.4. Shape selectivity of zeolite molecular sieves

The geometry and dimensionality of the channel system of zeolites play a decisive role in their shape selectivity properties [47]. This phenomenon arises from the well-defined sterically constrained environment in which either the molecules react or have to diffuse into and out of the zeolite pores. Three types of molecular sieve shape selectivity have been defined. Reactant selectivity facilitates or prevents penetration of the reactant molecules in to the zeolite channels, restricted transition state selectivity prevents against the formation of bulky reaction intermediates, while product selectivity preferably

removes smaller and readily diffusing products from the channels compared to larger product molecules held in the zeolite interior. Recently, another type of shape selectivity, the structure-directed transition state selectivity has been proposed [48, 49]. It involves reactions requiring a specific geometric approach of the reactant molecules, which is fulfilled by a certain dimension and architecture of the zeolite inner volume.

2.3.4. Use of Zeolites in Benzene Ethylation

Benzene ethylation has been studied over different kinds of zeolites. Levesque and Dao [20] studied the alkylation of benzene with ethanol using steamed-treated ZSM-5 zeolite and chryso-zeolite ZSM-5 catalysts. They reported that ethylbenzene selectivity increased at high benzene/ethanol molar ratio. Gao et al. [21] studied the effect of zinc salt on the synthesis of ZSM-5 for alkylation of benzene with ethanol. They observed that the increase in ethylbenzene selectivity was due to higher Lewis/Bronsted acid ratio and the smaller crystal size. Wang et al [30] studied the alkylation of benzene over three kinds of faujasite type zeolites from different company with different SiO_2/Al_2O_3 ratios. They found that USH-Y with SiO_2/Al_2O_3 ratio of 80 showed the highest conversion, up to 97.8% conversion for 1-dodecene. Yuan et al [31] investigated the alkylation of benzene over USY zeolite catalyst. The authors found that the catalytic activity and stability depends closely on the pretreatment temperature of catalyst and reaction conditions.

The main challenge in the area of catalyst development for benzene ethylation is the development of a catalyst which can;

(1) Produce high ethylbenzene selectivity while maintaining reasonable levels of benzene conversion.

(2) Limit the major co-reactions like ethylbenzene cracking, diethylbenzene cracking and ethanol decomposition which occur simultaneously with the main alkylation reaction.

(3) Resist quick deactivation.

Generally these may be achieved by modifying the physiochemical properties of zeolitic catalysts. The properties which are usually modified include the overall acidity of the zeolite, the number of the external acid sites on the zeolite crystal, pore size and crystal size.

2.3.5. Modification of external surface acid sites

As the selective synthesis and transformation of alkyl aromatics take place on acid sites located inside the zeolite channels, minimization or annihilation of the acid sites on the crystal surface, where the reaction environment is not limited by the steric constraints, is demanding. This can be achieved in two ways. By increasing crystal size of the zeolite, the relative concentration of acid sites inside the channels is increased compared to that on the crystal surface. However, due to the diffusional hindrance for alkyl aromatics inside the channels, the use of large crystals (ca > 2μm) leads to a substantial decrease in conversion values [11]

Another way of reduction of surface acid sites involves silylation of the crystal surface. This can be achieved by using the silylation reaction, which can take place either in solution or by the chemical vapor deposition (CVD) of chlorosilanes or alkoxysilanes [11]. To silylate exclusively the surface sites of ZSM-5 zeolite, tetraethyl- or isopropyl-orthosilicates can be advantageously used, i.e., molecules whose kinetic diameters do not

allow them to enter into the ZSM-5 zeolite pores, and the silylation reaction proceeds only with the protonic sites on the crystal surface.

It should be mentioned that the silylation reaction occurs besides with Si-OH-M groups also with Si-OH groups of the zeolite and with those OH groups formed by silylation. Thus, polymeric SiO_2 is formed on the external zeolite surface. Accordingly, silylation of the surface acid sites frequently also leads to a decrease in the pore openings of the channels or even plugging of a part of the channel entrances due to the formation of silica polymers. Pore narrowing imposes diffusional hindrances, which can be exploited for achieving higher para-selectivity as explained in the next section, but can also lead to retention of molecules inside the inner void volume, and finally, to increase coking compared to the original non-silylate zeolite. Niwa et al. [50] used the CVD technique with Si $(OCH_3)_4$ (TMOS), and $SiOCH_3$ $(OC_3H_7)_3$ (TMPOS). They were able to show that TMOS polymerizes readily, but that TNPOS, containing only one methyl group, appears to interact selectively with the surface strong acid sites. Thus, with a lower concentration of deposited silica, complete annihilation of the surface acid sites can be achieved by use of TMPOS.

2.4 Reaction Mechanism

2.4.1 Mechanism of Ethylation of Benzene with Ethanol

The alkylation of benzene with ethanol occurs through an electrophilic substitution on the aromatic ring and, likewise, it is considered to proceed via a carbonium ion-type mechanism [51-52]. The ethylation takes place by reaction of the activated alkene (formed in the case of ethanol by dehydration of the alcohol) on the acid

sites of the zeolite. However, when contacting ethanol or ethylene with benzene on a solid catalyst, the global process can follow two major routes:

(1) Alkylation of benzene with ethylene producing ethylbenzene, which can undergo other consecutive alkylation's yielding poly-ethyl benzenes, and

(2) Oligomerization of ethylene producing C4, C6 or even C8 species. The oligomers can be further transformed through cracking, isomerization and alkylation reactions, giving olefins and other alkylbenzenes (toluene, cumene, butyl benzenes, etc.).

It must be remarked that, from an industrial point of view, the formation of byproducts different from diethylbenzene has a negative effect, not only on the final yield, but also on the quality of the final product [4, 9, and 53].

One of the most comprehensive mechanistic studies of benzene ethylation with ethanol over ZSM-5 based catalyst is the one reported by Odedairo and Al-Khattaf [23]. In which, Surface proton attacks ethanol to form water and surface ethyl cation (ethoxy cation). An ethyl cation attacks benzene molecule to form protonated ethylbenzene on the surface. The protonated ethylbenzene returns a proton to the surface and forms ethylbenzene. Thereafter, surface ethyl cation (ethoxy cation) attacks ethylbenzene ring carbon atom at ortho, meta or para position atom to form a surface protonated diethylbenzene. The surface protonated diethylbenzene returns a proton to the surface and forms diethylbenzene.

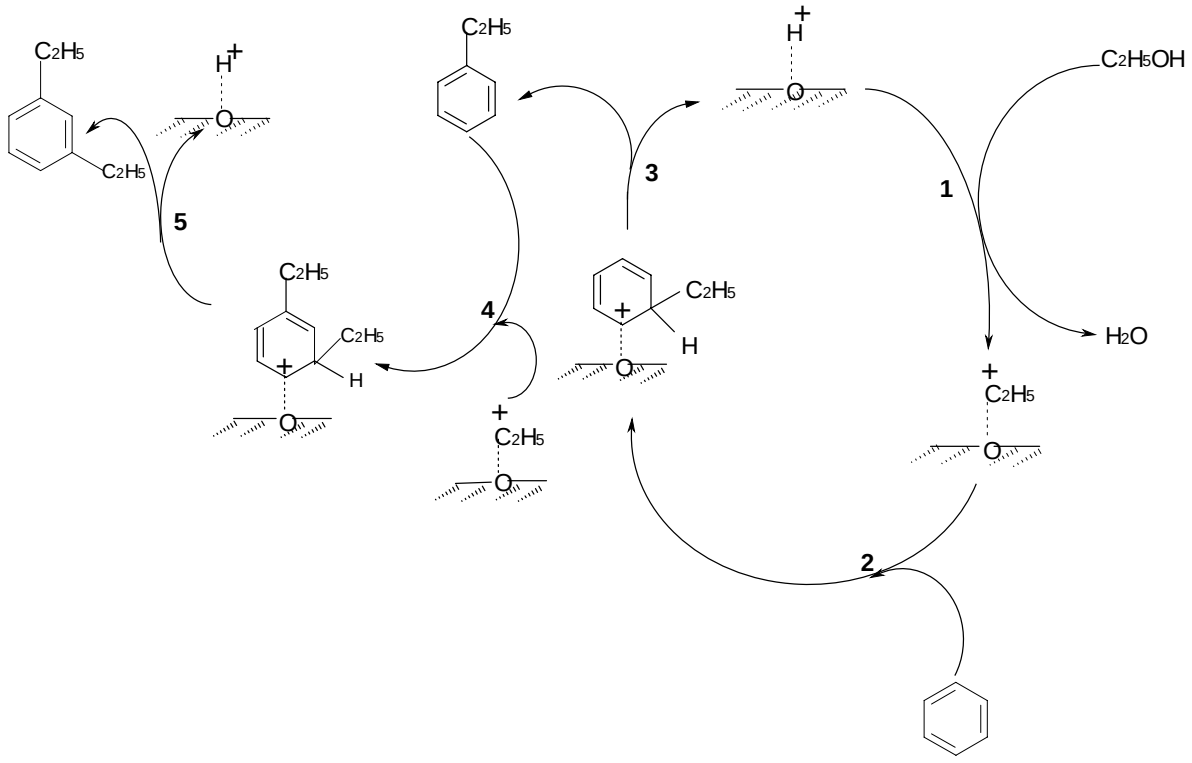

Figure 2.4 Proposed overall reaction scheme during benzene ethylation

Another comprehensive mechanistic study of benzene ethylation with ethanol over a catalyst based on Y zeolite is the one reported by Odedairo and Al-Khattaf [35]. In which, surface proton attacks ethanol to form water and surface ethyl cation (ethoxy cation). An ethyl cation attacks benzene molecule to form protonated ethylbenzene on the surface. The protonated ethylbenzene returns a proton to the surface and forms ethylbenzene. Surface proton reacts with ethylbenzene to form a carbonium ion I. These carbonium ion I forms surface methyl cation (methyoxy cation) and toluene. The surface methyl cation formed, reacts with benzene molecule to form protonated toluene. The protonated toluene returns a proton to the surface and forms toluene.

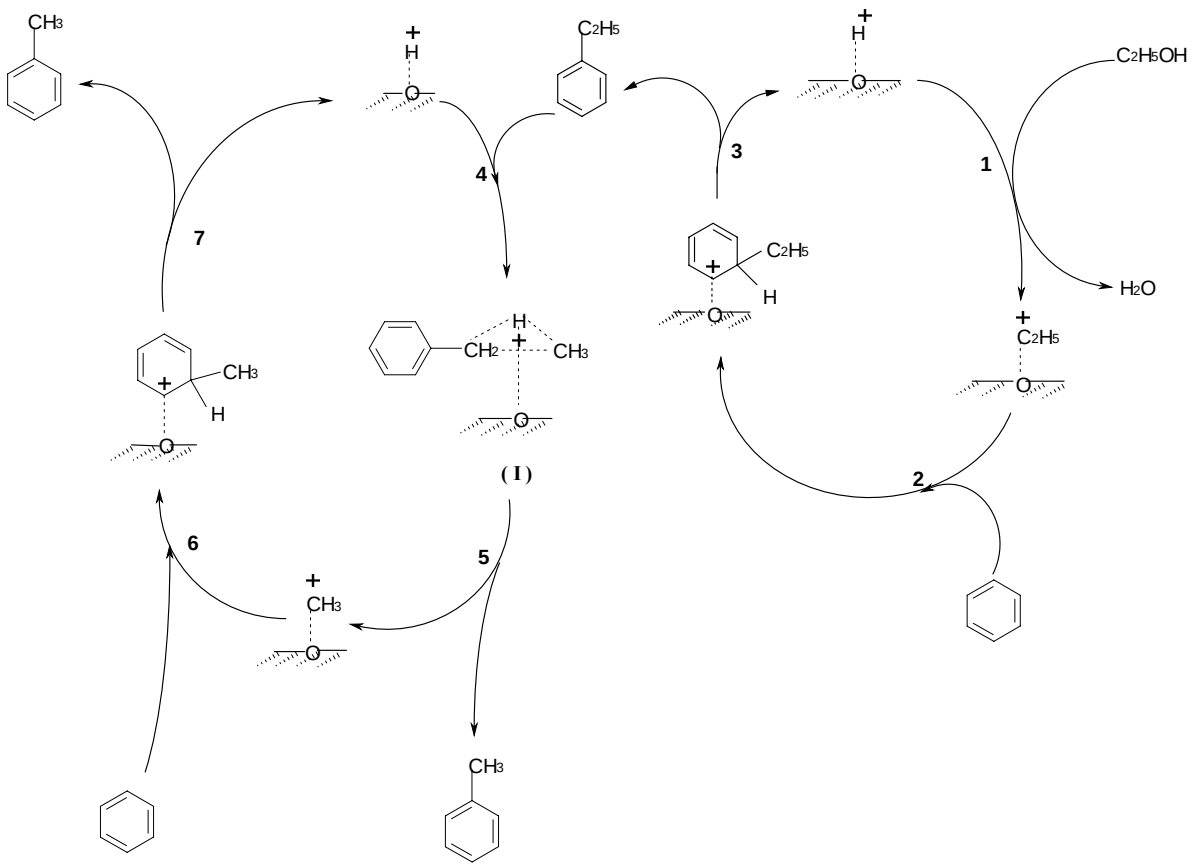

Figure 2.5 Proposed reaction scheme for toluene formation during benzene ethylation reaction with ethanol

CHAPTER 3

3 EXPERIMENTAL SECTION

The experimental section describes the equipment in the experimental set up and the procedures adopted in carrying out this work. The major tasks carried out here include catalyst preparation, characterization and evaluation.

3.1 Experimental Set-up

The experimental set-up used to carry out this work consists of five major equipments namely; **a novel riser simulator, a gas chromatograph, a x-ray diffraction crystallography, laser scattering particle size analyzer** and **a coke analyzer**.

3.1.1 Riser Simulator

All the experimental runs were carried out in a 45 cm^3 riser simulator (see Figure 3.1). This reactor is novel bench-scale equipment with an internal recycle unit invented by de Lasa [40]. The Riser Simulator consists of two outer shells, the lower section and the upper section which allow to load or to unload the catalyst easily. The reactor was designed in such way that an annular space is created between the outer portion of the basket and the inner part of the reactor shell. A metallic gasket seals the two chambers with an impeller located in the upper section. A packing gland assembly and a cooling

jacket surrounding the shaft provide support for the impeller. Upon rotation of the shaft, gas is forced outward from the centre of the impeller towards the walls. This creates a lower pressure in the centre region of the impeller thus inducing flow of gas upward through the catalyst chamber from the bottom of the reactor annular region where the pressure is slightly higher. The impeller provides a fluidized bed of catalyst particles as well as intense gas mixing inside the reactor. The riser simulator consists of two omega CN9000 series temperature controllers that control the vacuum box and reactor temperature. These controllers are calibrated to work with K type omega thermocouples. One of the thermocouple is connected to catalyst basket, from where the temperature in the reactor is measured as shown in Figure 3.1.

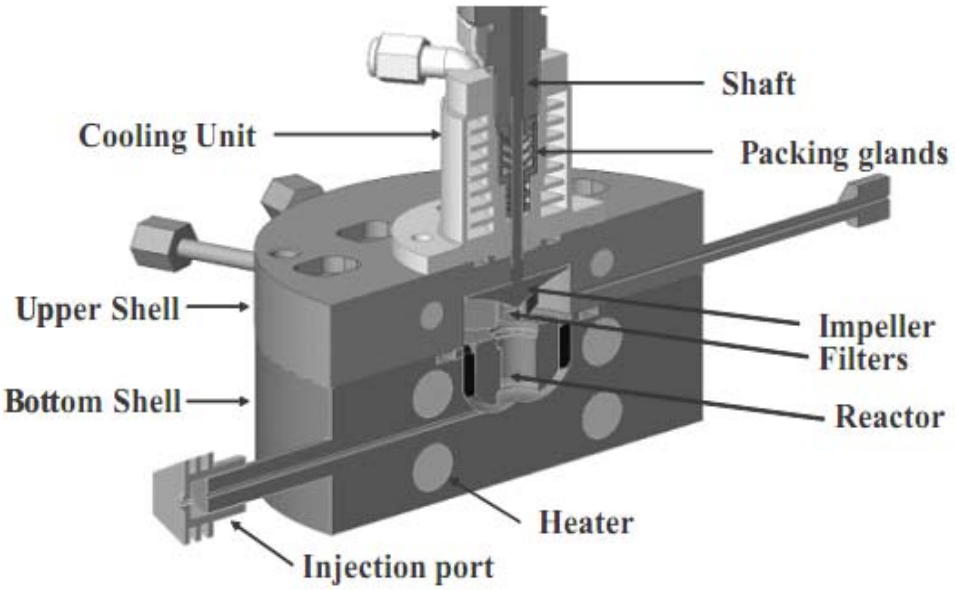

Figure 3.1 Schematic diagram of the Riser Simulator

The riser simulator operates in conjunction with series of sampling valves that allow for injection of the feedstock and withdrawal of reaction products in short periods of time, as shown in Figure 3.2. A four-port valve enables the connection and isolation of the 45cm^3 reactor and the vacuum box, and a six-port valve allows for the collection of a sample of reaction products in a sampling loop. Vacuum box and reactor pressure are displayed on two Omega DP series pressure displays. The pressures are displayed in psia (Pounds per Square Inch Absolute). These displays are calibrated for use with Omega pressure transducers, rated for 50psia maximum pressure.

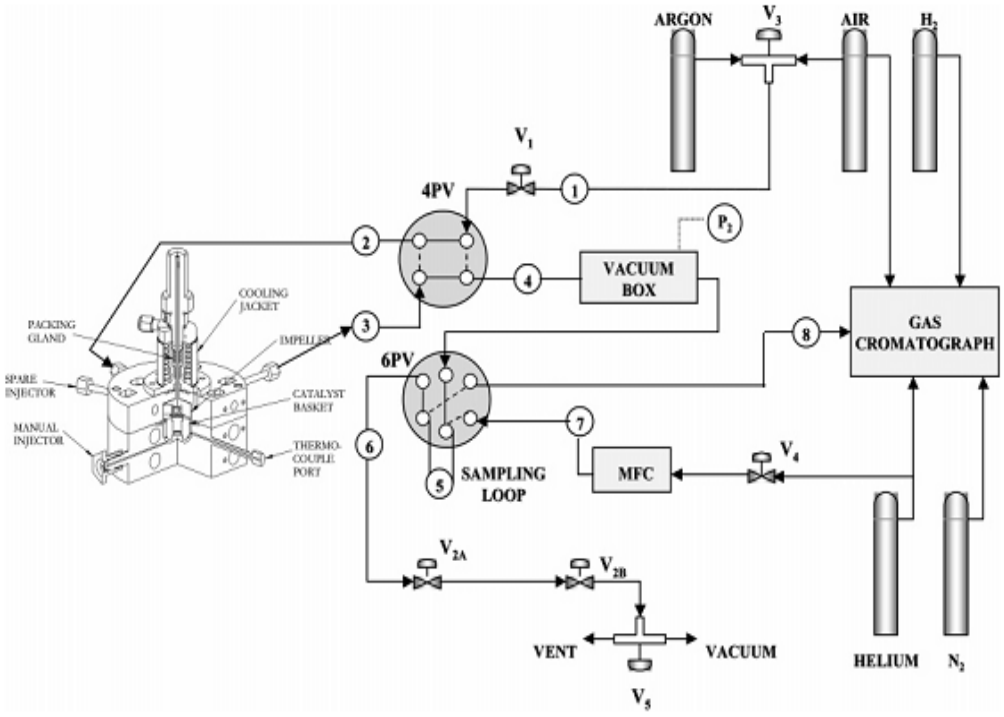

Figure 3.2 Schematic diagram of the riser simulator experimental set-up.

3.1.2 Gas Chromatograph (GC) system

The GC system consists of a 60 meters long INNOWAX capillary column, an FID-type detector and a temperature controlled oven. While helium is used as the sample carrier gas, air and hydrogen are used as the gases for the FID detector. Furthermore, liquid nitrogen is used to facilitate the initial cryogenic operation of the GC temperature program. The liquid nitrogen cools the GC oven to -30^0C. The flow of liquid nitrogen is administered by solenoid valve actuated from the GC's internal oven temperature controller. The integrator allows strip chart recording as well as integration of the GC detector signal. The integrator is connected to the GC via a HPIL instrument network cabling system.

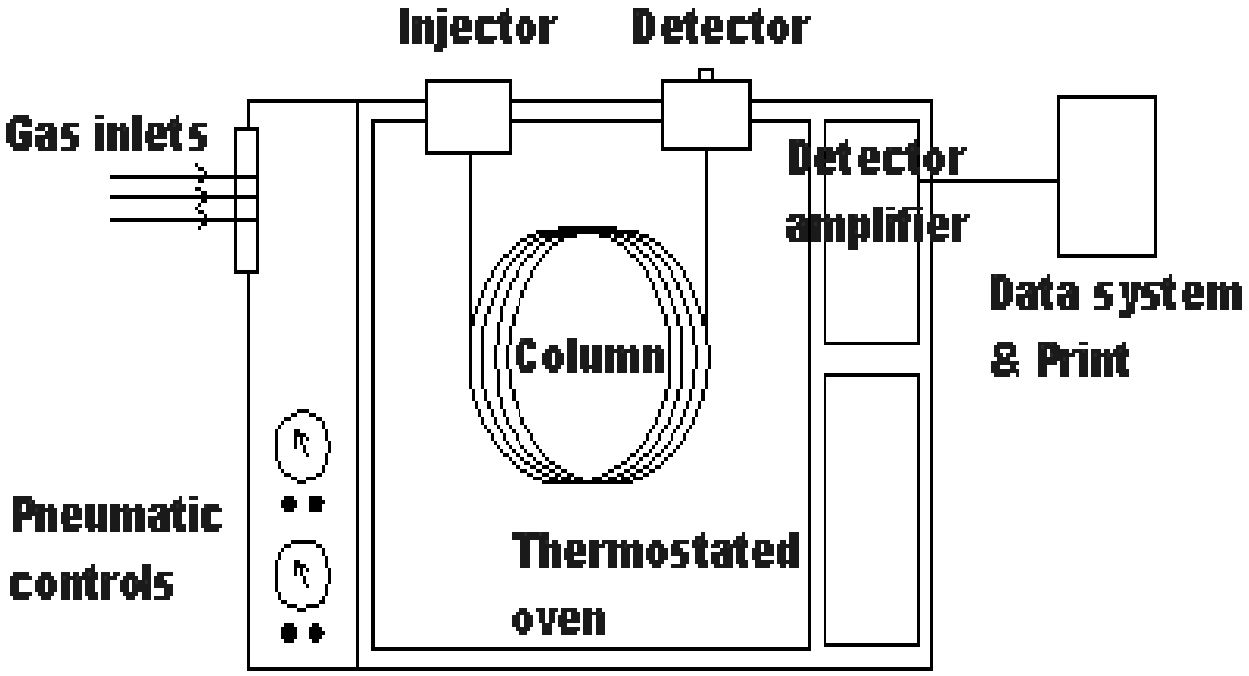

Figure 3.3 Schematic diagram of the gas chromatograph.

3.1.3 Coke Analyzer

Amount of coke deposited on spent catalyst was determined by a common combustion method. In this method, a carbon analyzer Cs-244 is used. Oxygen is supplied to the unit directly. A small amount of spent catalyst (0.25g) is used for the analysis. The coke laid out on the sample during reaction experiments is burnt completely converting the carbonaceous deposit into carbon dioxide. The amount of carbon dioxide formed is measured, and thus the amount of coke formed is determined.

3.2 Catalyst Preparation

3.2.1 Preparation of fresh fluidizable ZSM-5, Y, mordenite, SSZ-33 and TNU-9 based Catalysts

The ZSM-5 zeolite used in this work was obtained from Tosoh Company, Japan. The as-synthesized Na zeolite was ion-exchanged with NH_4NO_3 to replace the Na cation with NH_4^+. Following this, NH_3 was removed and the H form of the zeolite was spray dried using kaolin and alumina as the filler and a silica sol as the binder. Laser scattering particle size analyzer was used to determine the size of the catalyst particle. The resulting 60 μm catalyst particles had the following composition: 30 wt % zeolite, 50 wt % kaolin and alumina, and 20 wt % silica sol. The process of Na removal was repeated for the pelletized catalyst. Following this, the catalyst was calcined at 600 °C for 2 h. The total acidity was determined using NH_3 desorption method.

Another catalyst based on ZSM-5 zeolite, was also prepared and characterize. Kaolin was not added as filler in this catalyst based on ZSM-5, while silica sol was not used as the binder. The uncalcined proton form of ZSM-5 (CT-405) used in this study was obtained from CATAL, UK. The ZSM-5 has silica to alumina ratio of 30. An alumina binder (Cataloid AP-3) contains 75.4wt% alumina, 3.4% acetic acid and water as a balance obtained from CCIC Japan. The alumina binder was dispersed in water and stirred for 30min to produce thick slurry. The zeolite powder was then mixed with alumina slurry to produce a thick paste. The composition of the zeolite based catalyst in weight ratio is as follows: ZSM-5: AP-3 (2:1).

The uncalcined proton form of mordenite (H-mordenite) zeolite (HSZ-690HOA) used in this work was obtained from Tosoh Chemicals, Japan. The mordenite has silica to

alumina ratio of 240. Similar procedure used for the preparation of the ZSM-5 based catalyst discussed lately was also followed for the preparation of the mordenite based catalyst. Similarly, the SSZ-33 zeolite used in this present study was obtained from Chevron Energy and Technology Company, Richmond, CA, USA, while TNU-9 zeolite was obtained from J. Heyrovsky Institute of Physical Chemistry, Academy of Science of the Czech Republic, Prague, Czech Republic. Alumina was added to these zeolites (SSZ-33 and TNU-9) adopting the same procedure used for mordenite and ZSM-5 based catalyst.

Ultrastable Y zeolite (USY) used in this work was obtained from Tosoh Company in the Na form. The zeolite was ion exchanged with NH_4NO_3 to replace the sodium cation with $NH4^+$. Following this, NH_3 was removed and the H form of the zeolite was spray-dried using kaolin as the filler and silica sol as the binder. Catalysts and Chemicals Industries Co. Japan supplied both materials. The resulting 60-μm catalyst particles had the following compostions: 30 wt% zeolite, 50 wt% kaolin, and 20 wt% silica. The process of sodium removal was repeated for the pelletized catalyst. Following this, the catalyst was calcined for 2 hr at 600^oC. Finally, the fluidizable catalyst particles (60-μm average size) were treated with 100% steam at different temperatures and time to obtain the USY zeolites.

3.2.2 Preparation of precoked ZSM-5 based Catalyst

The precoked catalyst was prepared by treating 800mg of fresh catalyst with 100μL of carbonaceous 1,3,5-TIPB under mild reaction conditions (temperature 400^0C, reaction of 3s). 1,3,5-TIPB was used because its kinetic diameter is larger than the pore opening of ZSM-5, thereby restricting coke deposit to the external surface of the catalyst only. The catalytic cracking of 1,3,5-TIPB was carried out in the riser simulator at 400^0C for 3s. Less than 10% conversion was obtained at this reaction condition, with less than 3% propylene as product.

3.3 Catalyst Characterization

Since the behavior of a catalyst depends on its physical and chemical structure, a comprehensive catalyst characterization is of great importance. Characterization of the zeolite based catalysts used in thus work was carried out using the following well established standard procedures.

3.3.1 BET surface area determination

The BET surface area of the catalysts used in this work was measured according to the standard procedure ASTM D-3663 using Sorptomatic 1800 Carlo Erba Strumentazione unit, Italy.

3.3.2 Acidity of catalysts

The total acidity of the catalysts used aws characterized by NH_3 temperature programmed desorption (NH_3-TPD).

3.3.3 Unit cell size

The unit cell size of the catalysts was determined using X-ray diffraction following ASTM-D-3942-80.

3.4 Feed stock preparation

10g feed stock of benzene and ethanol in molar ratio of 1:1 (i.e 62.9% wt. benzene and 37.1% wt. of ethanol) was prepared by mixing 6.29g of benzene and 3.71g of ethanol in a clean sample bottle. The sample bottle was then well covered to make it air tight in order to prevent any possible evaporation of the components which may lead to a change in the composition of the feed stock. Fresh samples were prepared as neeeded during the course of the experimental work.

3.5 GC calibration

The calibration of the Gas Chromatograph for used in determining the product composition of the reaction of benzene and ethanol was done as explained in sections 3.5.1 and 3.5.2 below.

3.5.1 Determination of retention time for the different compounds

The retention times of all compounds of interest in this work were determined by analyzing pure samples of each of the compounds in the GC in turns. Table A3.1 (Appendix) shows the different compounds and their corresponding retention times. These retention times were used to identify each components of the reaction product.

3.5.2 Correlating GC response and actual weight percentage of each compound

In calibrating the GC, standard samples of digfferent compositions containing ethanol, benzene and the main reaction products (ethylbenzene, isomers of

diethylbenzene and toluene) were prepared. The composition of the prepared samples were carefully chosen to reflect all the possible product compositions (obtained from preliminary experimental runs) under the different reaction conditions to be investigated. 0.2µl of the first sample was then injected into the GC and the GC responses (area %) for each components in sample were obtained. The same procedure was repeated for all the othere samples Figure A3.1 (Appendix) shows GC output of the samples (M) while table A3.2 (Appendix) shows the sample composition and the corresponding GC responses for the different components in the sample. Based on the various GC outcomes, data points representing actual wt (%) of a component in a sample and the corresponding GC responses (% Area count) were generated. A calibration curve for each of the components was plotted as shown in figures A3.2-A3.4 (Appendix)

3.6 Catalyst Evaluation

Benzene ethylation was carried out over the prepared ZSM-5, Y, mordenite, SSZ-33 and TNU-9 fluidizable catalysts in order to test their catalytic activity. Each catalyst was evaluated for the alkylation reaction at temperatures of 250, 275, 300, 325, 350 and 400^0C for reaction times of 3, 5, 7, 10 13 and 15 sec. Furthermore, the reaction was carried out over the ZSM-5 based catalyst which has been pre-coked. The latter reaction was carried out to investigate the effect of catalyst pre-coking on the benzene conversion and the product distribution espescially the P/O ratio. To ensure the reproducibility of the data, experimental runs for each reaction condition was repeated at least twice.

3.7 Procedure for Benzene Ethylation using the fluidizable Zeolite based Catalysts.

Regarding the experimental procedure in the Riser Simulator, 0.81g of catalyst was loaded into the Riser Simulator basket. The system was then sealed and tested for any pressure leaks. Furthermore, the reactor was heated to the desired reaction temperature. The vacuum box was also heated to around 250^{o}C and evacuated to around 0.5 psi to prevent any condensation of hydrocarbons inside the box. The heating of the Riser Simulator was conducted under continuous flow of argon (inert gas), and it usually takes few hours until thermal equilibrium is finally attained. Before the initial experimental run, the catalyst was activated for 15 minutes at 620^{o}C in a stream of air. The temperature controller was set to the desired reaction temperature, in the same manner the timer was adjusted to the desired reaction time. At this point the gas chromatograph was started and set to the desired conditions.

Once the reactor and the gas chromatograph have reached the desired operating conditions, the feedstock (200µl) was injected directly into the reactor via a loaded syringe. After the reaction, the four port valve immediately opened ensuring that the reaction was terminated and the entire product stream was sent online to the analytical equipment via a pre-heated vacuum box chamber.

3.8 Procedure for Benzene Ethylation using pre-coked ZSM-5 based Catalysts.

Coke is selectively deposited on the external surface of zeolites in order to cover the external active sites which are responsible for undesirable secondary reactions. Generally, molecules with large kinetic diameters which cannot penetrate into zeolite pores are used thereby limiting the reaction of these compounds to the external surface of the zeolite. Hence, coke formed is essentially deposited on the catalyst external surface. Precoking using carbonaceous compounds with large molecules has been reported in the literature [54, 55]. Since coke is deposited only externally, it is assumed that the internal sites stay essentially unchanged. Therefore, although precoking generally reduces the total number of acid sites, it keeps enough acid sites to catalyze the reaction [54, 55]. Catalyst precoking has been observed to have a significant effect on para-selectivity. The significant increase in para-selectivity after precoking is attributed to the partial deactivation of the external active sites where p-isomers (generated inside ZSM-5 pores) undergo disproportionation reaction. Consequently, this leads to an increase in the rate of formation of p-isomers, while the rate of disproportionation reaction is significantly decreased.

In the experimental runs with the precoked catalyst, 100μL of 1,3,5-TIPB was injected at 400^0C into the reactor after loading the reactor basket with 800mg of fresh catalyst, and a limited reaction was allowed to take place for only 3s. The amount of coke deposited on the catalyst from 1,3,5-TIPB was found to be 0.15 wt%. The system was then purged and cleaned with argon for 30mins.

Regarding the nature of coke deposited, different analytical techniques have been used in the literature to characterize the coke formed over different zeolite catalyst at different temperatures. One of those methods is the one developed by Guisnet and

Magnoux [56] in which the coked catalyst is treated with HF solution and the soluble coke which dissolve in CH_2Cl_2, is analyzed through GC-MS coupling. Similar approach developed by Guisnet and Magnoux [56] describe above, was used to determine the developed formula for the components soluble in CH_2Cl_2 and was analyzed by an Agilent GC-MS (GC 6890N-MD 5973N) with a DB5-MS column (30m x 0.25mm). The column program is: injector temperature, 250^0C; initial column temperature, 40^0C; initial time, 5min; heating rate, 12^0C/min; final temperature, 320^0C; final time, 25min; carrier gas, He, 1mL/min; average velocity, 38cm/s; solvent delay, 6min. An alkyl benzene (methyl benzene) compounds were identified as the coke component over the precoked catalyst.

According to Guisnet and Magnoux [57], the H/C atomic ratio can be considered as a measurement of the aromaticity of the coke. The elemental analyzer (Model Vario EL) was also used to quantify the polyaromatic character of the coke over the precoked catalyst, by measuring the H/C atomic ratio. By applying this technique, any water released from the catalyst itself could interfere with the result, giving higher hydrogen (H) value [58]. To overcome this problem, water was quantified accurately in the catalyst sample by Karl Fischer titration. A Karl Fischer coulometer (Model Mettler DL 37) was used for water determination. Then, the hydrogen in water was subtracted from the total amount of H of the catalyst sample measured by elemental analyzer. The corrected H value is used in calculating the H/C ratio. The hydrogen to carbon ratio of the coke content over the precoked catalyst was found to be ~1.6.

It is of paramount importance to note that, the hydrogen to carbon atomic ratio as well as the obtained developed formula for the coke noticed from the coke over the precoked catalyst was not used in any section of this study; rather, the carbonaceous

compound was just used to cover part of external active sites which are responsible for undesirable secondary reactions.

CHAPTER 4

RESULTS AND DISCUSSIONS

This section presents and discusses the results of benzene ethylation over ZSM-5, Y-, mordenite, SSZ-33 and TNU-9 zeolite based catalyst. The effects of reaction conditions (temperature and time) on important variables such as benzene conversion, ethylbenzene yield, diethylbenzene yield, the P/O ratios are discussed in details. In addition a detailed kinetic modeling of the reaction over all zeolite based catalyts is presented starting first with model formulation and then model parameters determination using non-linear regressional anaylsis.

4.1. Benzene Ethylation over ZSM-5 based catalyst

4.1.1. Catalyst Characterization

Table 4.1 below shows the results of the charcterization of ZMS-5 based catalyst used in this work. As can be seen from the table, the acidity of the pre-coked catalyst is slightly lower than the fresh ZSM-5 based catalyst.

Table 4.1.Catalyst characterization of the ZSM-5 based catalyst used

Catalyst (%)	Surface Area (m^2/g)	Na_2O (%)	Acidity (mmol/g)	Weak acid sites (%)	Strong acid sites (%)
Fresh	70	Negligible	0.23	62.5	37.5
Precoked	63	Negligible	0.18	66.67	33.33

4.1.2. Effect of reaction conditions on benzene conversion

Figure 4.1 below shows the variation of benzene conversion with reaction time and temperature for the fresh ZSM-5 catalyst based on time on stream. It is evident from this figure that benzene conversion increased with both reaction time and temperature, reaching a maximum of ~ 17% at 400^0C for a reaction time of 15s. For all the reaction temperatures, it was observed that conversion increased by ~ 4 –5.33 times when reaction time was increased from 3 to 15s. Similarly, for all reaction times, benzene conversion was also found to increase as temperature was increased from 300 to 400^0C. This is in an agreement with observation made by Levesque and Dao [20] during the alkylation of benzene with aqueous ethanol solution over steamed-treated ZSM-5 and chryso-zeolite ZMS-5 catalysts. They reported that benzene conversion increased regularly with temperature to reach a maximum in the region of 725 K.

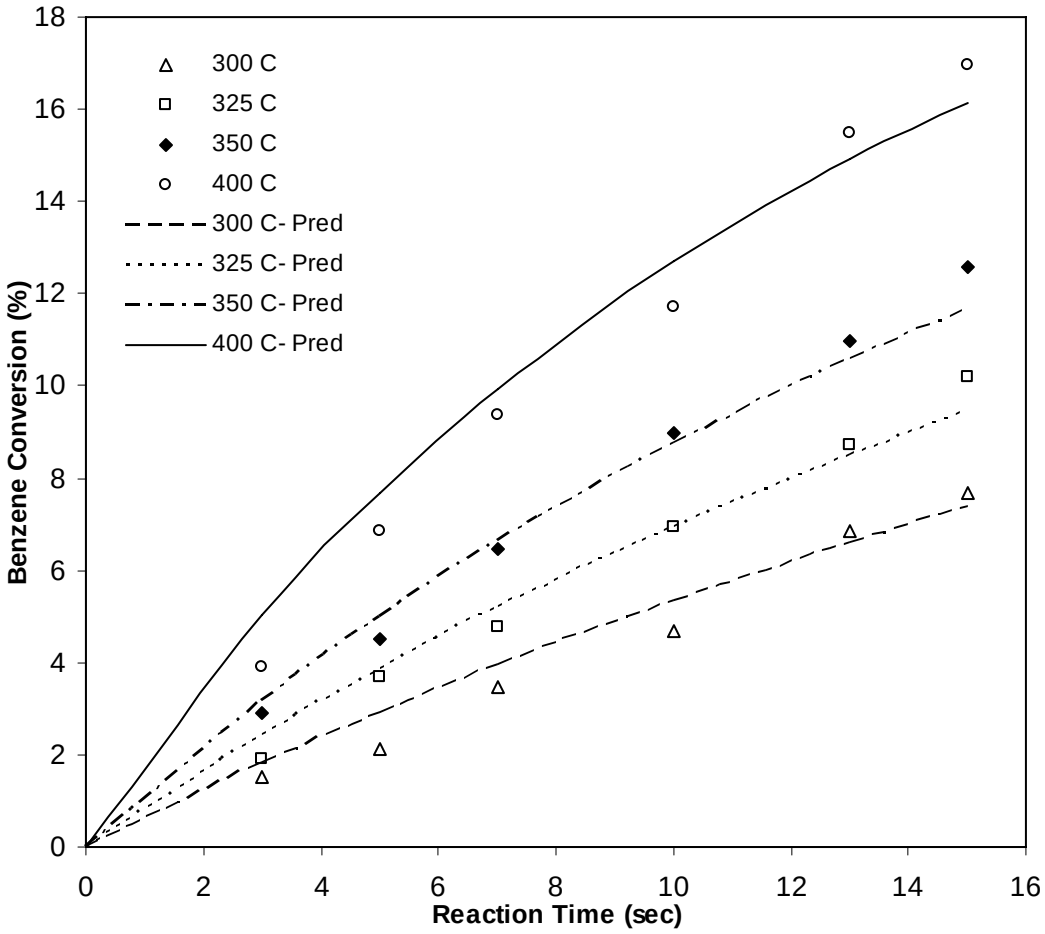

Figure 4.1 Variation of benzene conversion with different reaction conditions over ZSM-5 based catalyst

Benzene conversion was also observed over the precoked catalyst and it showed a similar dependence on temperature and reaction time as with the fresh catalyst, however, the values were slightly lower than those obtained over the fresh catalyst. Fig. 4.2 compares benzene conversion over the fresh and precoked catalyst at temperatures of 350 and 400^0C for reaction times of 5, 10, and 15sec. From Fig. 4.2, it can be seen that, at both 350 and 400^0C and a reaction time of 10s, less than 25% decrease was noticed in the benzene conversion between the fresh and precoked catalyst. However, conversion reduces to less than 17% at a reaction time of 15s, for both 350 and 400^0C. The mild effect of catalyst precoking on benzene conversion is an indication that coke deposit was restricted to the external surface of the catalyst without interfering much with the acid sites within the pores of the catalyst where alkylation largely takes place. The slight reduction in benzene conversion can be linked to the reduction of the total number of active sites due to partial deactivation and also due to problems of benzene diffusion, which may occur as a result of a possible blockage of some of the pore openings of the catalyst by the relatively larger molecules of 1,3,5-TIBP.

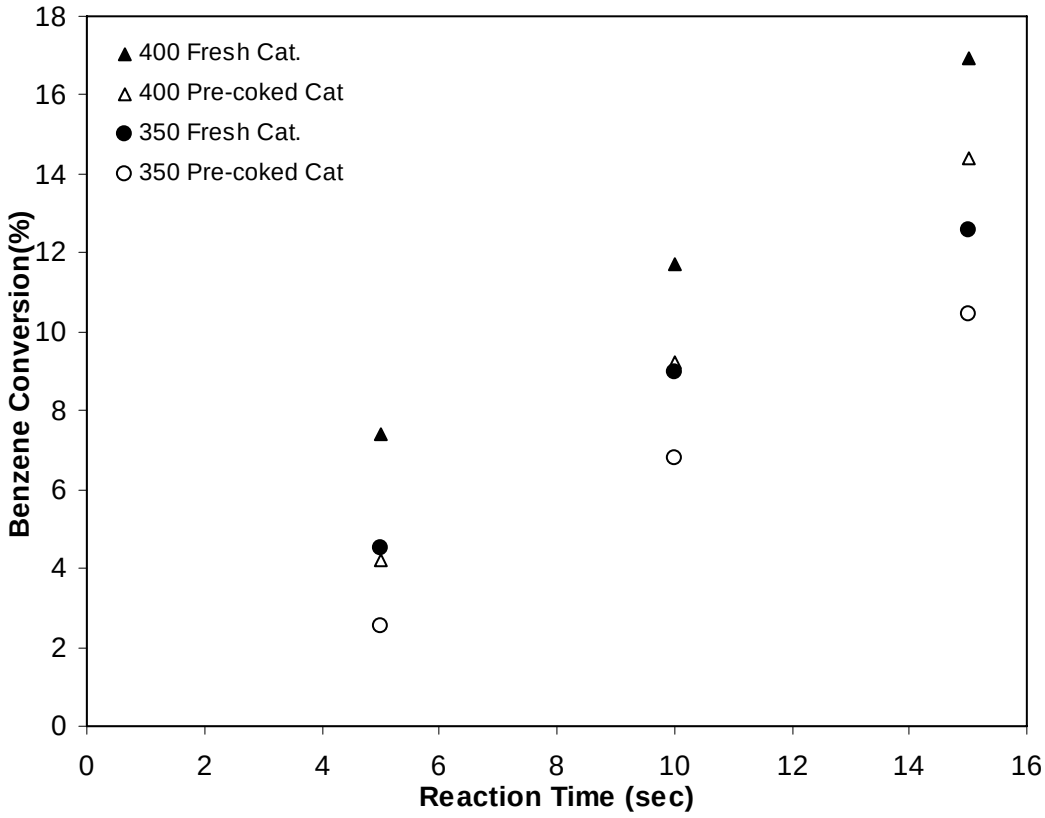

Figure 4.2 Comparison of benzene conversions for fresh and precoked catalyst

The effect of benzene conversion on ethylbenzene and diethylbenzene selectivity at 400^0C is given in Fig. 4.3. Diethylbenzene shows a high dependence on benzene conversion and was noticed to increase as benzene conversion increases. Ethylbenzene on the other hand, also shows a high dependence on benzene conversion, but was observed to decrease as benzene conversion increases.

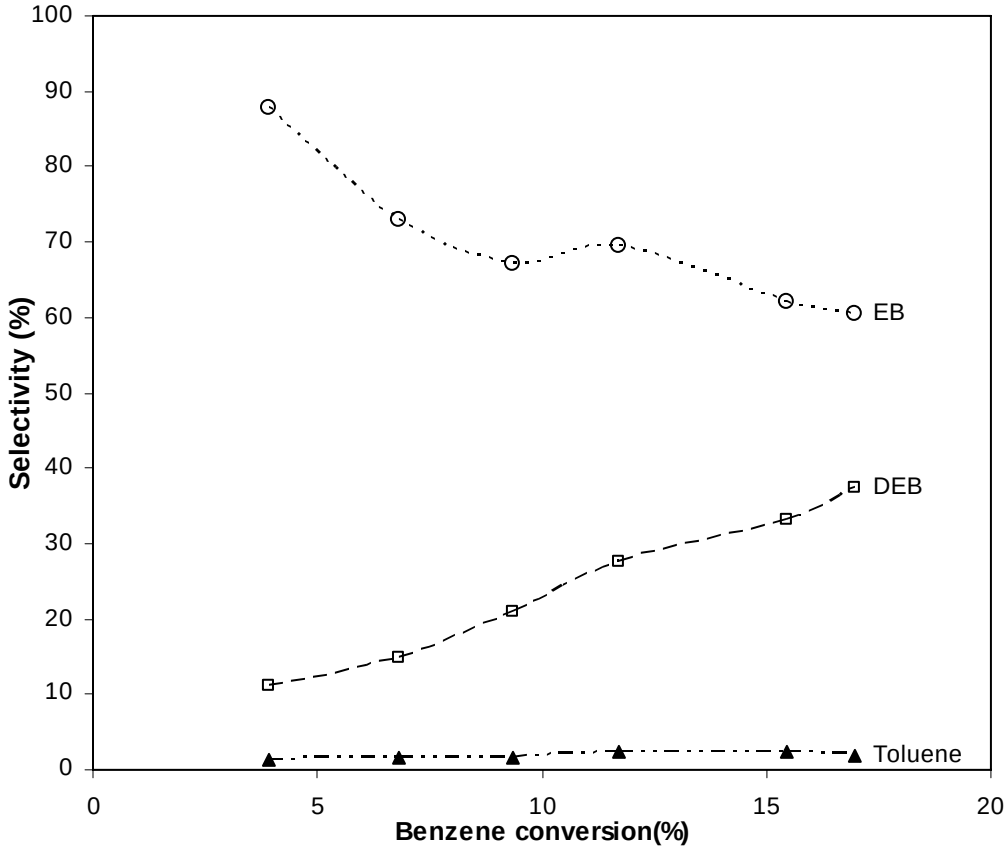

Figure 4.3 Effect of benzene conversion on products selectivity

4.1.3. Effect of feed mole ratio

The effect of feed mole ratios (benzene to ethanol) on benzene conversion, product selectivity and energies of activation were investigated over ZSM-5 based catalyst. Effect of benzene to ethanol mole ratio in the feed mixture on benzene conversion was studied by varying the ratio from 1:1 to 3:1 at 400^0C, for reaction times of 5, 10 and 15s. Table 4.1 presents the results of product selectivity over ZSM-5 based catalyst in the ethylation of benzene with ethanol with different feed mole ratios.

Table 4.2 Effect of feed ratio on products selectivity over ZSM-5

Performance	Feed ratio (benzene : Ethanol)		
	1:1	2:1	3:1
Benzene conversion	16.95	16.45	9.67
Selectivity (wt %)			
Ethylbenzene	60.41	81.61	86.69
Diethylbenzene	37.40	15.53	9.17
Others	2.19	2.86	4.14
Diethylbenzene isomers (%)			
Para	47.95	44.62	47.64
Meta	45.89	48.50	45.42
Ortho	6.15	6.88	6.94

Temperature = 400^0C, Reaction time = 15s.

Others: Toluene, xylene and unidentified compounds.

The conversion of benzene shows a significant decline with increasing feed mole ratio of benzene to ethanol from 1:1 to 3:1. The results are shown in Fig. 4.4. This is because most of the active sites of the catalyst surface were blocked by a large excess of aromatic reactant injected into the system. An increased dilution of ethanol by benzene, also account for the reduction in conversion. With increasing feed mole ratios of benzene to ethanol, the opportunity of benzene attacked by ethyl cations are reduced, and then a lower benzene conversion is obtained. This is in agreement with the findings of Levesque and Dao [20], in which the author reported similar drop for conversion of benzene over steamed-treated ZSM-5 zeolite catalyst. With an increase in the ratio of benzene to ethanol, the selectivity for ethylbenzene is improved at the expense of diethylbenzene. About ~44% increase in the selectivity of EB was noticed by increasing the feed mole ratio from 1:1 to 3:1 at 400^0C, for a reaction time of 15s. On other hand, selectivity of DEB decreased from ~37.40 to 9.17, representing a 75% decrease. The observed trend in the selectivity of the EB and DEB is consistent with the work of Levesque and Dao [20] during the alkylation of benzene over steamed-treated ZSM-5 zeolite and chryso-zeolite ZSM-5 based catalyst. The increase of feed mole ratios (benzene/ethanol) results in an increase of the primary alkylation and decrease of the secondary alkylation reaction.

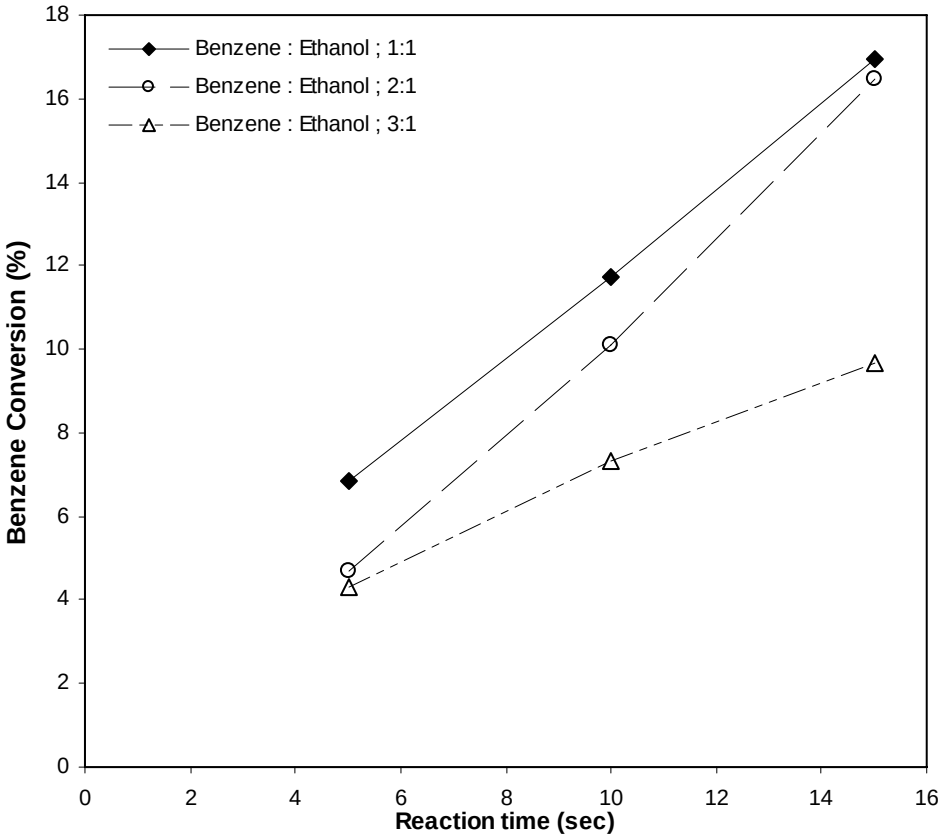

Figure 4.4 Effect of feed mole ratio (benzene to ethanol) on benzene conversion at 400^0C

4.1.4 Ethylbenzene yield and EB /DEB yield

As shown in Fig. 4.5, ethylbenzene yield, similarly to benzene conversion, increased with both reaction time and temperature over the fresh catalyst. A maximum yield of ~10.24% was achieved at 400^0C at 16.95% benzene conversion. This corresponds to an ethylbenzene selectivity of ~60.41%. Similarly, Fig. 4.6 shows diethylbenzene yield with reaction time and temperature over the fresh catalyst. From the fig., it is observed that diethylbenzene yield increased with both reaction time and temperature over the fresh catalyst. The highest diethylbenzene yield of ~ 6.34% was achieved at 400^0C at 16.95% benzene conversion, corresponding to a diethylbenzene selectivity of ~ 37.40%. Fig. 10 shows the variation of the ratio of ethylbenzene yield to the yield of diethylbenzene with temperature for a reaction time of 15s. It is observed from the figure that, as temperature was increased from 300 to 400^0C, the ratio of ethylbenzene yield to that of DEB decreased constantly, indicating that the secondary ethylbenzene alkylation with ethanol to produce diethylbenzene is highly sensitive to temperature.

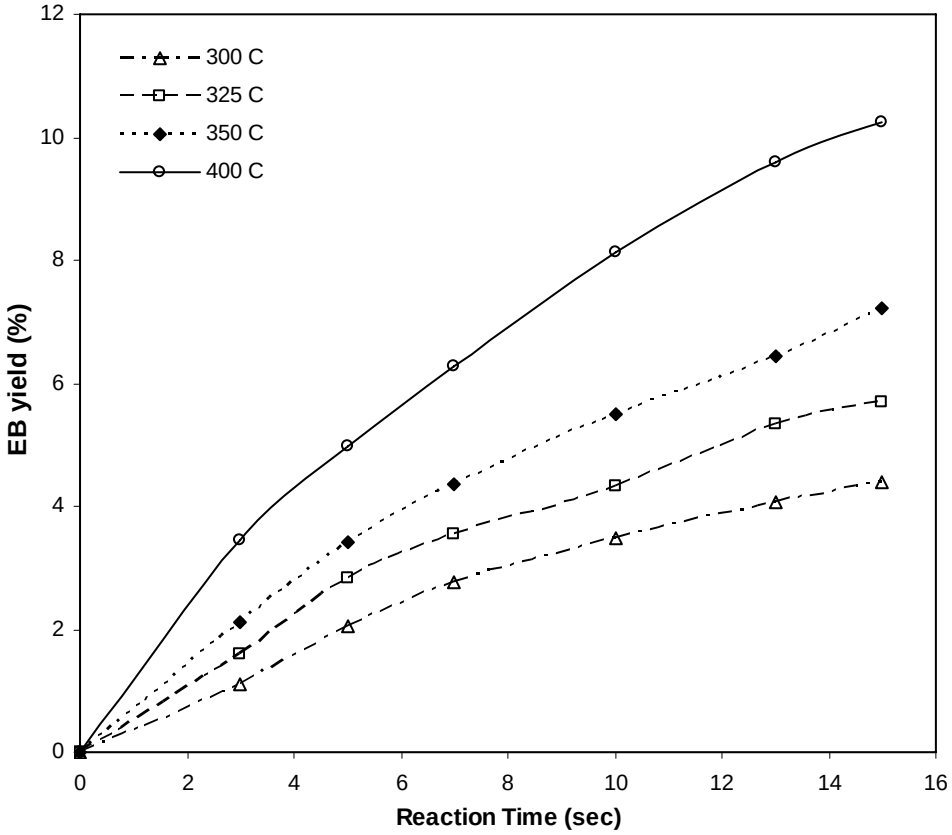

Figure 4.5 Variation of ethylbenzene yield with reaction conditions

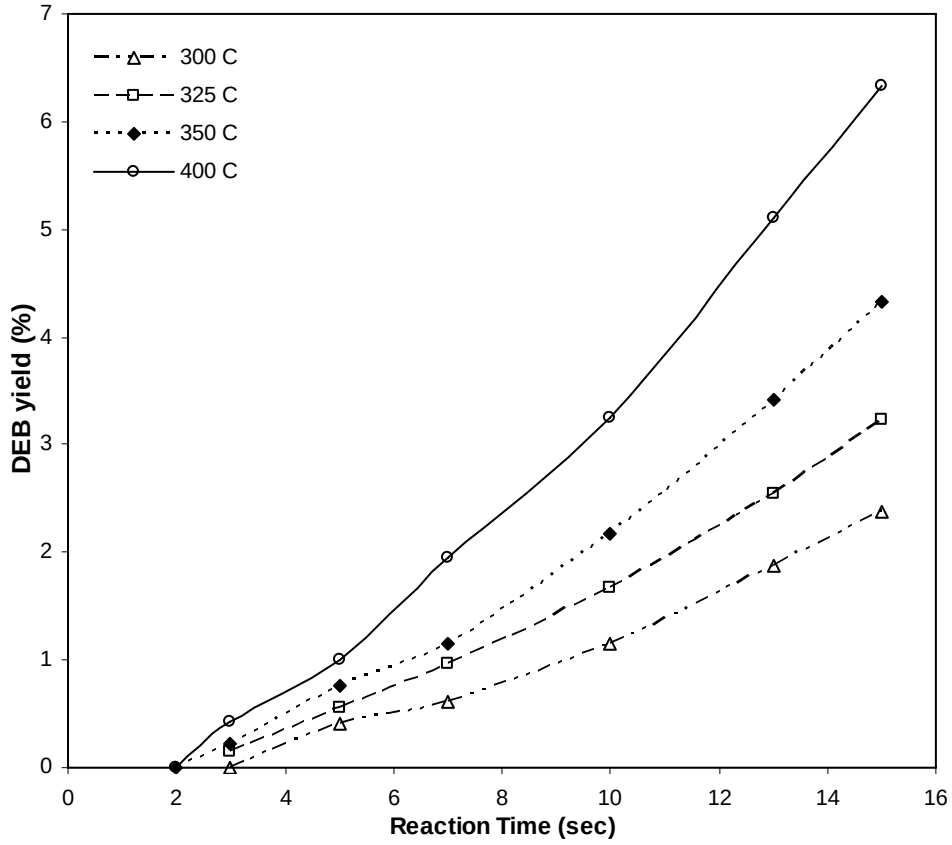

Figure 4.6 Variation of diethylbenzene yield with reaction conditions

Fig. 4.7 shows the variation of the ratio of ethylbenzene yield to the yield of diethylbenzene with temperature for a reaction time of 15s. It is observed from the figure that, as temperature was increased from 300 to 400^0C, the ratio of ethylbenzene yield to that of DEB decreased constantly, indicating that the secondary ethylbenzene alkylation with ethanol to produce diethylbenzene is highly sensitive to temperature.

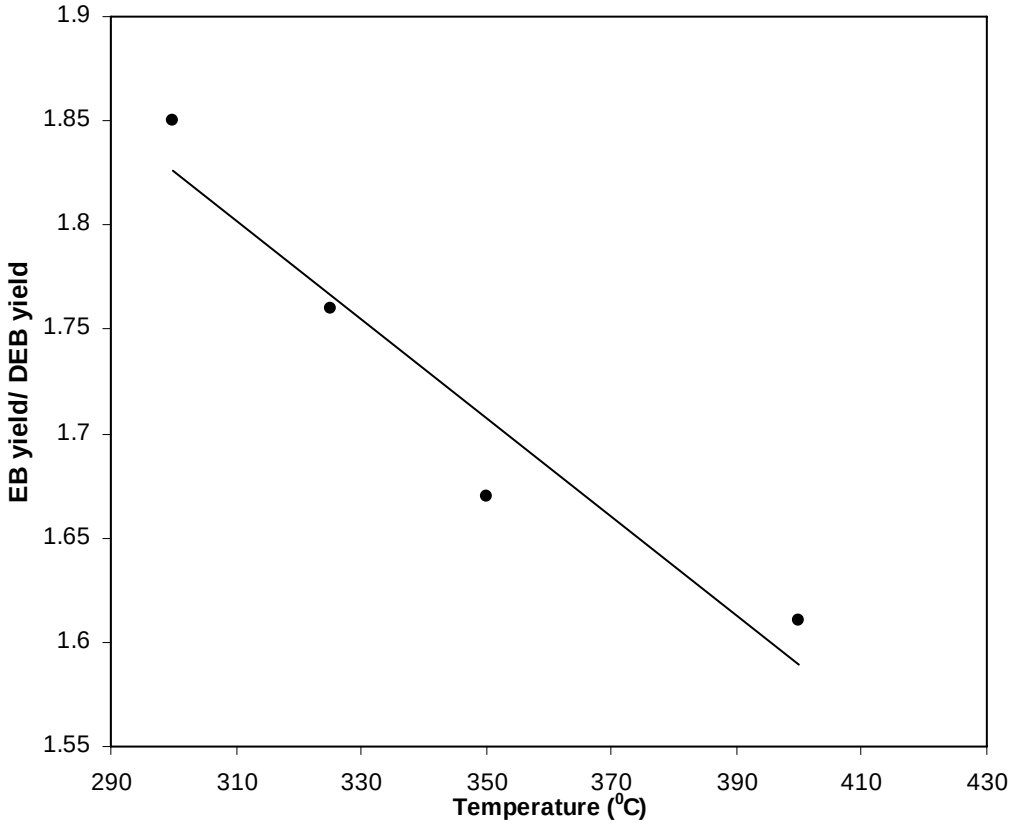

Figure 4.7 Variation of EB yield / diethylbenzene yield with temperature

4.1.5. para-DEB/ortho-DEB (P/O) ratio

Table 4.3 shows the variation of the reaction products for para, meta and ortho isomers. All the three isomers of diethylbenzene were detected in the GC analysis of the reaction product. However, the para-isomers were in higher proportion than the other isomers at all the conditions investigated in this study. Raj et al. [22], had reported that the critical diameter of p-isomer is smaller than meta, which implies that para isomers diffuse out of the pores faster than the bulky meta isomers, leading to greater para selectivity. The ortho isomer is not formed in significant amount in the ethylation reactions over ZMS-5 due to steric hindrance and low density of acid sites on external surface.

Table 4.3 Product distribution of benzene ethylation over the fresh ZSM-5catalyst at 400 and 350^{0}C, benzene/ethanol ratio =1:1

Temperature (^{0}C)	Time (s)	Yield (%)							Benzene Conversion (%)	P/O
		Ben.	Eth.	EB	m-DEB	p-DEB	o-DEB	T-DEB		
Fresh catalyst 400	5	58.60	30.16	5.15	0.42	0.45	0.14	1.12	6.84	3.21
	10	55.53	25.19	8.13	1.45	1.61	0.19	3.24	11.72	8.47
	15	52.24	21.07	10.24	2.91	3.04	0.39	6.34	16.95	7.79
300										
	5	60.07	32.07	3.41	0.30	0.41	0.04	0.75	4.50	10.25
	10	57.24	26.53	6.31	0.75	1.34	0.09	2.17	8.99	14.89
	15	55.00	20.99	7.22	1.76	2.38	0.19	4.33	12.56	12.53

Figure 4.8 shows the variation of P/O ratios with reaction time at different temperatures. As can be seen from the figure, there is significant decrease in the P/O ratio as the temperature is increased. At 350^0C, P/O ratio was found to increase with reaction time up to 10s, but a sharp decrease in P/O ratio was noticed as the reaction time was further increased to 15s. The observed decrease of P/O ratio as temperature was increased from 350 to 400^0C can be explained in terms of the effect of temperature on strength of adsorption of ethylbenzene and ethyl cation on the catalyst surface. The mechanism of the ethylation of ethylbenzene with ethanol was studied by Vijayaraghavan et al.[7] , they reported that the formation of p-DEB would require reaction between ethylbenzene in the vapor phase and ethyl cation on the catalyst surface while formation of m-DEB would require reaction between co-adsorbed ethylbenzene and ethyl cation on the catalyst surface. At lower temperature, most of the ethylbenzene is in the vapor state without much adsorption. Rajesh et al. [59] reported that when ethylbenzene in the vapor state approaches the layer of ethyl cations on the catalyst surface, it can better use its para position for electrophilic attack to produce p-DEB, as its ortho position offers little steric hindrance and the meta position demand high activation energy for electrophilic attack.

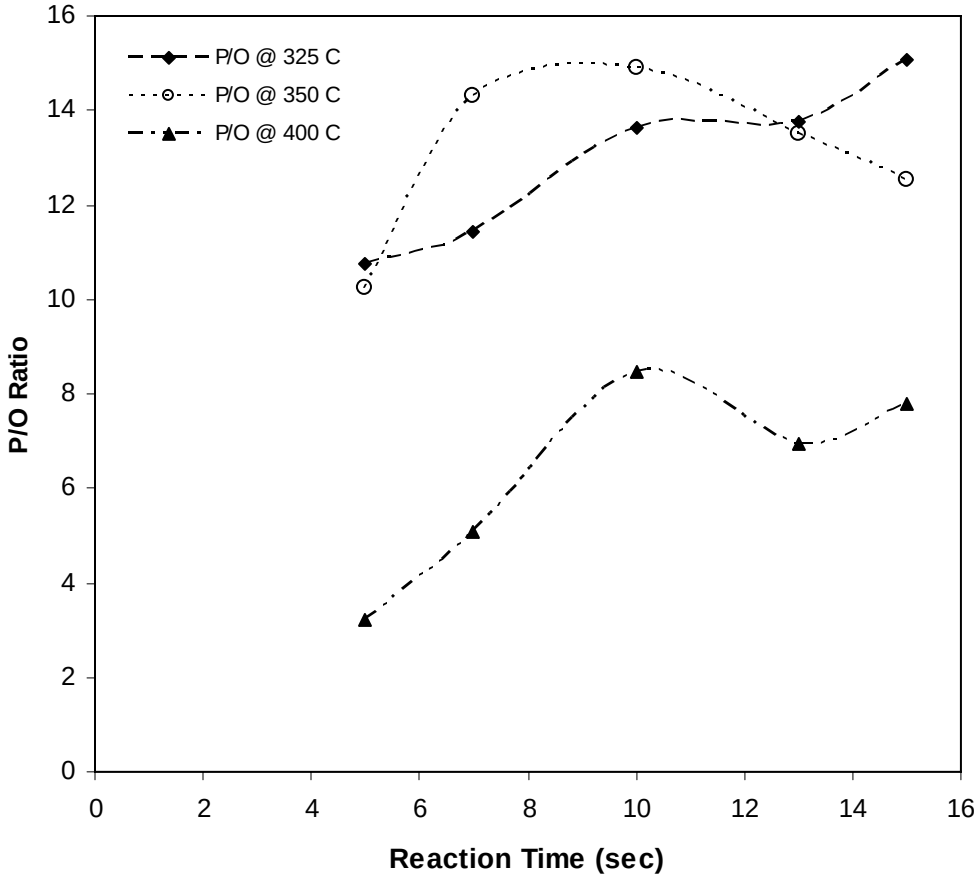

Figure 4.8 Variation of P/O with reaction time at different temperatures

It is well-known that a post synthesis modification of the HZSM-5, such as impregnation with coke deposition, can improve para-selectivity dramatically [60]. Catalyst precoking was observed to have a significant effect on the P/O ratio. This is due to the partial deactivation of the external active sites, which are responsible for the undesirable isomerization of the p-DEB formed in the pores of the catalyst into the other isomers. The ratio of p- to o-DEB (P/O) for the fresh and precoked catalyst at 350 and 400^0C for a benzene conversion of 10%, is presented in Fig. 4.9. It can be seen from this figure that, at 350^0C, the P/O ratio increased from ~ 14.14 to ~ 17.80, representing an increase of 26%. The effect of catalyst precoking became more visible at 400^0C, with P/O increasing from ~6.80 to ~ 16.12, representing a 137% increase. It is evident from this figure that, for all the reaction conditions studied, P/O was found to be much higher than the equilibrium value, which was reported by Halgeri [61] to be ~1.875.

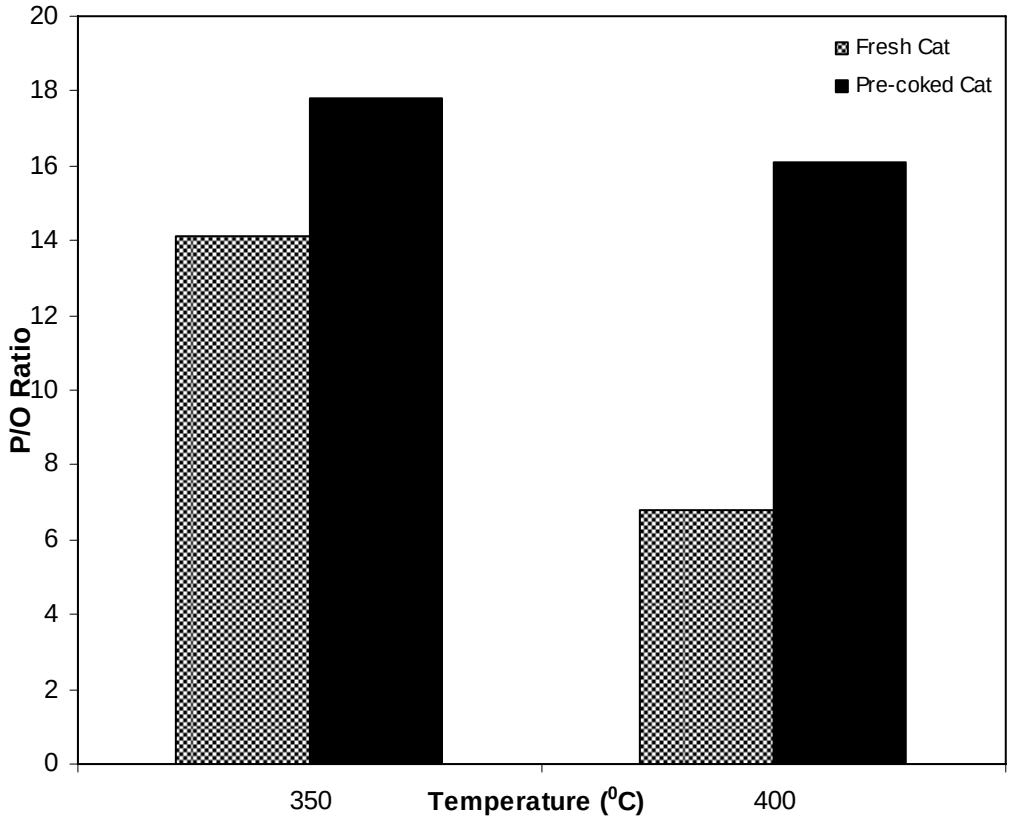

Figure 4.9 Effect of catalyst precoking on P/O ratio

4.1.6. Coke content measurement

Cokes are mainly responsible for the deactivation of catalysts. The coke formation in zeolite has been widely studied [62] and depends on the size and shape of the space available near the active sites as well as the diffusion path of the organic molecules in the pores of zeolites. Coke was also measured at different conditions. Table 4.4 reveals the amount of coke deposition. It is clear that the ratio of coke weight percent to percent conversion is very small, ranging from 0.015 and 0.028 at all reaction conditions. This implies that the ethylation of benzene with ethanol over ZSM-5 based catalyst is not accompanied by appreciable coke deposition.

Table 4.4 Coke formation for benzene ethylation with ethanol at different reaction conditions

Temp (^{0}C/time (s)		Conversion (%)	Coke (wt %)	Coke/ conv.
350	5	4.50	0.127	0.028
	10	8.99	0.150	0.017
	15	12.56	0.227	0.018
400	5	6.84	0.149	0.022
	10	11.72	0.213	0.018
	15	16.95	0.247	0.015

4.1.7 Kinetic modeling

4.1.7.1 Model development

The experimental results were modeled using catalyst deactivation function based on two different models. One of the catalyst activity decay model was based on time-on-stream (TOS), while the other was based on reactant conversion (RC) model.

4.1.7.2 Catalyst activity decay function based on time-on-stream (TOS).

The catalyst activity decay model based on time-on-stream was initially suggested by Voorhies [63]. This model, the so called "time on stream" model (TOS) was also successfully tested, for the ethylation of ethylbenzene with ethanol [64]. To develop a suitable kinetic model representing the overall ethylation of benzene, the reaction network shown in Scheme 1 is used. The following set of species balances and catalytic reactions can be written:

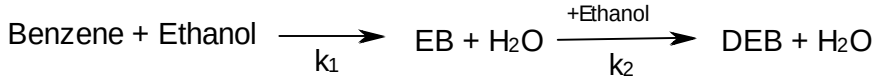

Scheme 1

Rate of disappearance of benzene

$$-\frac{V}{W_c}\frac{dC_{BZ}}{dt} = \eta k_1 C_{BZ} C_E \exp(-\alpha t) \tag{4.1}$$

Rate of formation of ethylbenzene

$$\frac{V}{W_c}\frac{dC_{EB}}{dt} = \left(\eta k_1 C_{BZ} C_E - \eta k_2 C_{EB} C_E\right)\exp(-\alpha t) \tag{4.2}$$

Rate of formation of diethyl benzene

$$\frac{V}{W_c}\frac{dC_{DEB}}{dt} = \eta k_2 C_{EB} C_E \exp(-\alpha t) \tag{4.3}$$

The measurable variables from our chromatographic analysis are the weight fraction of the species, $y_{x,}$ in the system. By definition the molar concentration, c_x of every species in the system can be related to its mass fraction, y_x by the following relation:

$$c_x = \frac{y_x W_{hc}}{V\, MW_x} \tag{4.4}$$

Where W_{hc} is the weight of feedstock injected into the reactor, MW_x is the molecular weight of specie x in the system, V is the volume of riser simulator, t = time, α = catalyst decay constant and η = an effectiveness factor to account for the diffusion of benzene and ethanol into the pores of the catalyst. Benzene and ethylbenzene have almost the same critical molecular diameter, therefore a single effectiveness factor was considered for them. Substituting Eq. (4.4) into Eqs.(4.1) – (4.3), we have the following first order differential equations which are in terms of weight fractions of the species:

$$\frac{dy_{BZ}}{dt} = -\eta B_1 k_1 y_{BZ} y_E \frac{W_c}{V} \exp(-\alpha t) \tag{4.5}$$

$$\frac{dy_{EB}}{dt} = \left[\eta B_2 k_1 y_{BZ} y_E - \eta B_1 k_2 y_{EB} y_E\right] \frac{W_c}{V} \exp(-\alpha t) \tag{4.6}$$

$$\frac{dy_{DEB}}{dt} = \eta B_3 k_2 y_{EB} y_E \frac{W_c}{V} \exp(-\alpha t) \tag{4.7}$$

$B_{1,}$ B_2 and B_3 are lumped constants given below.

$$B_1 = \frac{W_{hc}}{VMW_E} \tag{4.8}$$

$$B_2 = \frac{MW_{EB} W_{hc}}{VMW_{BZ} MW_E} \tag{4.9}$$

$$B_3 = \frac{MW_{DEB} W_{hc}}{VMW_{EB} MW_E} \tag{4.10}$$

Equations (4.5) - (4.7) contain 5 parameters, k_1, k_2, E_1, E_2, and α, which are to be determined by fitting into experimental data.

The temperature dependence of the rate constants was represented with the centered temperature form of the Arrhenius equation, i.e.

$$k_i = k_{oi} \exp\left[\frac{-E_i}{R}\left(\frac{1}{T} - \frac{1}{T_o}\right)\right] \tag{4.11}$$

Since the experimental runs were done at 300, 325, 350 and 400^{0}C, T_0 was calculated to be 343.75^{0}C.

Where T_o is an average temperature introduced to reduce parameter interaction [65], k_{oi} is the rate constant for reaction i at T_o, W_c is the weight of catalyst and E_i is the activation energy for reaction i.

The above proposed model equations were based on the following simplifying assumptions:

(1) The ethylation of benzene for both molar ratios of benzene to ethanol (1:1 and 2:1), follows simple second-order kinetics. A third order kinetics was found not suitable for the 2:1 (benzene/ethanol) molar ratio.

(2) Catalysts deactivation is assumed to be a function of time on stream (TOS). And a single deactivation function was defined for all the reactions.

(3) Ethylation reactions were all assumed to occur via an irreversible reaction path. A similar assumption has been made by previous workers in the area [1, 5]

(4) Isothermal operating conditions can also be assumed given the design of the riser simulator unit and the relatively small amount of reacting species [40]. This is justified by the negligible temperature change observed during the reactions.

(5) A pseudo-first order reaction kinetic for all species involved in the reactions.

(6) Negligible thermal conversion.

(7) Since, benzene and ethylbenzene have almost the same critical molecular diameter, a single effectiveness factor was considered for them.

(8) The effectiveness factor η was taken to be unity. This is justified by the fact that p-xylene formed by catalytic reaction can easily escape via the pores of ZSM-5 [66], comparing benzene and ethylbenzene with almost the same critical diameter as p-xylene; negligible diffusion limitation is also expected in this reaction.

4.1.7.3 Catalyst activity decay function based on reactant conversion (RC)

The catalyst activity decay function can be conveniently expressed as a function of reactant converted. This meaningful deactivation function (reactant conversion model) was proposed by de Lasa [67]. The following set of species balances and catalytic reactions can be written based on the reaction network shown in Scheme 1.

Rate of disappearance of benzene

$$-\frac{V}{W_C}\frac{dC_{BZ}}{dt} = \eta k_1 C_{BZ} C_E \varphi \tag{4.12}$$

Rate of formation of ethylbenzene

$$\frac{V}{W_c}\frac{dC_{EB}}{dt} = \left(\eta k_1 C_{BZ} C_E - \eta k_2 C_{EB} C_E\right)\varphi \tag{4.13}$$

Rate of formation of diethyl benzene

$$\frac{V}{W_c}\frac{dC_{DEB}}{dt} = \eta k_2 C_{EB} C_E \varphi \tag{4.14}$$

Where η is the effectiveness factor and $\varphi = \exp(-\lambda(1 - y_{BZ})$ represents catalyst deactivation based on reactant converted (RC) model proposed by de Lasa [67]. This type of model has been reported to incorporate a sound mechanistic description of catalyst deactivation [68], and also allows for changes of chemical species without extra requirement of measuring the coke concentration [67]:

$$k_i = k_{oi} \exp\left[\frac{-E_i}{R}\left(\frac{1}{T} - \frac{1}{T_o}\right)\right] \tag{4.15}$$

Where T_o is the average reaction temperature introduced for re-parameterization of kinetic constants [65]:

Substituting Eq. (4.4) into Eqs.(4.12) – (4.14), we have the following first order differential equations which are in terms of weight fractions of the species:

$$\frac{dy_{BZ}}{dt} = -\eta B_1 k_1 y_{BZ} y_E \frac{W_c}{V} \exp(-\lambda(1 - y_{BZ})) \tag{4.16}$$

$$\frac{dy_{EB}}{dt} = \left[\eta B_2 k_1 y_{BZ} y_E - \eta B_1 k_2 y_{EB} y_E\right]\frac{W_c}{V} \exp(-\lambda(1 - y_{BZ})) \tag{4.17}$$

$$\frac{dy_{DEB}}{dt} = \eta B_3 k_2 y_{EB} y_E \frac{W_c}{V} \exp(-\lambda(1 - y_{BZ})) \tag{4.18}$$

B_1, B_2 and B_3 are lumped constants given in equations (4.8), (4.9) and (4.10) above. Similar assumptions made for the proposed model equations in catalyst activity decay function based on time-on-stream (TOS) are also applicable in this model.

Equations (4.16) - (4.18) contain 5 parameters, k_1, k_2, E_1, E_2, and λ which are to be determined by fitting into experimental data.

4.1.7.4 Determination of model parameters

The kinetic parameters k_{0i}, E_i, and α for the ethylation reaction for both benzene to ethanol molar ratios of 1:1 and 2:1 were obtained by fitting experimental results into the rate equations (4.5)-(4.7) using nonlinear regression (MATLAB package). The values of the model parameters along with their corresponding 95% confidence limits (CLs) are shown in Tables 4.5 and 4.6 (TOS model), while the resulting cross-correlation matrices are also given in Tables 4.7 and 4.8. From the results of the kinetic parameters presented in Table 4.5, it is observed that catalyst deactivation for the feed mole ratio of 1:1 (benzene/ethanol) was found to be small, α = 0.025, indicating low coke formation in agreement with the data shown in Table 4.4, indicating very low coke yield. It can also be observed from Tables 4.5 and 4.6 that E_1 for the feed mole ratio of 1:1 (benzene/ethanol) is higher than the E_1 for the feed mole ratio of 2:1 (benzene/ethanol), which indicates that the activation energy required to attach activated ethyl cations to an activated benzene molecules as a result of benzene ethylation for the feed mole ratio of 1:1 is higher than that for 2:1 (benzene/ethanol) by 4–5kJ/mol. Furthermore, it was also noted that the activation energy for the ethylation of ethylbenzene (E_2) for the feed mole ratio of 2:1 is higher than the E_2 for the feed mole ratio of 1:1 (benzene/ethanol). This can be easily

understood as the increased dilution of ethanol by benzene reduces the accessibility of EB to yield subsequent alkylated products.

Table 4.5 Estimated kinetic parameters based on time on stream (TOS-model) Feed ratio = 1:1 (benzene: ethanol)

Parameters	k_1	k_2	α (1/s)	r^2
Ei (kJ/ mol)	34.69	9.53	0.0250	0.99
95% CL	0.59	1.43	0.0035	
k_{0i} X 10^4 (m3/ (kg of cat. s))	0.170	1.118		
95% CL x 10^4	0.004	0.033		

[a] Pre-exponential factor as obtained from eq.4.11 ; unit for second order (m^6 /kg of catalyst.s).

Table 4.6 Estimated kinetic parameters based on time on stream (TOS-model) Feed ratio = 2:1 (benzene: ethanol)

Parameters	k_1	k_2	α (1/s)	r^2
E_i (kJ/ mol)	29.95	11.03	0.0925	0.99
95% CL	2.71	8.62	0.0146	
k_{0i} X 10^4 (m3/ (kg of cat. s))	0.153	0.627		
95% CL x 10^4	0.018	0.099		

[a] Pre-exponential factor as obtained from eq.4.11 ; unit for second order (m^6 /kg of catalyst.s).

Table 4.7 Correlation matrix for benzene ethylation (TOS model) (feed ratio = 1:1 (benzene: ethanol))

	k_1	E_1	α
k_1	1.0000	-0.2205	0.9461
E_1	-0.2205	1.0000	-0.1230
α	0.9461	-0.1230	1.0000

Table 4.8 Correlation matrix for ethylbenzene ethylation (TOS model) (feed ratio = 1:1 (benzene: ethanol))

	k_2	E_2	α
k_2	1.0000	-0.3331	0.7932
E_2	-0.3331	1.0000	-0.0517
α	0.7932	-0.0517	1.0000

Next, a nonlinear regression involving equations (4.16) – (4.18), the same experimental data as used with the TOS model and three adjustable parameters was considered using MATLAB software. Table 4.9 reports the parameters obtained while the resulting cross-correlation matrices are also given in Tables 4.10 and 4.11. Based on the parameters obtained with the RC model in Table 4.9, it goes to show the accuracy and soundness of the kinetic parameters obtained using the TOS model. Table 4.7, shows the very low correlations between k_1 and E_1 and E_1 and α and the moderate correlation between k_1 and α. Similar to Table 4.7, Table 4.8, reports the very low correlations between k_2 and E_2 and E_2 and α and the moderate correlation between k_2 and α. Table 4.10, shows the low correlation between k_1 and E_1 and a moderate correlation between E_1 and λ, while Table 4.11, reports the low correlations between k_2 and E_2 and E_2 and λ and the moderate correlation between k_2 and λ. It can be observed that in the cross-correlation matrices presented in this study, most of the coefficients remain in the low level with only a few exceptions.

Table 4.9 Estimated kinetic parameters based on reactant conversion (RC-model) Feed ratio = 1:1 (benzene: ethanol)

Parameters	k_1	k_2	λ
E_i (kJ/ mol)	32.28	8.59	2.083
95% CL	0.92	1.91	0.739
k_{0i} X 10^3 (m3/ (kg of cat. s))	0.0085	0.0553	
95% CL x 10^3	0.0025	0.0167	

[a] Pre-exponential factor as obtained from eq.4.11 ; unit for second order (m^6 /kg of catalyst.s).

Table 4.10 Correlation matrix for benzene ethylation (RC model) (feed ratio = 1:1 (benzene: ethanol))

	k_1	E_1	λ
k_1	1.0000	0.6526	0.9900
E_1	0.6526	1.0000	-0.6601
λ	0.9900	-0.6601	1.0000

Table 4.11 Correlation matrix for ethylbenzene ethylation (RC model) (feed ratio = 1:1 (benzene: ethanol))

	k_2	E_2	λ
k_2	1.0000	0.3191	0.9846
E_2	0.3191	1.0000	-0.3552
λ	0.9846	-0.3552	1.0000

Table 4.12 shows the comparison between the previously reported energies of activation for benzene ethylation and that of the present study. From the results of the activation energies presented in Table 4.12, it is observed that, value of our activation energy for benzene ethylation is lower than the one reported by Barman et al. [1] who obtained an apparent energy of activation of 56kJ/mol for alkylation of benzene over cerium exchanged NaX zeolite catalyst. Barman et al. [1] investigations were carried out in a fixed-bed reactor at much lower temperatures of 225 – 275^{0}C. Similarly, Sridevi et al. [5] reported an apparent activation energy of 60.03kJ/mol for alkylation of benzene with ethanol over $AlCl_3$ impregnated 13X zeolites catalyst in a fixed-bed reactor but at much higher temperatures of 400 – 450^{0}C.

Table 4.12 Activation energies at different reaction conditions

References	Activation Energy (kJ/mol)	Catalyst	Reactor	Benzene to Ethanol molar ratio.	Temperature Range.
Sridevi et al.[5]	60.03	$AlCl_3$ impregnated13X zeolite.	Fixed-bed.	3:1	400 – 450^{0}C.
Barman et al.[1]	56.00	Cerium exchanged NaX zeolite.	Fixed-bed.	3:1	225 – 275^{0}C.
Present Study.	34.69	ZSM-5 zeolite.	Fluidized-bed.	1:1	300 – 400^{0}C.

It is important to point out the significant difference between the activation energies for benzene ethylation (34.69kJ/mol and 29.95kJ/mol) and ethylbenzene ethylation to form diethylbenzene (9.53kJ/mol and 11.03kJ/mol) for both molar ratios. However, this is not unexpected because it is consistent with the observation made by Kaeding [69] that alkylation, dealkylation and disproportionation reactions of long substituted benzenes generally occur with greater ease compared to their shorter substituted counterparts. This is also in agreement with the observation made by Al-Khattaf et al. [70] in their study of catalytic transformation of three methylbenzenes (toluene, m-xylene and 1,2,4-trimethylbenzene) over USY-based FCC zeolite catalyst in a riser simulator. They noticed that the sequence of reactivity of the alkylbenzenes decreases as the number of methyl group per benzene ring decreases.

To check the validity of the estimated kinetics parameters for use at conditions beyond those of the present study, the fitted parameters were substituted into the comprehensive model developed for this scheme and the equations were solved numerically using the fourth-order-Runge-Kutta routine. Graphical comparisons between experimental and model predictions for the time on stream model (TOS) based on the optimized parameters for scheme 1 are shown in Figure 4.1. It can be seen that the model predictions compared very well with the experimental data. Further comparisons between model predictions and experimental data also based on time on stream model are presented in Figs. 4.10 and 4.11. As observed in these plots, the model predictions compares favorably with the obtained experimental data for the various conditions, indicating the model can be used to accurately represent the experimental data following

the assumptions made, coupled with the peculiar nature of this process in the riser simulator. In addition, the reconciliation plot (Fig. 4.12) between the experimental data and the model predictions for the time on stream model, display a normal distribution of residuals, besides, the adequacy of the model and the selected parameters to fit the data as shown in Tables 4.5 and 4.6 gave 0.9921 regression coefficients.

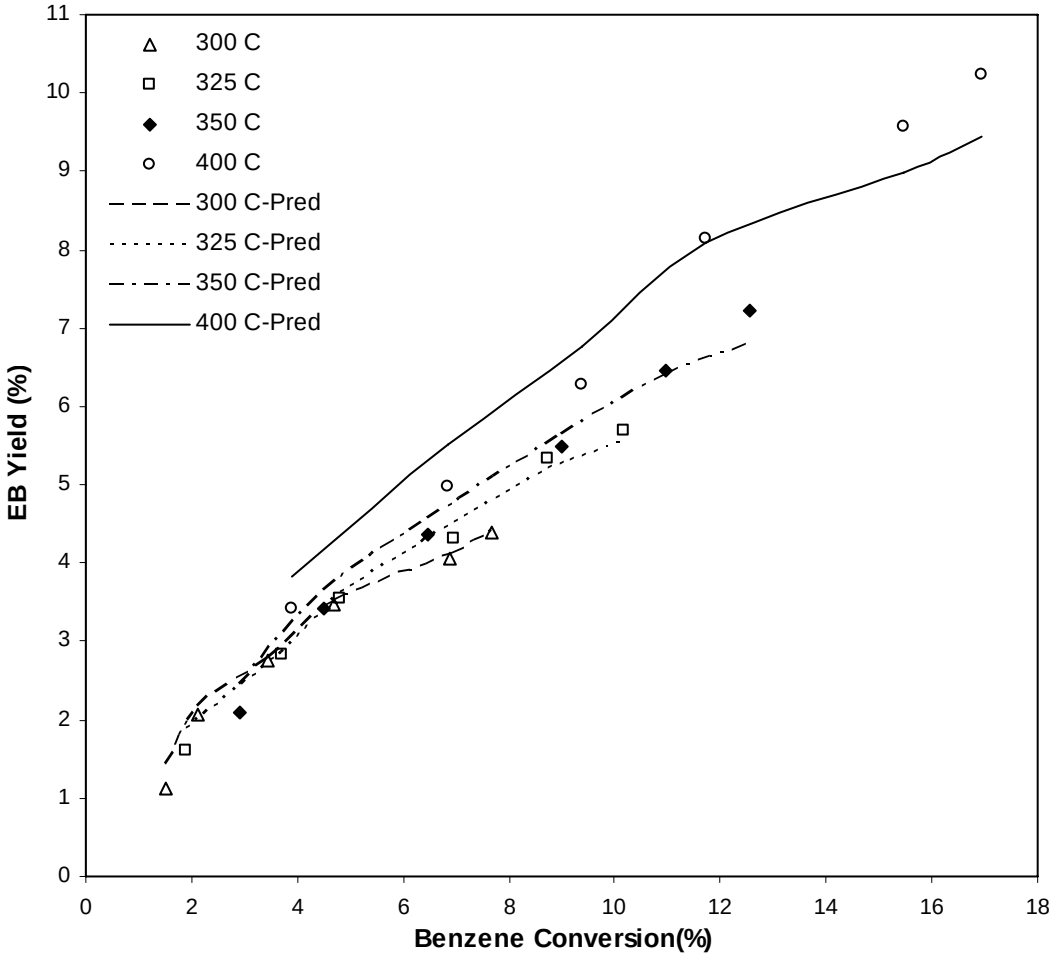

Figure 4.10 Ethylbenzene yield vs benzene conversion at various temperatures

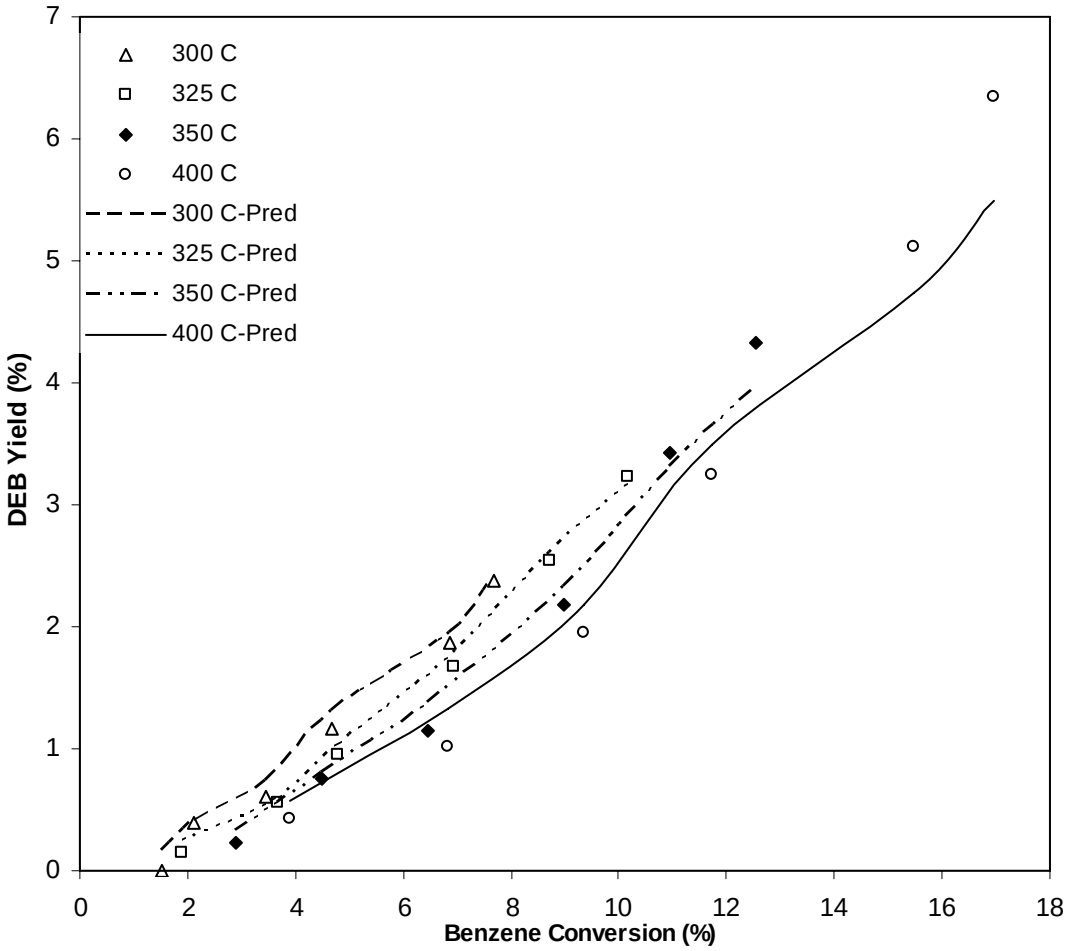

Figure 4.11 Diethylbenzene yield vs benzene conversion at various temperatures

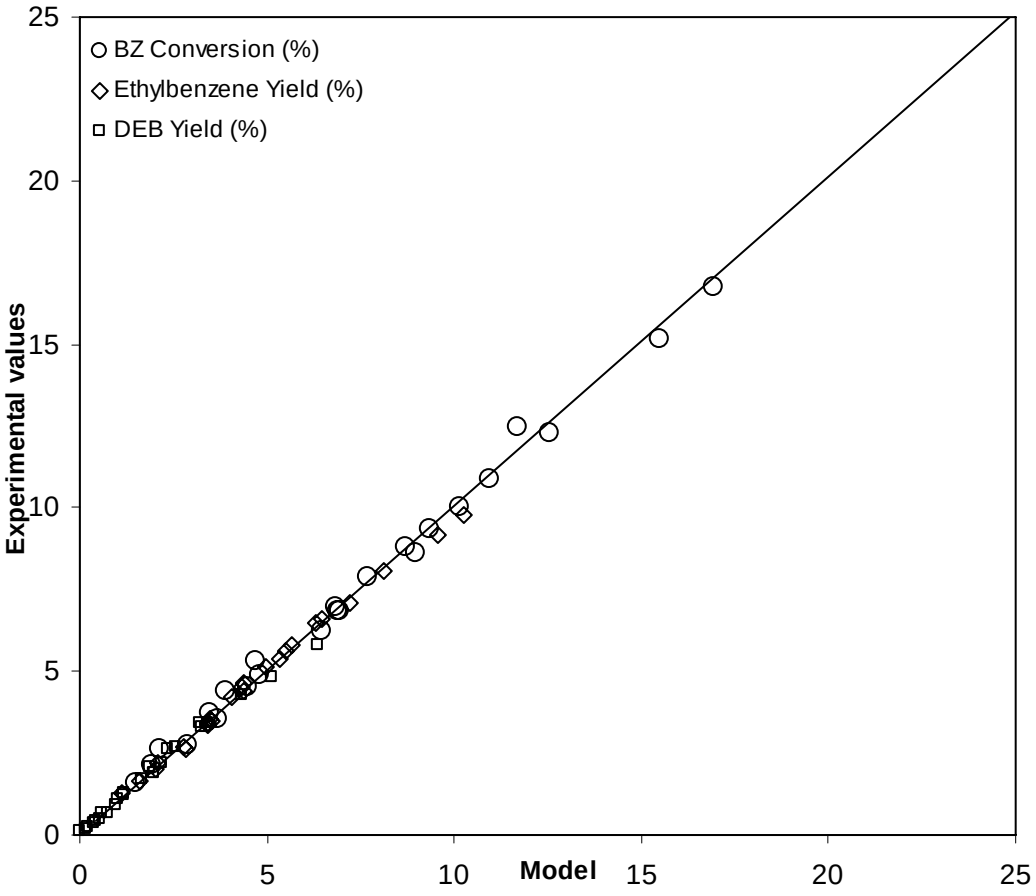

Figure 4.12 Overall comparison between the experimental results and model predictions

4.2. Benzene ethylation reaction over USY catalyst.

4.2.1. Catalyst Characterization.

The physicochemical properties of the catalysts used in this study are presented in Table 4.13. The total acidity for each catalyst was determined by NH_3 adsorption (TPD). Results are summarized in Table 4.13. It can be seen that USY-2 has 0.200 mmol/g acidity, which is about 6 times higher that of the USY-1 catalyst.

Table 4.13 Characterization of used catalysts

	USY-1	USY-2
Total acidty (mmol/g)	0.033	0.200
Unit cell size (Å)	24.28	24.45
SiO_2/Al_2O_3	31.7	10.5
Steamin temperature (^0C)	800	600
Steaming time (h)	6	2
BET surface area (m^2/g)	155	177
Na_2O (wt %)	Negligible	Negligible

4.2.2 Benzene ethylation reaction over USY-1 catalyst.

The ethylation of benzene with ethanol was carried out at 300, 350 and 400^0C over USY-1 catalyst for residence times of 3, 5, 7, 10, 13, and 15s with constant benzene to ethanol molar ratio of 1:1. Ethylation of benzene over USY-1 catalyst with SiO_2/Al_2O_3 ratio of 31.7 and 0.033mmol/g of acid sites gave negligible benzene conversion at all temperatures studied. The only product noticed over USY-1 catalyst was ethylbenzene in small amount, with negligible amounts of toluene and diethylbenzene at 400^0C for a reaction time of 15s. The insignificant benzene conversion observed over USY-1 catalyst, is as a result of low concentration of acid sites that is associated with this catalyst.

4.2.3. Benzene ethylation reaction over USY-2 catalyst.

4.2.3.1 Benzene conversion.

The ethylation of benzene with ethanol over USY-2 catalyst was studied at variable temperature ranges (300, 350, 400^0C) for residence times of 3, 5, 7, 10, 13, and 15s. The product distributions for benzene ethylation over USY-2 zeolite catalyst under the conditions of the present study were mainly ethylbenzene, toluene and diethylbenzene (Figure 4.13, Table 4.14). Traces of m-xylene and gaseous hydrocarbons (mainly ethylene) were also observed; however, the yields of these products were consistently very low and as a result were neglected in subsequent analysis. Ethylation reaction was observed to be the major reaction, while at elevated temperatures cracking reaction is also important. A possible reaction scheme to represent the observed products distribution is shown in Scheme 2. The primary reaction pathway is ethylation of benzene with ethanol to produce EB and water, while the formation of DEB indicates the secondary ethylation step of ethylbenzene with ethanol. Cracking reaction of DEB to produce ethylbenzene

(EB) and ethylene was also assumed due to appearance of increased cracking products at elevated temperatures.

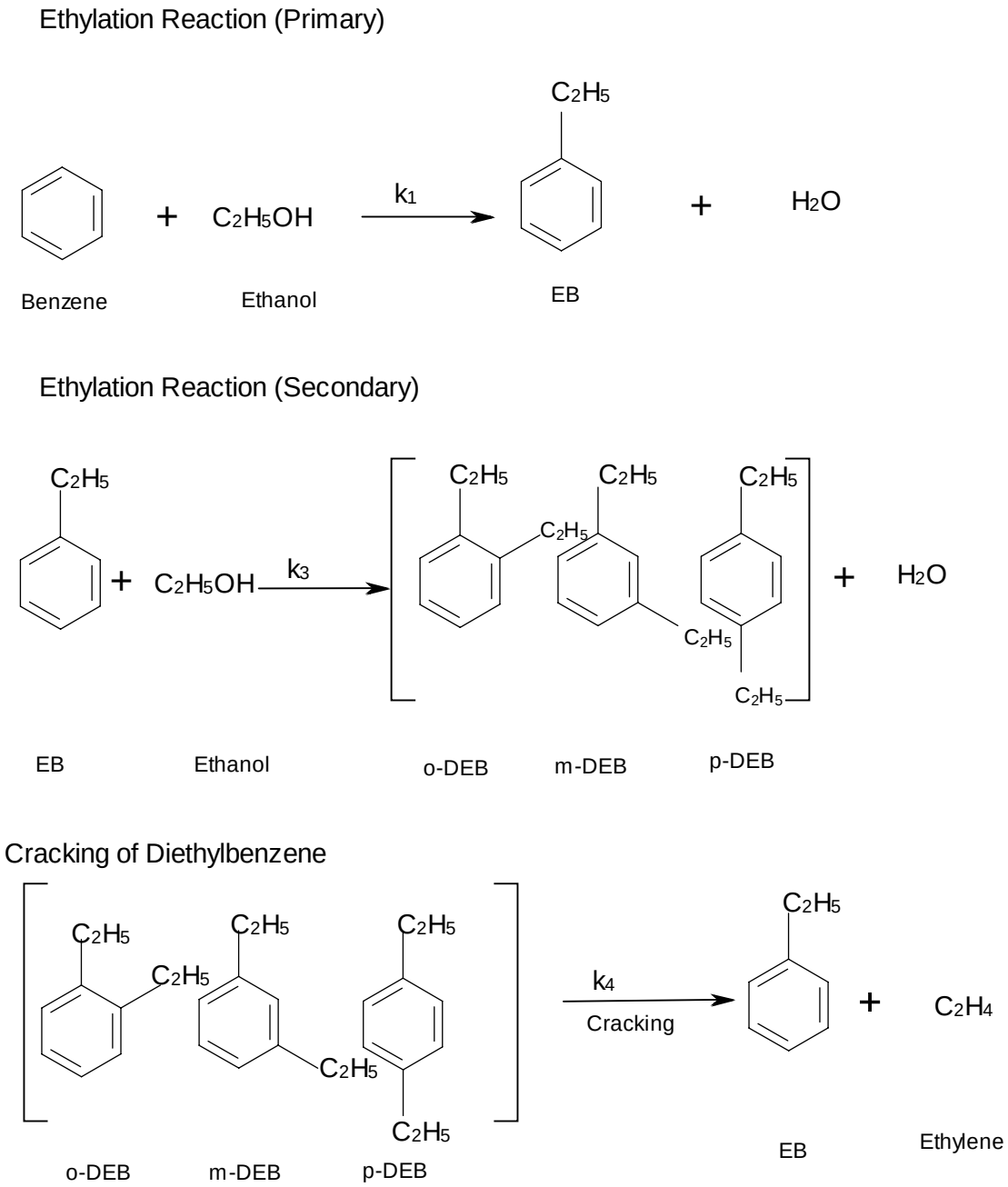

Figure 4.13 Reactions occurring during ethylation of benzene with ethanol over USY-2 catalyst

Table 4.14 Product distribution (wt %) at various reaction conditions for the ethylation of benzene over USY-2 catalyst

Temp (^{0} C)	Time (s)	Ben. Conv. (%)	EB	Toluene	m-DEB	p-DEB	o-DEB	Total DEB
300	5	2.00	1.44	0.07	0.29	0.15	0.05	0.49
	10	4.85	3.23	0.33	0.78	0.40	0.12	1.31
	15	8.16	5.15	0.67	1.38	0.60	0.22	2.29
400	5	3.57	1.78	1.29	0.19	0.10	0.03	0.33
	10	8.10	3.76	3.28	0.40	0.21	0.07	0.68
	15	12.13	5.39	5.03	0.55	0.27	0.09	0.92

The cracking of EB results in the formation of toluene. The cracking reaction involves the formation of 2 mol of toluene and 1 mol of ethylene from 2 mol of ethylbenzene (EB). The product distribution for USY-2 catalyst is given in Table 4.14. Benzene conversion was found to increase with reaction time and temperature, reaching a maximum of ~ 12.1% at 400^0C for a reaction time of 15s, as shown in Figure 4.14.

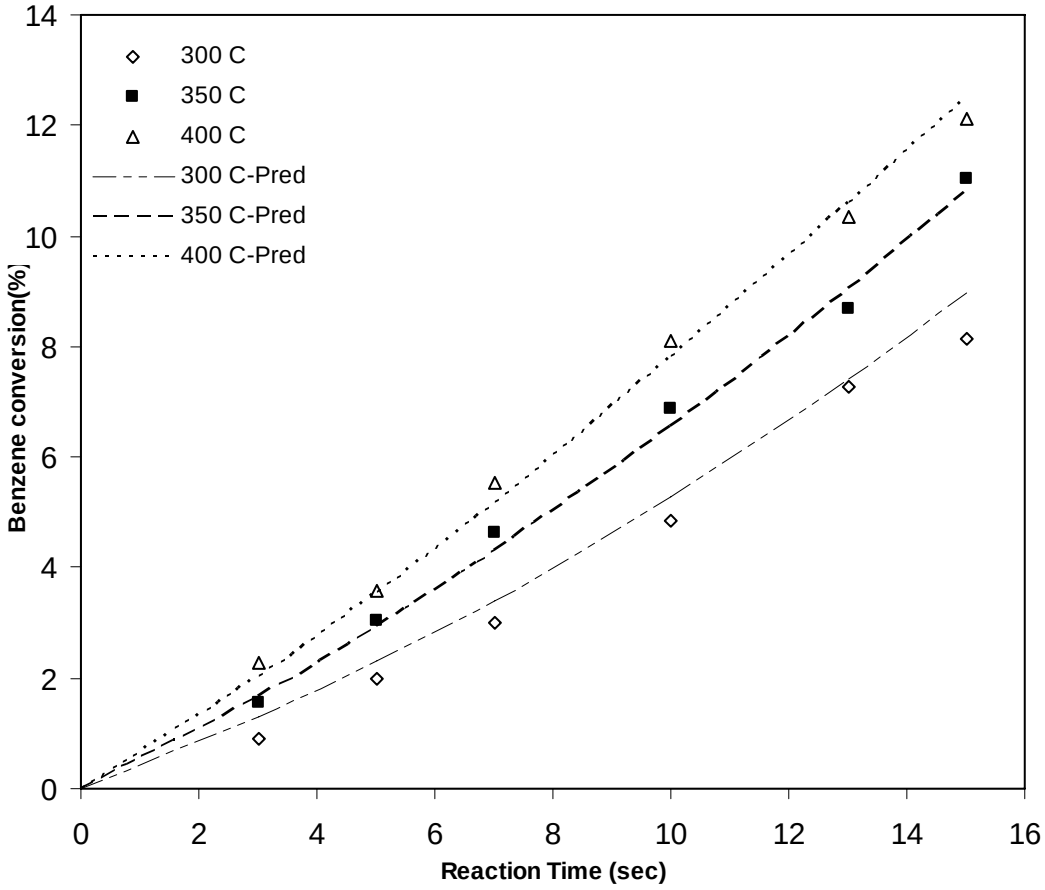

Figure 4.14 Conversion of benzene with respect to time at various temperatures

4.2.3.2. Ethylbenzene Selectivity.

The effect of temperature on ethylbenzene selectivity for a reaction time of 15s is shown in Figure 4.15. As shown in Figure 4.15, ethylbenzene selectivity decreased steadily with temperature over USY-2 catalyst to a minimum of ~ 44.4%. It is evident from the figure that, at 300^0C, less ethylbenzene cracking is occurring, with an ethylbenzene selectivity of ~62.9%. But as temperature was increased from 300 to 400^0C, more toluene was formed due to ethylbenzene cracking, leading to a decrease in the selectivity of ethylbenzene at higher temperature. This drop suggests that EB undergoes secondary reactions. Moreover, the simultaneous rise in the selectivity of toluene indicates that it is probably the products of such secondary reactions. Li et al. [71] observed similar drop in the selectivity of ethylbenzene over HZSM-5-200 and they reported that the decline in EB selectivity can be ascribed to the subsequent side reactions of EB.

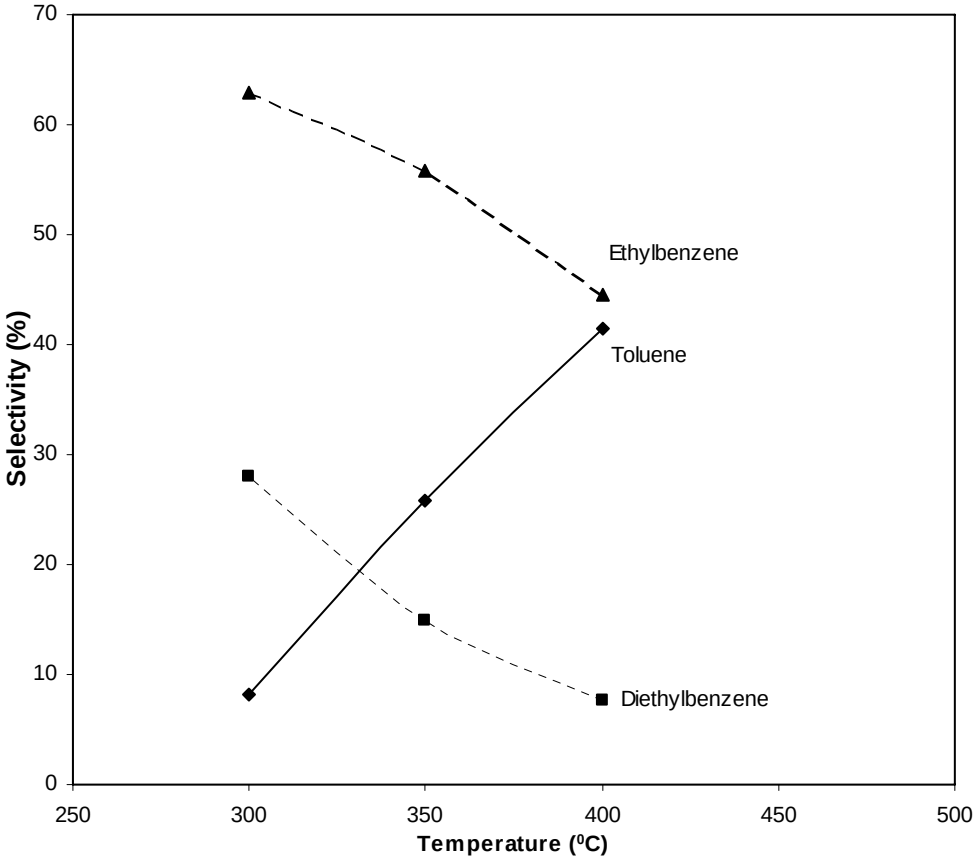

Figure 4.15 Selectivity of USY-2 catalyst as a function of temperature

4.2.3.3 Toluene Selectivity.

Figure 4.16 shows toluene selectivity with reaction time and temperature over USY-2 catalyst. Toluene selectivity shows a high dependence on temperature over USY-2 catalyst, showing a toluene selectivity rise from 6.85% to 23.58% and then to 40.43% for temperatures of 300, 350 and 400^0C, and for 10 s reaction time, respectively. The selectivity of toluene increased with increase in temperature. The substantial increase in toluene selectivity indicates that the EB formed undergoes cracking at higher temperature, leading to the significant increase in toluene formation at 350 and 400^0C. This is consistent with the observation made by Li et al. [72] that, toluene was found to increase significantly as temperature increases, indicating that higher temperature was favorable for the cracking of ethylbenzene to obtain toluene. Similar explanation was given by Gao et al. [21] when traces of toluene were found in the alkylation of benzene with ethanol over ZSM-5 based catalyst. They attributed the formation of toluene to the cracking of ethylbenzene over Bronsted acid sites.

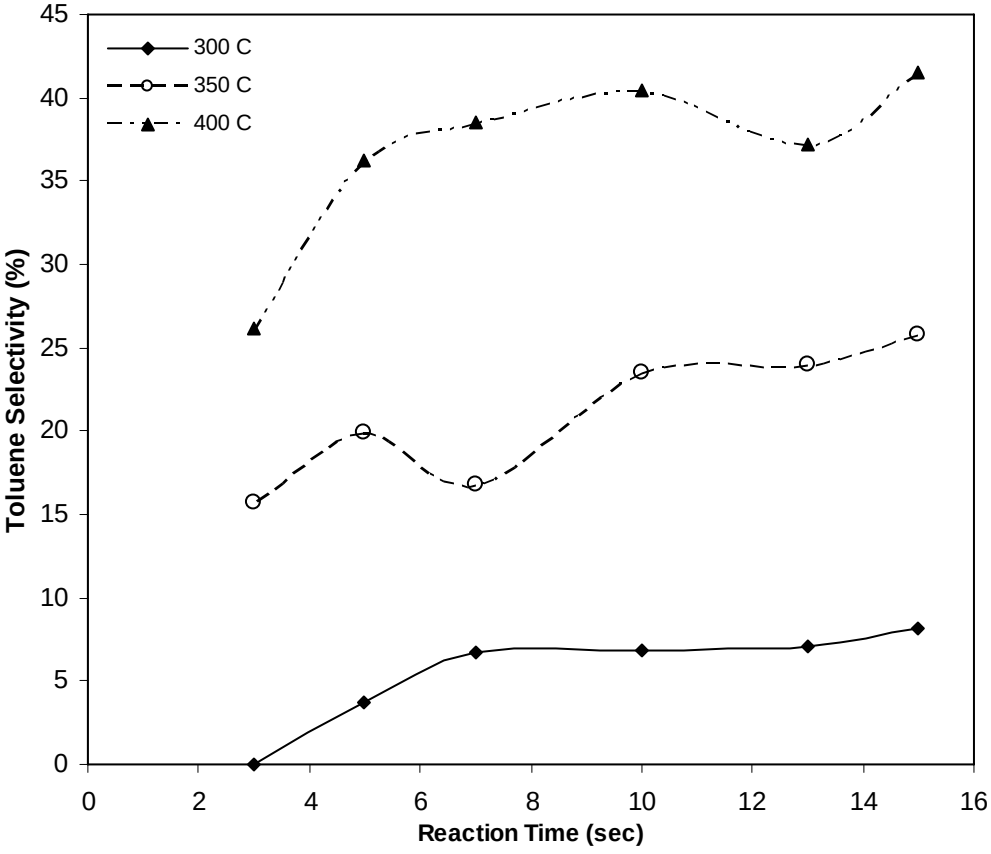

Figure 4.16 Variation of toluene selectivity with reaction conditions

In order to validate our argument that toluene is been formed from the cracking of EB, we carried out an investigation of EB alone over USY-2 catalyst at the same reaction conditions with that of the ethylation of benzene with ethanol over USY-2 catalyst. It was observed that, toluene selectivity of about 18.74% was obtained at 400^0C for a reaction time of 15s. Similarly, at 350^0C, toluene selectivity of about 10.61% was noticed for a reaction time of 15s.

The ratio of toluene yield to EB yield has been plotted versus benzene conversion for its ethylation reaction over USY-2 catalyst in Figure 4.17. The ratio is between 0.05 and 0.12 at 300^0C for the benzene ethylation over USY-2 catalyst. However, as temperature increases, the ratio increased from 0.12 to about 0.93 (i.e., 8 times more). Cracking of the ethylation product (EB) is responsible for the higher toluene-to-EB ratio at higher temperatures.

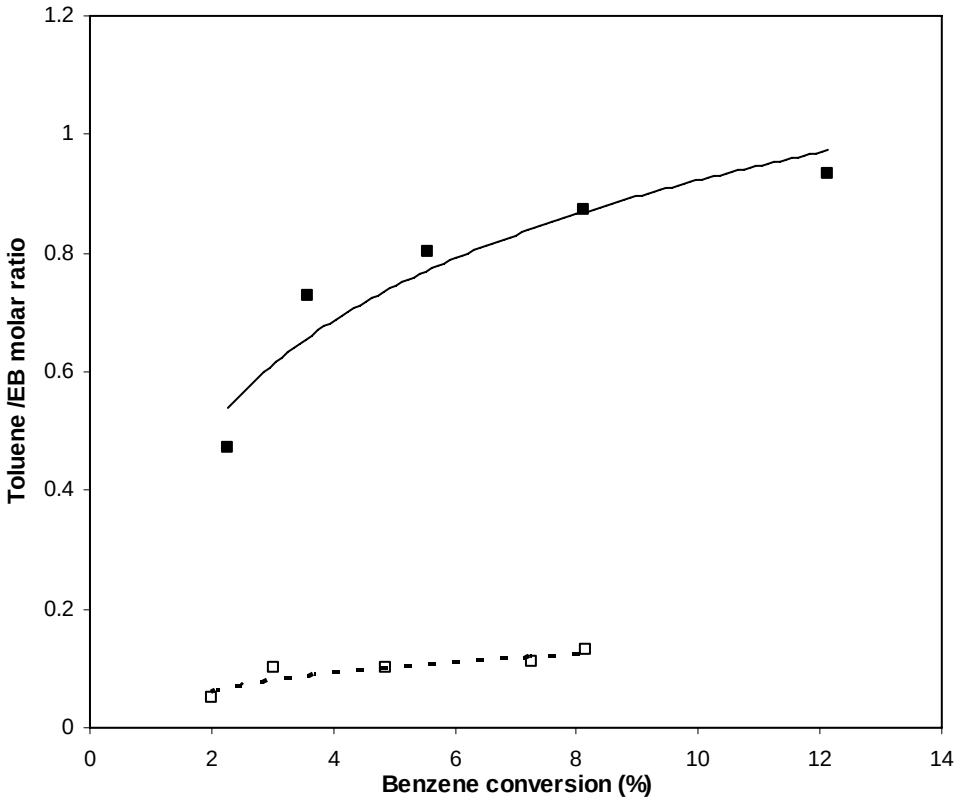

Figure 4.17 Toluene/EB ratio with benzene conversion at (□) 300^{0}C and (■) 400^{0}C.

4.2.3.4 Diethylbenzene Selectivity.

Figure 4.18 shows that the selectivity of diethylbenzene drops from 26.81% to 15.78% and then to 8.43% for the temperatures of 300, 350 and 400^{0}C for 10 s reaction time, respectively over USY-2 catalyst. It is evident from the Figure 4.18 that, less cracking of diethylbenzene (DEB) to EB is taking place at 300^{0}C, leading to higher selectivity of diethylbenzene at the lower temperature. The significant decrease in the selectivity of DEB at 350 and 400^{0}C indicates the cracking of DEB to produce ethylbenzene (EB) and ethylene.

Table 4.14 shows the distribution of the reaction products for para, meta and ortho isomers over USY-2 catalyst. Generally, in the case of zeolites this is strongly influenced by the channel geometry and the transport of individual isomers into channel structure. It is clear from the Table that, for all the reaction conditions investigated, meta-diethylbenzene was found to be higher than the para- and ortho-diethylbenzene in the ethylation reaction over USY-2 catalyst. However, this is not surprising because it is consistent with the observation made by Raj et al. [22] that medium pore zeolites exhibiting channels with dimensions of about 0.55nm have led to shape selectivity in the processing of alkyl aromatics, particularly with respect to para isomers of dialkyl aromatic hydrocarbons while large pore zeolites of the Y, Beta and MCM-22 do not exhibit para selectivity. It can be noticed from Table 2 that, for all the reaction conditions studied; P/O ratio was found to be between the range of ~2.73 and ~3.33, while the P/M ratio was observed to be between the range of ~0.43 and ~0.53. Kaeding [69] and Halgeri [61] reported that ethylation of ethylbenzene with ethylene/ethanol over ZSM-5 yields a thermodynamic equilibrium mixture of diethylbenzenes (DEBs) (para: meta: ortho = 30:54:16). This gives a P/O ratio of 1.875 and P/M ratio of 0.56. Therefore, the P/O ratios

for the EB ethylation reaction under the current experimental conditions are higher than the above equilibrium value, while the P/M is almost the same with the equilibrium value stated above.

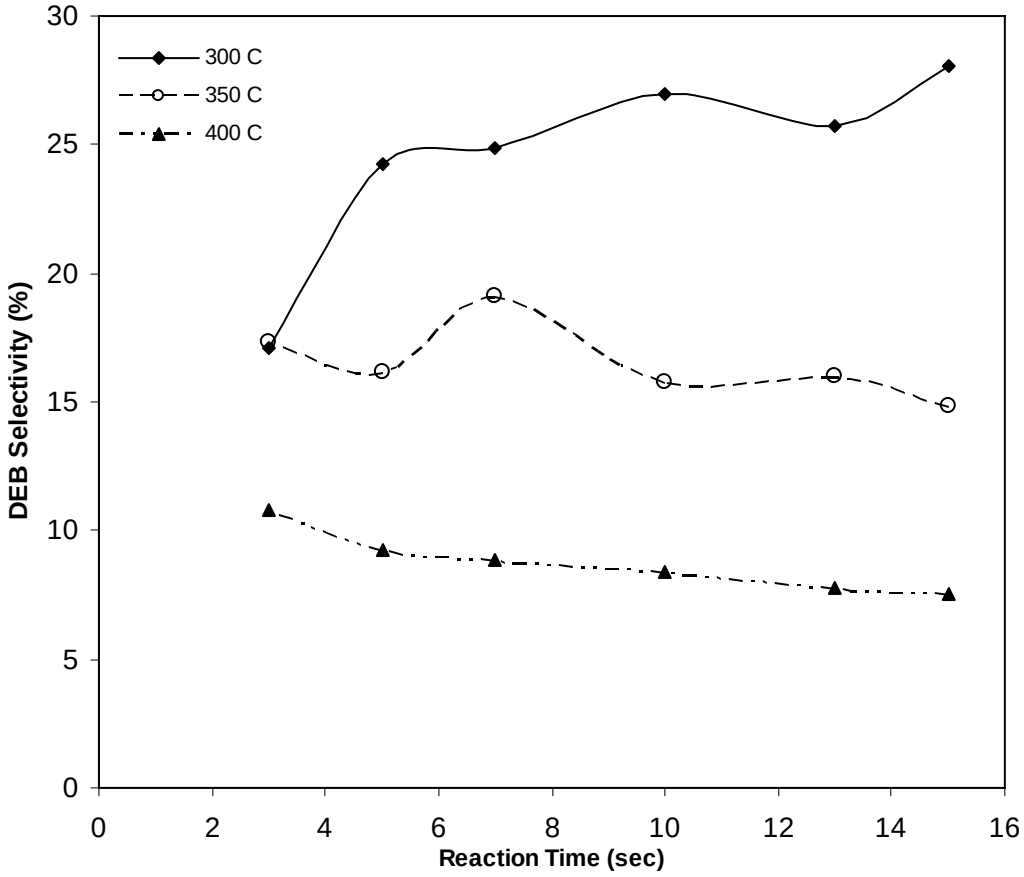

Figure 4.18 Variation of diethylbenzene selectivity with reaction conditions

4.2.3.5 Coke content measurement.

The coke formation in zeolite has been widely studied [62, 73] and depends on the size and shape of the space available near the active sites as well as the diffusion path of the organic molecules in the pores of zeolites. Coke formation can be consecutive or competitive to the reaction leading to the desired product [74]. Coke was also measured at different conditions. Table 4.15 reveals the amount of coke deposition for different reaction times. From the Table, it can be seen that, as reaction time increased from 5s to 15s, the coke increased from ~0.402 to ~ 0.887 at 400^0C. Similar increase was noticed at 350^0C. It has been reported that more coke is expected to be deposited on catalysts as the reaction time increases [74]. It is clear that ratio of coke weight percent to percent conversion is small, ranging from 0.073 to 0.132 at all reaction conditions. This implies that the ethylation of benzene with ethanol over USY-2 catalyst is not accompanied by substantial coke deposition.

Table 4.15 Coke formation for benzene ethylation with ethanol at different reaction conditions

Temp (^{0} C)	Time (s)	Convn. (%)	Coke USY-2 (wt %)	Coke (USY-2)/ Coke (ZSM-5)
350	5	3.03	0.400	3.150
	10	6.89	0.673	4.487
	15	11.03	0.805	3.546
400	5	3.57	0.402	2.698
	10	8.10	0.690	3.239
	15	12.13	0.887	3.591

4.3. Benzene ethylation reaction over USY-2 catalyst vs. results of ethylation reaction over ZSM-5 based catalyst

4.3.1 Benzene conversion.

Ethylation reaction of benzene with ethanol over ZSM-5 based catalyst was reported in our earlier publication [23]. The experimental results showed that the ethylation reaction is the main reaction. Benzene conversions are plotted versus reaction time in Figure 4.19 at 300, 350 and 400^0C. USY-2 catalyst and ZSM-5 based catalyst showed nearly the same benzene conversion at 300^0C. But as temperature was increased to 350 and 400^0C, a clear difference between the conversions was noticed. Benzene conversion of ~16.95% was obtained at 400^0C for a reaction time of 15s over ZSM-5 based catalyst with constant benzene to ethanol mole ratio of 1:1 as earlier reported in our recent publication [23]. This conversion is higher than the value obtained over USY-2 catalyst (12.13%) with the same benzene to ethanol mole ratio. The difference in benzene conversion noticed at 350 and 400^0C, is probably due to higher acid strength of ZSM-5 or the smaller crystal size of ZSM-5 based catalyst compared with that of USY-2 catalyst. This is in agreement with the observation made by Du et al. [52] that, the conversion of benzene is expected to increase clearly with an increase in catalyst acidity because strong acid sites were required for the activation of carbocations.

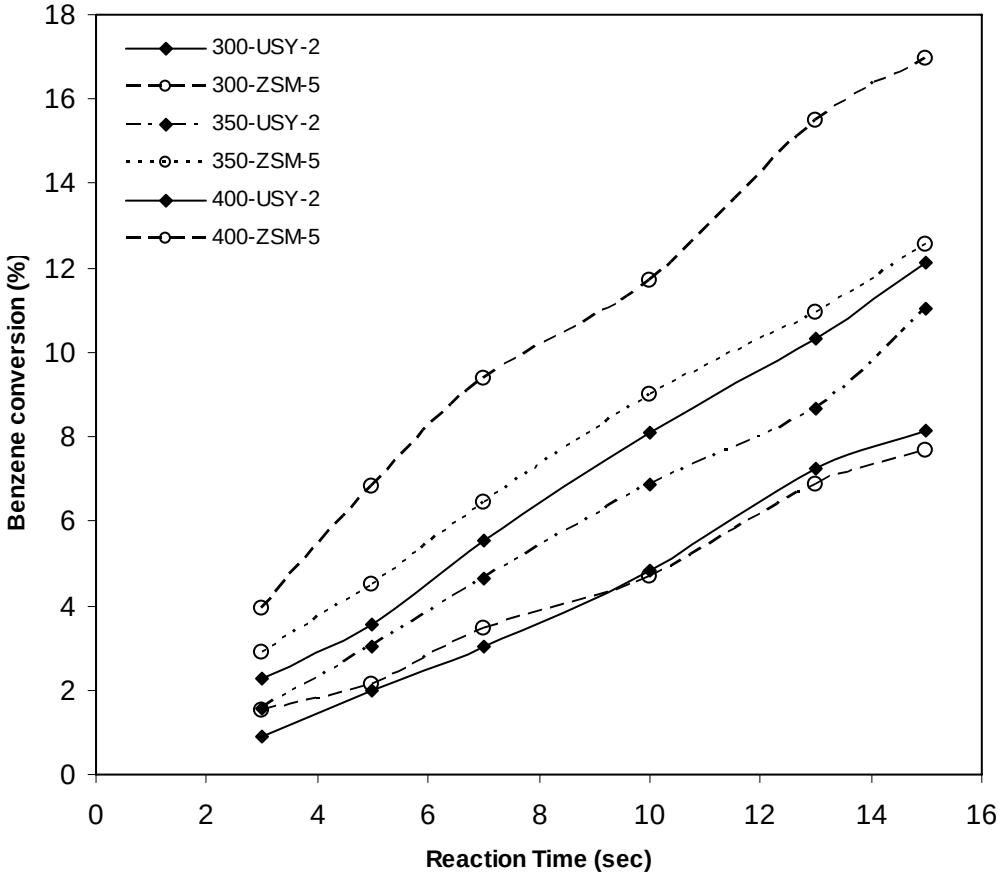

Figure 4.19 Benzene conversion vs. reaction time at 300, 350 and 400^{0}C on catalysts ZSM-5 (○) and USY-2 (◆)

4.3.2. Products distribution.

Two different reaction mechanisms were observed over USY-2 and ZSM-5 based catalysts, leading to the difference in products selectivity noticed over these catalysts. Ethylation of benzene over ZSM-5 based catalyst was observed to follow a series reaction, in which the ethylation of benzene with ethanol to produce EB represents primary reaction while the formation of DEB from ethylbenzene ethylation represents the secondary ethylation step. On the other hand, a more complex reaction mechanism was noticed in the ethylation reaction over USY-2 catalyst. The primary reaction pathway is ethylation of benzene with ethanol to produce EB and water. A parallel reaction was then found to occur at both high and low temperatures over this primary product (EB). Ethylbenzene ethylation to produce DEB was found to dominate at low temperature (300^0C), while cracking reaction producing toluene and ethylene becomes significant at higher temperatures. Cracking reaction of DEB to produce ethylbenzene and ethylene was observed at elevated temperatures, while further cracking of EB to produce toluene was also noticed at these temperatures. This is better depicted by the plot of the products selectivity versus reaction temperature for USY-2 catalyst (Figure 4.15). The selectivity of gaseous hydrocarbons (mainly ethylene) in the ethylation reaction over USY-2 catalyst was found to be ~7.57% at a constant conversion level of 12% at 400^0C compared to ~1.67% obtained in the ethylation reaction over ZSM-5, at the same benzene conversion. Similarly, a selectivity of ~7.37% was noticed at 350^0C over USY-2 compared to ~1.20% observed over ZSM-5, at a constant conversion level of 11%. This observation shows the extent of cracking of ethylation product noticed in the ethylation reaction over USY-2 catalyst compared with ZSM-5.

The product distribution during the ethylation of benzene at 400^0C over ZSM-5 and USY-2 catalyst is compared in Figure 4.20 at constant conversion level of 12%. The results showed that ethylbenzene has the highest yield over both catalysts. However, considerable amount of toluene was found in the ethylation of benzene with ethanol over USY-2 catalyst as compared to the negligible amount noticed over ZSM-5 based catalyst. Toluene selectivity is about 23 times more over USY-2 catalyst as compared to its selectivity with ZSM-5 based catalyst at 400^0C. All the three isomers of DEB were detected in considerable amount over both catalysts. For all temperatures investigated, meta-diethylbenzene was found to be higher than the para- and ortho-diethylbenzene in the ethylation reaction over USY-2 catalyst. However, for the ethylation reaction over ZSM-5 based catalyst, para-diethylbenzene was noticed to be higher than both the meta- and ortho-diethylbenzene. This observation is expected as USY-2 catalyst has been reported not to exhibit para selectivity as explained earlier.

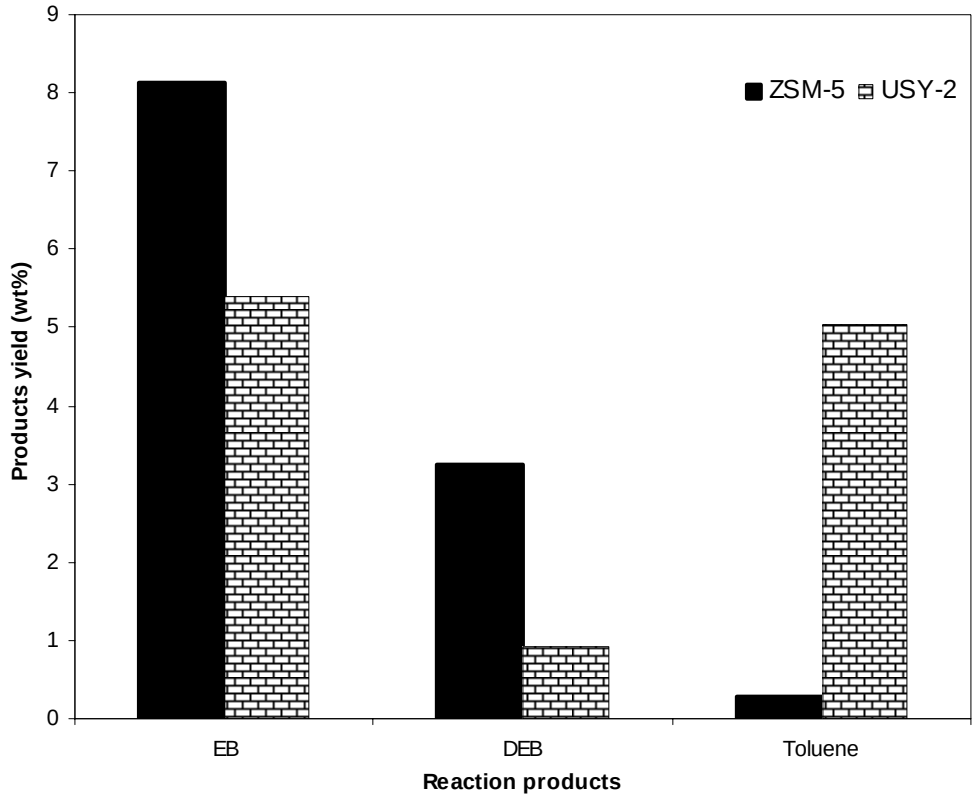

Figure 4.20 Product distribution of benzene ethylation over USY-2 catalyst and ZSM-5 at 12% conversion and 400^0C reaction temperature

4.3.3 Kinetic Modeling

4.3.3.1 Model development for ethylation reaction over USY-2.

In this section, a comprehensive kinetic model for benzene ethylation over the USY-2 catalyst was developed. The experimental results were modeled using steady-state approximations with catalyst decay to be a function of time on stream. The catalyst activity decay model based on time-on-stream was initially suggested by Voorhies. To develop a suitable kinetic model representing the overall ethylation of benzene, we propose the reaction network shown in Scheme 2. The following set of species balances and catalytic reactions can be written:

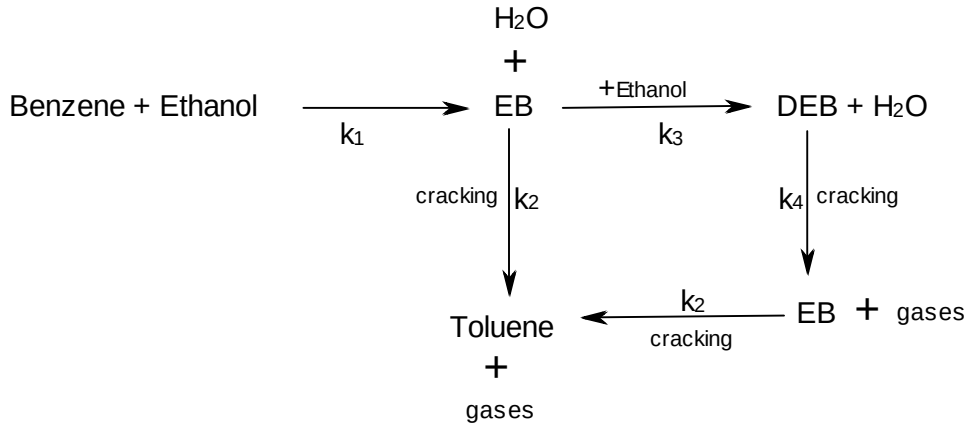

Scheme 2

Rate of disappearance of benzene, r_B

$$-\frac{V}{W_C}\frac{dC_B}{dt} = k_1 C_B C_E \exp(-\alpha t) \tag{4.19}$$

Rate of formation of ethylbenzene, r_{EB}

$$\frac{V}{W_C}\frac{dC_{EB}}{dt} = \left(k_1 C_B C_E - \left(k_2 C_{EB} + k_3 C_{EB} C_E\right)\right)\exp(-\alpha t) \tag{4.20}$$

Rate of formation of toluene, r_T

$$\frac{V}{W_C}\frac{dC_T}{dt} = k_2 C_{EB}\exp(-\alpha t) \tag{4.21}$$

Rate of diethylbenzene formation ,r_{DEB}

$$\frac{V}{W_C}\frac{dC_{DEB}}{dt} = \left(k_3 C_{EB} C_E - k_4 C_{DEB}\right)\exp(-\alpha t) \tag{4.22}$$

where C_B is the benzene concentration, C_{EB} is the concentration of ethylbenzene, C_{DEB} is the concentration of diethylbenzene, C_T is the concentration of toluene in the riser simulator, V is the volume of the riser (45 cm^3), W_C is the mass of the catalyst (0.81g of catalyst), t is the time (s), α is the deactivation constant and k is the rate constant (cm^3 /(g of catalyst .s)). By definition the molar concentration, C_x of every species in the system can be related to its mass fraction, y_x (measurable from GC), by the following relation:

$$c_x = \frac{y_x W_{hc}}{V\ MW_x} \tag{4.23}$$

Where W_{hc} is the weight of feedstock injected into the reactor, MW_x is the molecular weight of specie x in the system, V is the volume of riser simulator.

It should be noted that the following assumptions were made in deriving the reaction network:

1. The cracking of ethylbenzene follows simple first-order kinetics, while the ethylation reactions follow second order kinetics.

2. An irreversible reaction path is assumed for both the ethylation and cracking reactions. Sridevi et al. [11] made similar assumption since the conversion of benzene is small.

3. Catalysts deactivation is assumed to be a function of time on stream (TOS). A single deactivation function is defined for all the reactions taking place.

4. Isothermal operating conditions can also be assumed given the design of the riser simulator unit and the relatively small amount of reacting species. This is justified by the negligible temperature change observed during the reactions.

5. A pseudo-first order reaction kinetic for all species involved in the reactions.

6. Negligible thermal conversion.

Substituting Eq.(4.23) into Eqs. (4.19) – (4.22), we have the following first order differential equations which are in terms of weight fractions of the species:

$$\frac{dy_B}{dt} = -A_1 k_1 y_B y_E \frac{W_c}{V} \exp(-\alpha t) \tag{4.24}$$

$$\frac{dy_{EB}}{dt} = \left[A_2 k_1 y_B y_E - \left(k_2 y_{EB} + A_1 k_3 y_{EB} y_E\right)\right] \frac{W_c}{V} \exp(-\alpha t) \tag{4.25}$$

$$\frac{dy_T}{dt} = A_3 k_2 y_{EB} \frac{W_c}{V} \exp(-\alpha t) \tag{4.26}$$

$$\frac{dy_{DEB}}{dt} = \left(A_4 k_3 y_{EB} y_E - k_4 y_{DEB}\right) \frac{W_c}{V} \exp(-\alpha t) \tag{4.27}$$

A_1, A_2, A_3 and A_4 are lumped constants given below.

$$A_1 = \frac{W_{hc}}{VMW_E}$$

$$A_2 = \frac{MW_{EB} W_{hc}}{VMW_B MW_E}$$

$$A_3 = \frac{MW_T}{MW_{EB}}$$

$$A_4 = \frac{MW_{DEB} W_{hc}}{VMW_{EB} MW_E}$$

Equations (4.24) - (4.27) contain 9 parameters, k_1- k_4, E_1- E_4 and α, which are to be determined by fitting into experimental data.

The temperature dependence of the rate constants was represented with the centered temperature form of the Arrhenius equation, i.e.

$$k_i = k_{oi} \exp\left[\frac{-E_i}{R}\left(\frac{1}{T} - \frac{1}{T_o}\right)\right] \qquad (4.28)$$

Since the experimental runs were done at 300, 350 and 400^{0}C, T_0 was calculated to be 350^{0}C. Where T_o is an average temperature introduced to reduce parameter interaction, k_{oi} is the rate constant for reaction i at T_o, W_c is the weight of catalyst and E_i is the activation energy for reaction i.

4.3.3.2 Discussion of Kinetic Modeling Results.

The kinetic parameters k_{0i}, E_i, and α for the ethylation reaction were obtained using nonlinear regression (MATLAB package). Table 4.16 reports the parameters obtained along with the corresponding 95% confidence limits, while Tables 4.17- 4.20 presents the

correlation matrices for the parameters. The correlation matrices of the regression analysis show that the parameters are highly correlated. From the results of the kinetic parameters presented in Table 4.16, it is observed that catalyst deactivation was found to be small, α = 0.0776. This value is higher than α (0.0250) reported by Odedairo and Al-Khattaf [23] over ZSM-5 based catalyst for benzene to ethanol mole ratio of 1:1. This significant result is in perfect agreement with the findings of refs 75, 76 and 77, in which the authors reported that cage-type zeolites like faujasite shows a lower resistance to coking compared with ZSM-5 based catalyst. It was also observed that the ratio of the coke weight percent in the ethylation reaction over USY-2 catalyst to coke weight percent in the ethylation reaction over ZSM-5 earlier reported was noticed to be between the range of 2.7 to 4.5 as shown in Table 4.15. It was observed that the ratio of catalyst deactivation constant for both catalysts $(\alpha_{(USY-2)}/\alpha_{(ZSM-5)})$ is 3.10, which is in the same range of the coke ratio of the two catalysts. This observation confirms that, the catalyst deactivation in both catalysts is directly related to coke deposition.

Table 4.16 Estimated kinetic parameters based on time on stream (TOS-model) Feed ratio = 1:1 (benzene: ethanol)

Parameters	k_1	k_2	k_3	k_4	α
E_i (kJ/ mol)	15.39	27.21	24.71	16.32	0.0776
95% CL	1.51	6.92	7.39	12.85	0.0088
k_{0i} X 10^3 (m3/ (kg of cat. s))	0.0102	1.0775	0.1266	10.6285	
95% CL x 10^3	0.0006	0.1208	0.0177	2.5213	

Table 4.17 Correlation matrix for benzene ethylation (TOS model) (feed ratio = 1:1 (benzene: ethanol))

	k_1	E_1	α
k_1	1.0000	-0.1016	0.9542
E_1	-0.1016	1.0000	-0.0607
α	0.9542	-0.0607	1.0000

Table 4.18 Correlation matrix for ethylbenzene cracking (TOS model) (feed ratio = 1:1 (benzene: ethanol))

	k_2	E_2	α
k_2	1.0000	-0.3245	0.7577
E_2	-0.3245	1.0000	-0.0886
α	0.7577	-0.0886	1.0000

Table 4.19 Correlation matrix for ethylbenzene ethylation (TOS model) (feed ratio = 1:1 (benzene: ethanol))

	k_3	E_3	α
k_3	1.0000	-0.4895	0.7298
E_3	-0.4895	1.0000	-0.1122
α	0.7298	-0.1122	1.0000

Table 4.20 Correlation matrix for diethylbenzene cracking (TOS model) (feed ratio = 1:1 (benzene: ethanol))

	k_2	E_2	α
k_2	1.0000	-0.1880	0.6935
E_2	-0.1880	1.0000	-0.0627
α	0.6935	-0.0627	1.0000

Apparent activation energies of 27.21, 24.71, 16.32 and 15.39kJ/mol were obtained for the cracking of EB, ethylbenzene ethylation, cracking of DEB and benzene ethylation respectively. It can be seen from the table that the apparent activation energies for the benzene ethylation, cracking of DEB, ethylbenzene ethylation and cracking of EB follows the increasing order: $E_1 < E_4 < E_3 < E_2$. Odedairo and Al-Khattaf [23] recently reported apparent energies of activation of 34.69kJ/mol for benzene ethylation over ZSM-5 based catalyst, and 9.53kJ/mol for the secondary ethylation reaction.

The apparent activation energy obtained for benzene ethylation over ZSM-5 based catalyst (34.69kJ/mol) earlier reported is higher than the 15.39kJ/mol obtained in the present study over USY-2 catalyst. Looking to their pore opening and their pore geometry, this result is not surprising. USY-2 catalyst with a diameter of 7.4 Å and the free diameter inside the cages of 12 Å is large enough for the reactants and reaction products as compared to the medium pore zeolite (ZSM-5) with almost the same critical diameter with benzene. Therefore, the activation energy for benzene diffusion (E_D) over ZSM-5 based catalyst is greater than the E_D in USY-2 catalyst. According to Levenspiel [78] the apparent activation energy (E_{App}) is equivalent to half of the summation of the intrinsic activation energy (E_{in}) and the diffusion activation energy (E_D) as follows;

$$E_{App} = \frac{E_{in} + E_D}{2}$$

Since $E_{D\ (ZSM-5)} > E_{D\ (USY-2)}$, therefore the apparent activation energy for benzene ethylation over ZSM-5 ($E_{App\text{-}ZSM\text{-}5}$) is greater than the apparent activation energy for benzene ethylation over USY-2 catalyst ($E_{App\text{-}USY\text{-}2}$).

It is of great interest to note that the apparent activation energy for ethylbenzene cracking (27.21kJ/mol) is higher than the apparent energy of activation for benzene

ethylation (15.39kJ/mol). This clearly suggests that an increase in temperature leads to a larger fraction of cracking products, as shown in Table 4.14. Similar explanation was given by Atias et al. [79] during the catalytic conversion of 1,2,4- Trimethylbenzene when a higher apparent energy of activation was obtained for the isomerization of 1,2,4-TMB as compared with its disproportionation. The lower apparent energy of activation obtained for benzene ethylation indicates that the ethylation reaction is less sensitive to temperature variations. Therefore, EB formation is not expected to change significantly with temperature, as shown in Table 4.14.

The apparent activation energy (E_2) of 27.21kJ/mol was obtained for the formation of toluene during the cracking of EB over USY-2 catalyst. This value is higher than the 16.32kJ/mol obtained for the cracking of DEB (E_4). This indicates that the activation energy required to form toluene as a result of ethylbenzene cracking is higher than the apparent activation energy required for removing an ethyl group from diethylbenzene as a result of DEB cracking by magnitudes of 10-11kJ/mol. From a comparison of the apparent activation energies for ethylbenzene ethylation (9.53kJ/mol) over ZSM-5 based catalyst earlier reported and ethylbenzene ethylation (24.71kJ/mol) over USY-2 catalyst, the difference in the apparent activation energies over the two catalysts is probably due to the formation of DEB within the pores of USY-2 catalyst as compared with the formation of DEB on the crystal surface of ZSM-5 based catalyst.

To check the validity of the estimated kinetic parameters for use under conditions beyond those of the present study, the fitted parameters were substituted into the comprehensive model developed for this scheme and the equations were solved

numerically using the fourth-order-Runge-Kutta routine. The numerical results were compared with the experimental data as shown in Figure 4.14. It can be observed from this figure that the calculated results compare very well with the experimental data. Further comparisons between model predictions and experimental data are presented in Figures 4.21 and 4.22. It can be seen that the model predictions compared very well with the experimental data. This demonstrates that the proposed kinetic model fits well into our experimental observations. In addition, the reconciliation plot (Fig. 4.23) between the experimental data and the model predictions display a normal distribution of residuals, besides, the adequacy of the model and the selected parameters to fit the data as shown in Table 4.16 gave 0.9830 regression coefficients.

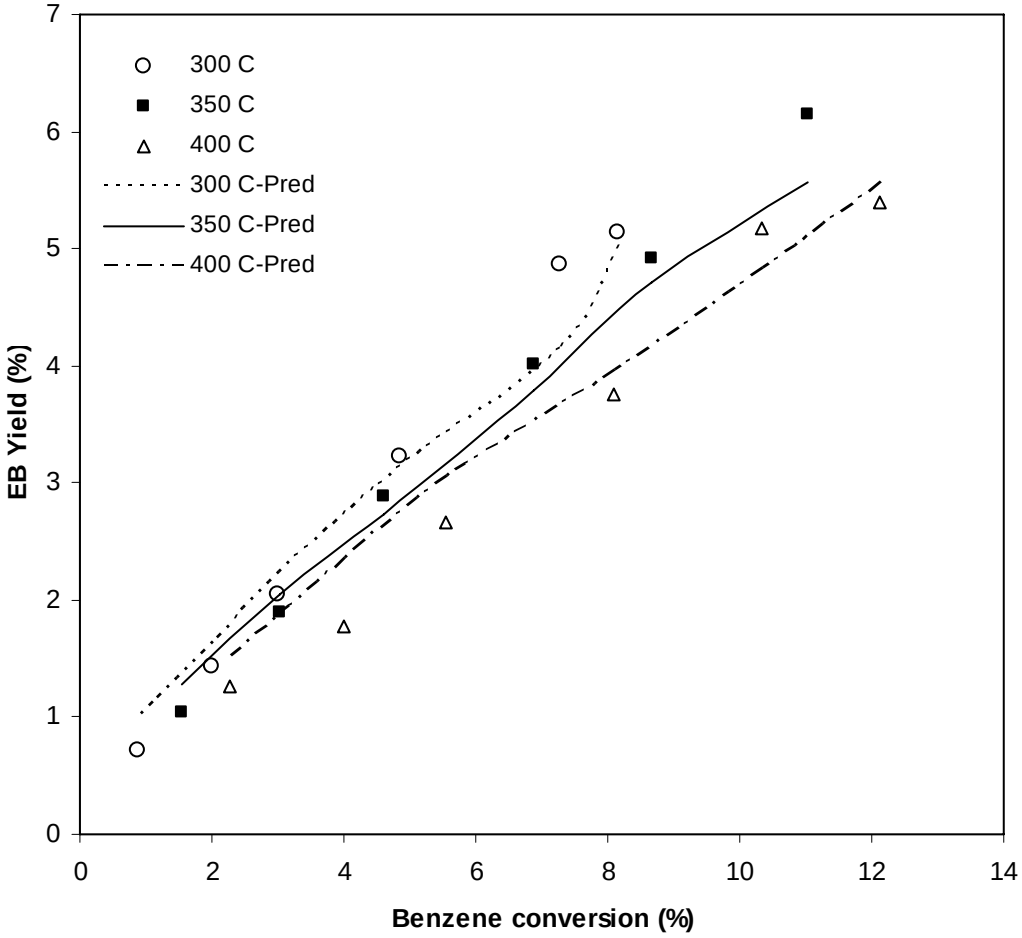

Figure 4.21 Ethylbenzene yield vs. benzene conversion at various temperatures

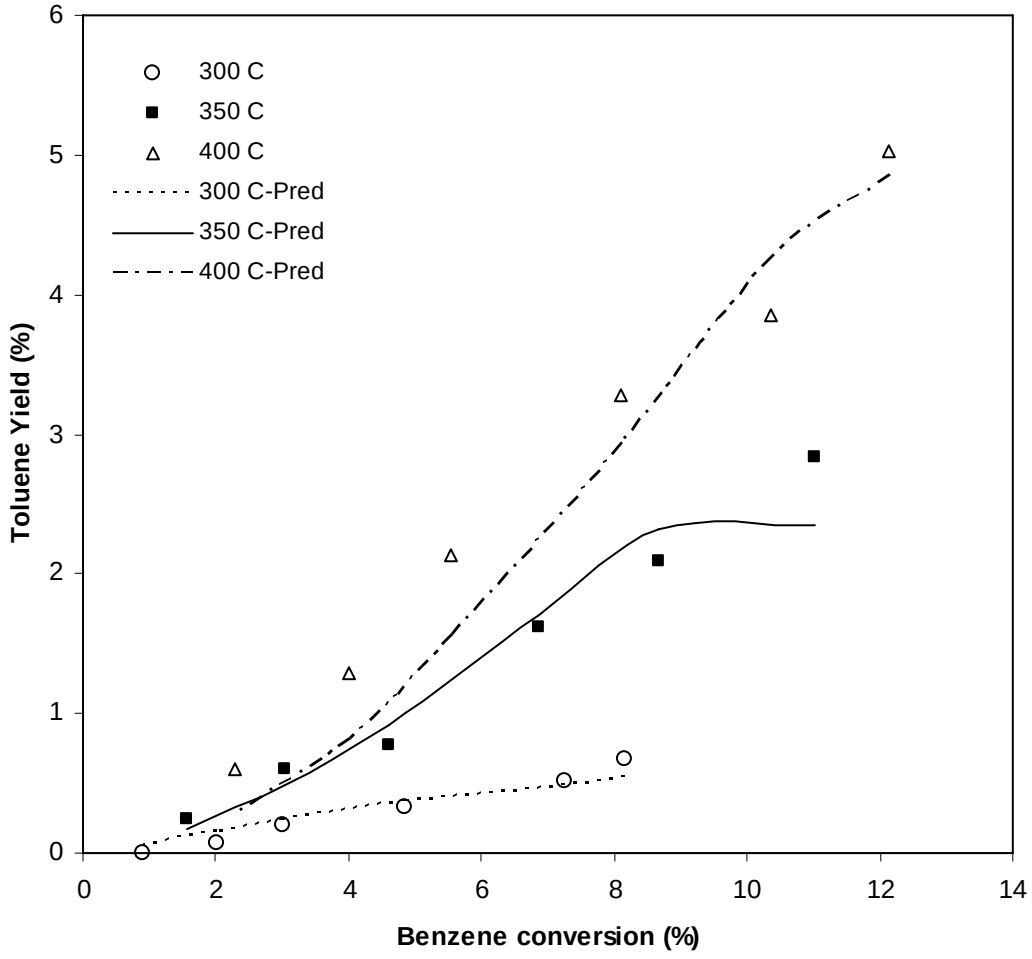

Figure 4.22 Toluene yield vs. benzene conversion at various temperatures

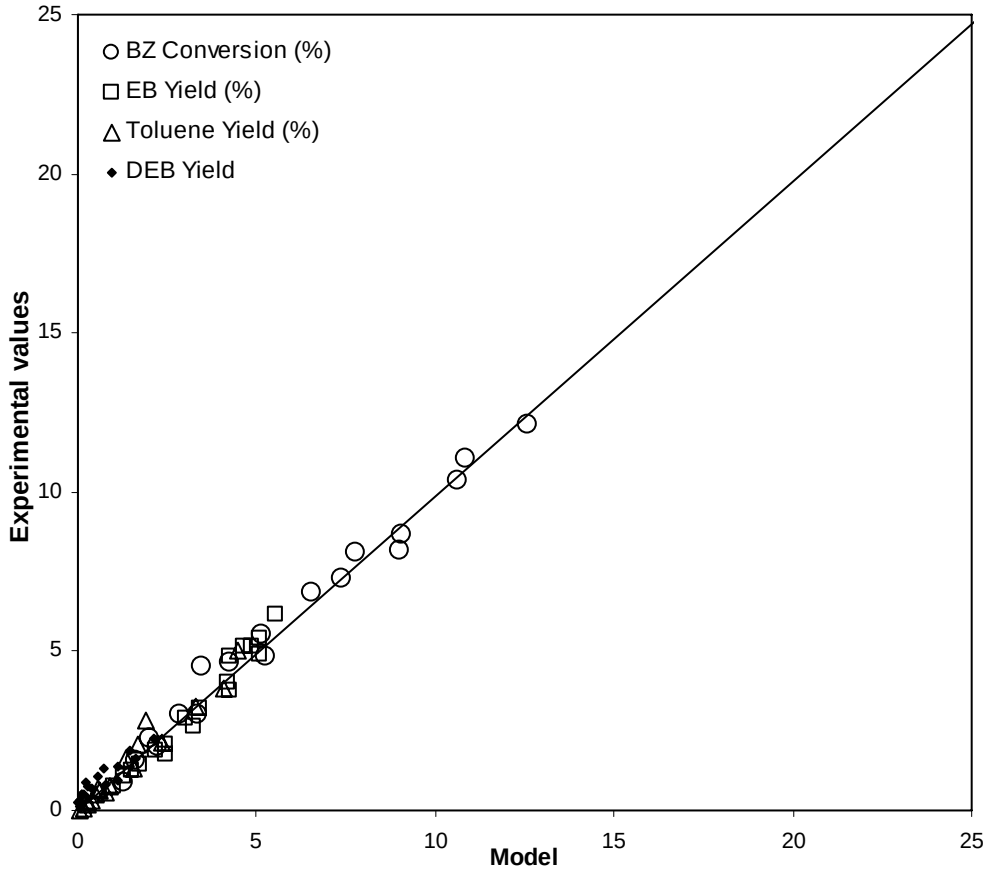

Figure 4.23 Overall comparison between the experimental results and model predictions

4.4 The roles of acidity and structure of zeolite for catalyzing benzene ethylation

In this section of the research work, the catalytic activity of a novel zeolite TNU-9 possessing 10-10-10-ring system is compared with SSZ-33, ZSM-5 and mordenite in benzene ethylation. Although there are many studies on ethylation of benzene with ethanol over ZSM-5 and mordenite based catalyst, while a few has been reported over SSZ-33 and none over TNU-9 based catalyst. Most of them are related to catalyst development and elucidation of reaction mechanism. To our knowledge, the kinetic study over TNU-9, SSZ-33 and mordenite based catalyst in the ethylation of benzene with ethanol has not been reported in the open literature and has not been carried out in a riser simulator.

4.4.1 Preparation of catalysts

The uncalcined proton form of mordenite (H-mordenite) zeolite (HSZ-690HOA) used in this work was obtained from Tosoh Chemicals, Japan. The mordenite has silica to alumina ratio of 240. An alumina binder (Cataloid AP-3) contains 75.4wt% alumina, 3.4% acetic acid and water as a balance obtained from CCIC Japan. The alumina binder was dispersed in water and stirred for 30min to produce thick slurry. The zeolite powder was then mixed with alumina slurry to produce a thick paste. The composition of the zeolite based catalyst in weight ratio is as follows: Mordenite: AP-3 (2:1). The uncalcined proton form of ZSM-5 (CT-405) used in this study was obtained from CATAL, UK. The ZSM-5 has silica to alumina ratio of 30. Similar procedure used for the preparation of the mordenite based catalyst used in this study was also followed for the preparation of the ZSM-5 based catalyst. The composition of the ZSM-5 zeolite based catalyst in weight

ratio is as follows: ZSM-5: AP-3 (2:1). Zeolite SSZ-33 and TNU-9 used in this study were obtained from J. Heyrovsky Institute of Physical Chemistry, Academy of Science of the Czech Republic, Prague, Czech Republic. Alumina was added to these zeolites (SSZ-33 and TNU-9) adopting the same procedure used for mordenite and ZSM-5 based catalyst.

4.4.2 Characterization of catalysts

Surface areas were obtained from N_2 physical adsorption isotherms by applying BET method with Quantachrome AUTO-SORB-1 (model # ASI-CT-8). The samples were preheated at 373k for 3h in flowing N_2. Type and concentration of acid sites in all zeolites was determined by adsorption of pyridine as probe molecules followed by FTIR spectroscopy (Nicolet 6700 FTIR) using the self-supported wafers technique. Prior to adsorption, self-supporting zeolite wafers were activated in situ by evacuation at temperature 450^0C over night. Adsorption of pyridine proceeded at 150^0C for 20 min at partial pressure 5 Torr.

The concentrations of Bronsted and Lewis acid sites were calculated from the integral intensities of individual bands characteristic of pyridine on Bronsted acid sites at 1550cm^{-1} and band of pyridine on Lewis acid sites at 1455cm^{-1} and molar absorption coefficient [80] of $\varepsilon(B) = 1.67 \pm 0.1$cm μmol^{-1} and $\varepsilon(L) = 2.22 \pm 0.1$ cm $\mu mol^{-1,}$ respectively. The infrared spectra of absorbed pyridine on SSZ-33 were recently discussed in detail by Gil et al. [81]. The characteristics of all samples are given in Table 4.21.

Table 4.21 Characteristics of sample used in this work

Sample	ZSM-5	TNU-9	Mordenite	SSZ-33
Si/Al	20.3	19.3	135.9	13.6
Bronsted acid sites (mmol/g)	0.21	0.33	0.03	0.18
Lewis acid sites (mmol/g)	0.28	0.25	0.12	0.48
Bronsted sites (%)	43	57	20	28
Lewis sites (%)	57	43	80	72
Total acid sites (mmol/g)	0.49	0.58	0.15	0.66
BET surface area (m^2/g)	304	330	441	448

4.4.3 Ethylation of benzene over mordenite based catalyst (M-catalyst)

4.4.3.1 Benzene conversion

The formation of ethylbenzene (EB), diethylbenzene (DEB) and triethylbenzene (TEB) (Table 4.22) via ethylation of benzene with ethanol was studied over mordenite based catalyst at 250, 275, and 300^{0}C for residence times of 3, 5, 7, 10, 13, 15 and 20s. Benzene conversions of approximately 20.16, 14.53, and 9.72% were achieved at 300, 275 and 250^{0}C respectively for a reaction time of 20s, as shown in Fig.4.24. At all reaction times studied, the maximum benzene conversion was obtained at 300^{0}C. The experimental results showed that the conversion occurred via ethylation. The major product of the ethylation reaction over M-catalyst is ethylbenzene. A maximum EB yield of ~10.2% was obtained at 300^{0}C at a benzene conversion of 20.16% for a reaction time of 20s. Diethylbenzene was also observed in significant amount in the ethylation reaction over mordenite based catalyst. The highest triethylbenzene (TEB) yield of ~3.0% was achieved at 300^{0}C at 20.16% benzene conversion. The product distribution is partially reproduced in Table 4.22. Formation of ethylbenzene represents the primary ethylation step, while the ethylation reaction of EB with ethanol represents the secondary ethylation reaction. A tertiary ethylation reaction was also observed in this reaction, which led to the formation of triethylbenzene (TEB). The formation of TEB is as a result of the channel opening of mordenite that is large enough for the alkylation reaction. The channel opening provides larger reaction volume enabling consecutive reactions of DEB to proceed.

Table 4.22 Product distribution (wt %) at various reaction conditions for the ethylation of benzene over mordenite based catalyst

Temp	Ben. Conv. (%)	EB	Toluene	Gases	m-DEB	p-DEB	o-DEB	T. DEB	TEB
250									
5	0.81	0.49	-	-	0.08	0.03	0.02	0.13	0.19
15	7.92	4.05	-	0.23	1.08	0.44	0.22	1.74	1.90
20	9.72	4.83	-	0.26	1.44	0.55	0.28	2.27	2.36
275									
5	4.30	2.51	-	-	0.59	0.22	0.12	0.93	0.86
15	13.51	6.67	-	0.36	2.28	0.98	0.36	3.62	2.86
20	14.53	7.26	-	0.36	2.55	1.12	0.37	4.04	2.87
300									
5	8.07	4.61	-	0.12	1.40	0.63	0.21	2.24	1.10
15	18.16	9.30	0.18	0.45	3.47	1.57	0.49	5.53	2.70
20	20.16	10.23	0.25	0.46	3.93	1.78	0.55	6.26	2.96

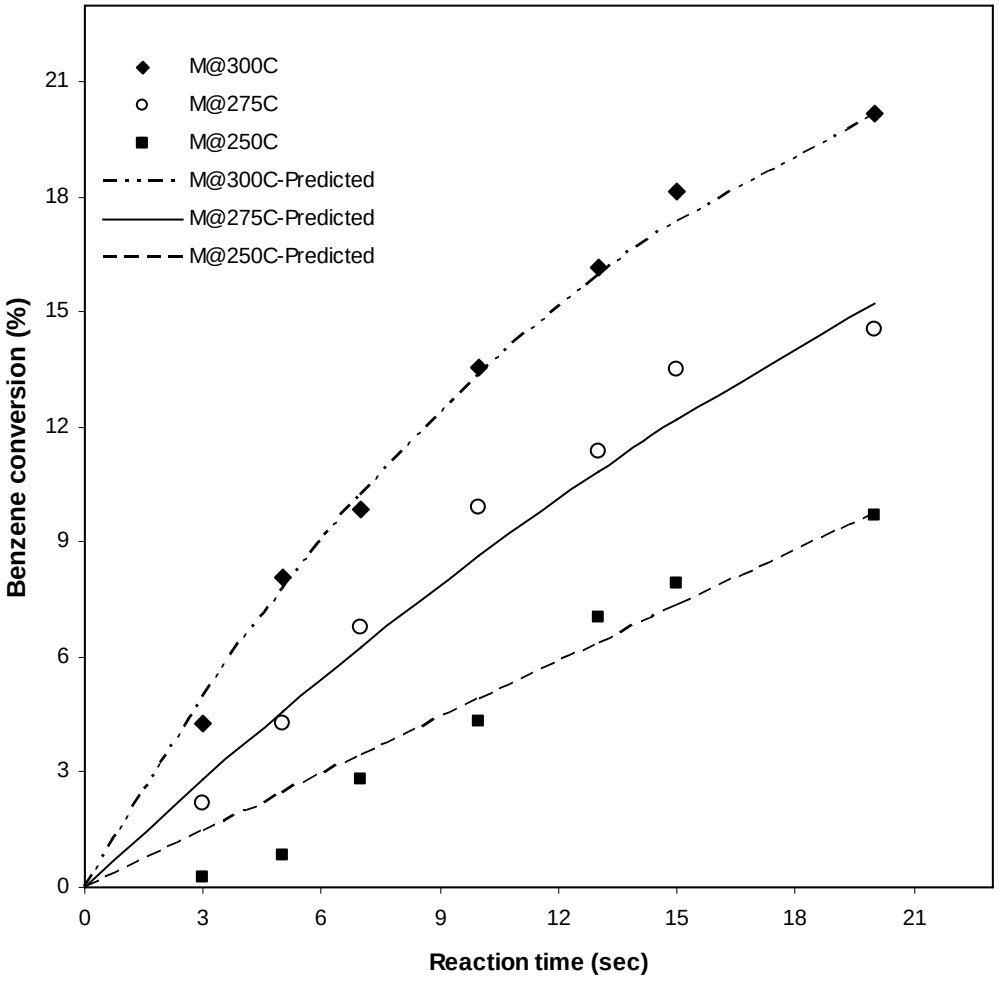

Figure 4.24 Effect of reaction conditions on benzene conversion over mordenite based catalyst

4.4.3.2 Ethylbenzene and DEB Yield

The yield of ethylbenzene was found to increase with both temperature and time, up to a maximum of ~10.2% at 300^0C for a reaction time of 20s. This corresponds to an ethylbenzene selectivity of ~50.7%. Cracking of ethylbenzene to produce toluene was not observed in this reaction compared to the pronounced EB cracking reported in our recent publication [35] over USY-zeolite based catalyst.

Similarly to ethylbenzene yield, diethylbenzene yield was noticed to increase with both time and temperature. A maximum of ~6.3% yield of DEB was obtained at 300^0C at a benzene conversion of ~20.2% for a reaction time of 20s. The experimental results showed that m-DEB was found to be in significant amount more than other DEB isomers detected in this ethylation reaction. The thermodynamic equilibrium mixture of diethylbenzenes (para: meta: ortho = 30:54:16) reported by Kaeding [69] and Halgeri [61] was compared with the DEB isomers obtained under this present study. It can be observed from Table 4.22 that, for all the reaction conditions studied; p/o ratio was found to be between 1.50 and 3.24, which compared favorably well with the thermodynamic equilibrium values given by previous researchers.

4.4.4 Ethylation of benzene over ZSM-5 based catalyst (Z-catalyst)

4.4.4.1 Benzene conversion

The main products obtained from the ethylation reaction of benzene with ethanol over ZSM-5 based catalyst were ethylbenzene and diethylbenzene (Table 4.23). Small amount of toluene and gaseous hydrocarbon was also noticed from the reaction products. A maximum benzene conversion of ~21.7% was obtained at 300^0C for a reaction of 20s.

The conversion of benzene was observed to increase with reaction temperature and time, as shown in Fig. 4.25. This is in conformity with observation made by Odedairo and Al-Khattaf [23] during the ethylation of benzene over ZSM-5 based catalyst, in which kaolin and alumina were used as the filler and silica sol was used as the binder. About 2.2-8.6% of toluene was also noticed in this ethylation reaction over ZSM-5 based catalyst, as compared with a negligible amount reported in our recent publication over another catalyst which was also based on ZSM-5 [23]. The small amount of toluene observed in this ethylation reaction is due to the higher acidity of the ZSM-5 used in this present study as compared with the one previously reported, which was of a lower acidity (0.23 mmol/g). The noticeable amount of toluene observed at the higher temperatures, is probably formed from the cracking of ethylbenzene.

Table 4.23 Product distribution (wt %) at various reaction conditions for the ethylation of benzene over ZSM-5 based catalyst

Temp	Ben. Conv. (%)	EB	Toluene	Gases	m-DEB	p-DEB	o-DEB	T. DEB
250								
5	4.31	3.01	0.09	0.08	0.50	0.43	0.03	0.95
15	12.74	8.90	0.48	0.30	1.49	1.46	0.11	3.06
20	16.10	11.23	0.70	0.34	1.94	1.72	0.17	3.83
275								
5	8.24	5.96	0.32	0.20	0.93	0.75	0.08	1.76
15	17.54	12.21	0.87	0.37	2.13	1.78	0.18	4.09
20	19.29	13.29	1.12	0.52	2.33	1.81	0.22	4.36
300								
5	7.78	5.62	0.54	0.26	0.73	0.73	0.08	1.36
15	19.02	13.20	1.42	0.68	2.06	1.42	0.23	3.71
20	21.70	14.94	1.88	0.88	2.29	1.44	0.27	4.00

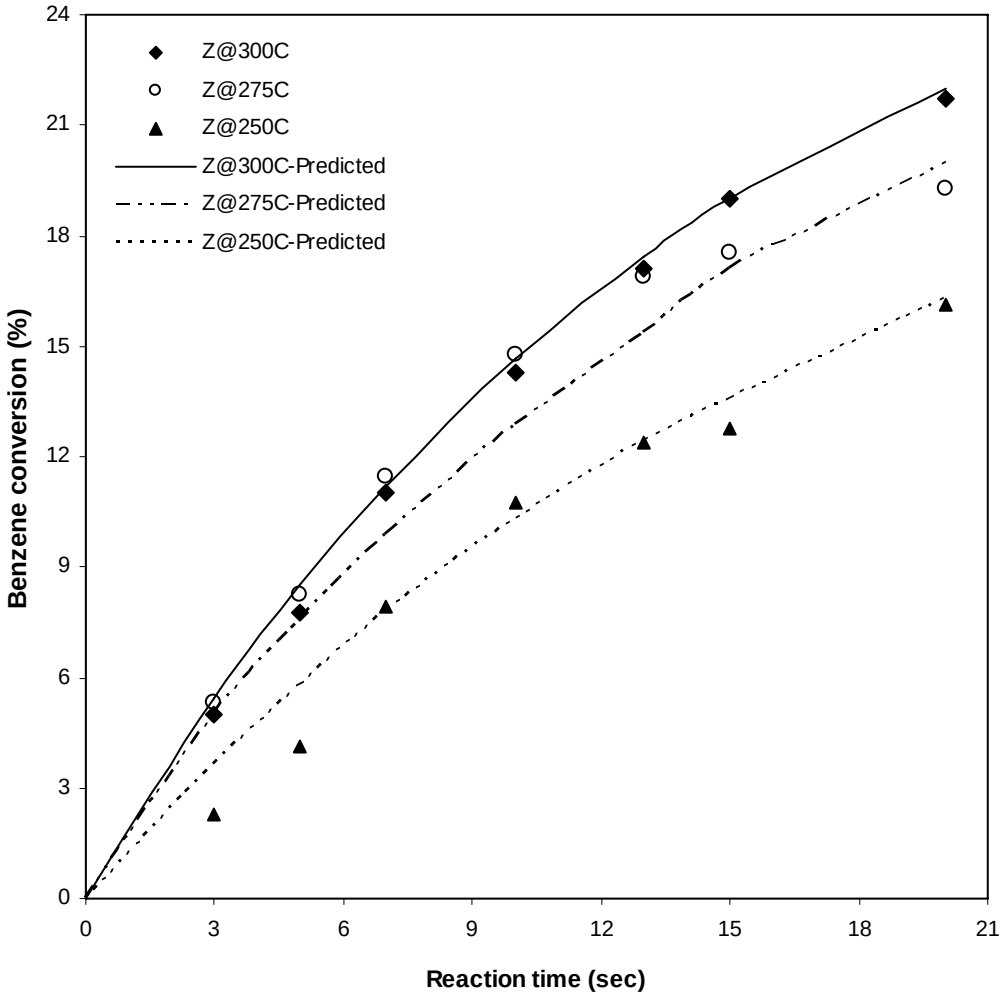

Figure 4.25 Effect of reaction conditions on benzene conversion over ZSM-5 based catalyst

4.4.4.2 Ethylbenzene and DEB Yield

The yield of ethylbenzene increased with reaction time and temperature, up to ~14.9% at 300^0C, for a reaction time of 20s. EB yield of 13.3% and 11.2% was also obtained at 275^0C and 250^0C, respectively. An optimum yield of ~4.4% of DEB was noticed at 275^0C for a reaction time of 20s. As temperature was further increased to 300^0C, a slight decrease in DEB yield was observed to a value of ~4.0%. In the ethylation reaction of benzene with ethanol over ZSM-5 based catalyst, the formation of para-isomers can be expected to proceed almost entirely in the zeolite channel system, while the formation of meta- and ortho-isomers proceeds on the external surface. The p/o ratio obtained from the ethylation of benzene with ethanol over ZSM-5 based catalyst was found to range between ~5.3 and ~14.3. This value was noticed to be far above the thermodynamic equilibrium value given by Kaeding [69] and Halgeri [61].

It is of paramount importance to note that triethylbenzene was not formed in the ethylation reaction over ZSM-based catalyst. Even if the alkylation product (TEB) is formed in the large channel intersections, its chances to leave the channel would be very small. This also goes to ascertain the fact that zeolite with 10 rings usually exhibit restricted transition-state and product shape selectivity being particularly important in para-selective reactions such as toluene disproportionation, xylene isomerization, and toluene alkylation with methanol, ethylene/ethanol and propylene/propanol [82-84].

4.4.5 Ethylation of benzene over SSZ-33 based catalyst

Ethylbenzene and toluene were observed to be the main products obtained from the ethylation of benzene with ethanol over SSZ-33. Benzene conversion was found to increase with reaction time for all temperatures studied, reaching maximum of ~27% at 275^0C. Toluene selectivity shows a high dependence on reaction temperature over SSZ-33 catalyst, showing a toluene selectivity rise from ~25% to ~43% and then to ~54% for temperatures of 250, 275, and 300^0C, for 20s reaction time, respectively. The selectivity of toluene increased with increase in temperature. The significant increase in the selectivity of toluene indicates that the ethylbenzene formed undergoes cracking at higher temperature. Gao et al. [21] gave similar explanation when traces of toluene were found in the alkylation of benzene with ethanol over ZSM-5-based catalyst. They attributed the formation of toluene to the cracking of ethylbenzene over Bronsted acid sites.

Ethylbenzene selectivity decreased steadily with increase in temperature over SSZ-33 based catalyst to minimum of ~34% at 300^0C for a reaction time of 20s. It is evident from Table 4.24 that as temperature was increased from 250^0C to 300^0C; more toluene was formed due to ethylbenzene cracking, leading to a decrease in the selectivity of ethylbenzene at higher temperature. Negligible amount of DEB was noticed at 250^0C, while no DEB was formed at the higher temperatures.

Table 4.24 Product distribution (wt %) at various reaction conditions for the ethylation of benzene over SSZ-33 based catalyst

Temp	Ben. Conv. (%)	EB	Toluene	Gases	m-DEB	p-DEB	o-DEB	T. DEB
250								
5	12.08	7.81	2.01	1.33	0.56	0.29	0.08	0.93
15	24.17	15.41	4.95	2.11	1.04	0.53	0.13	1.70
20	25.28	14.94	6.26	2.32	1.04	0.58	0.14	1.76
275								
5	12.85	8.03	3.25	1.57	-	-	-	-
15	25.43	11.85	10.76	2.82	-	-	-	-
20	27.24	12.35	11.75	3.14	-	-	-	-
300								
5	16.26	6.76	7.39	2.11	-	-	-	-
15	24.97	8.25	13.89	2.83	-	-	-	-
20	26.38	8.87	14.18	3.33	-	-	-	-

4.4.6 Ethylation of benzene over TNU-9 based catalyst

Table 4.25 shows the product distribution of TNU-9 catalyst in the ethylation of benzene with ethanol at variable temperature of 250, 275 and 300^0C. EB, toluene, DEB and gaseous hydrocarbons were found in the ethylation reaction. Benzene conversion increased with reaction time, up to a maximum of ~25.0% at 300^0C.

Ethylation was noticed to be the major reaction, while at elevated temperatures the cracking reaction is also important. Cracking reaction of EB and DEB was observed at elevated temperatures, leading to increased cracking product (toluene) at elevated temperatures. The ethylation and cracking reaction noticed over TNU-9 based catalyst in the ethylation reaction of benzene with ethanol is similar to the reactions observed during benzene ethylation with ethanol over USY catalyst reported in our recent publication [35]. Both toluene and EB selectivity shows a high dependence on temperature over TNU-9 catalyst. The selectivity of toluene increased with increase in temperature, while the selectivity of ethylbenzene and DEB decreased with increase in temperature.

Table 4.25 Product distribution (wt %) at various reaction conditions for the ethylation of benzene over TNU-9 based catalyst

Temp	Ben. Conv. (%)	EB	Toluene	Gases	m-DEB	p-DEB	o-DEB	T. DEB
250								
5	10.92	6.90	1.43	0.81	1.09	0.58	0.11	0.95
15	23.78	14.84	3.37	1.63	2.44	1.27	0.23	3.94
20	25.01	15.19	3.95	1.73	2.57	1.34	0.23	4.14
275								
5	12.19	7.46	1.87	0.85	1.23	0.65	0.13	2.01
15	24.20	13.55	5.07	2.23	2.08	1.07	0.20	3.35
20	24.58	13.60	5.29	2.25	2.12	1.10	0.22	3.44
300								
5	12.41	6.09	2.91	1.38	1.19	0.45	0.10	1.38
15	24.31	11.54	7.64	2.16	1.72	1.07	0.81	2.97
20	25.06	11.78	7.83	2.26	1.97	1.01	0.21	3.19

4.4.7 Comparison of catalysts in the ethylation of benzene with ethanol

Figure 4.26 provides time-on-stream dependence of benzene conversion at 300^0C over zeolite based catalysts prepared from ZSM-5, TNU-9, SSZ-33 and mordenite materials. It is evident from this figure that, over all the catalysts studied, benzene conversion increases as expected with increase in reaction time (5-20s). The conversion of benzene in the ethylation reaction of benzene with ethanol carried out at 300^0C for a contact time of 20s, follows the order: SSZ-33 (26%) > TNU-9 (25%) > ZSM-5 (22%) > mordenite (20%).

Based on the comparison of the role of structure of the zeolites on benzene conversion in ethylation reaction of benzene with ethanol, it can be inferred that more open structure of SSZ-33 based catalyst (12-12-10-ring), which have been known to combine both large and medium pore channels [85], allows a higher reaction rate and faster diffusion of both reactants and products in comparison with the medium pore (10-ring) ZSM-5 and TNU-9 zeolite. Similar explanation was given during toluene disproportionation reaction over zeolite based catalysts when an increase in toluene conversion was observed [86]. They attributed the increase in conversion to the increase in the size of channels from medium to large pore zeolites.

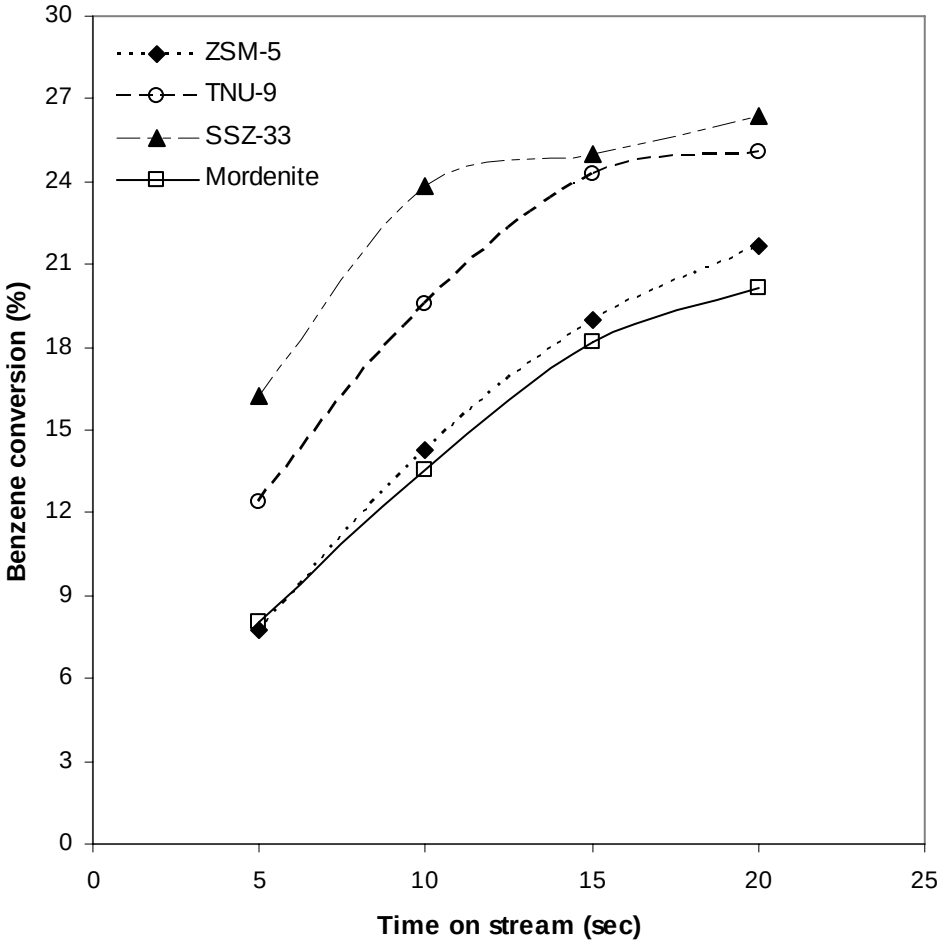

Figure 4.26 Time-on-stream dependence of benzene conversion in benzene ethylation over different zeolite based catalysts at 300^0C

The product selectivity during the ethylation of benzene with ethanol over ZSM-5, TNU-9, SSZ-33 and mordenite based catalyst are compared in Fig. 4.27 at constant conversion level of 18%. The results show that ethylbenzene (EB) is obtained as the most predominant product over all the catalysts. The formation of EB with high selectivity over all the catalysts might be due to its free diffusion without steric hindrance through the pores of the catalysts. Catalyst based on ZSM-5 gave the highest EB selectivity of ~70%, and mordenite based catalyst gave the lowest with an EB selectivity of ~51%. SSZ-33 gave the highest toluene selectivity of ~34% among all the catalysts studied, at a constant benzene conversion of 18%. It is worth mentioning that DEB was not observed over SSZ-33 catalyst at all conversion levels, except at 250^0C, which gave negligible amount of DEB. In contrast, a significant amount of DEB was obtained over mordenite as compared to SSZ-33 catalyst. Mordenite, however, gave the lowest selectivity towards toluene, particularly at lower reaction temperatures.

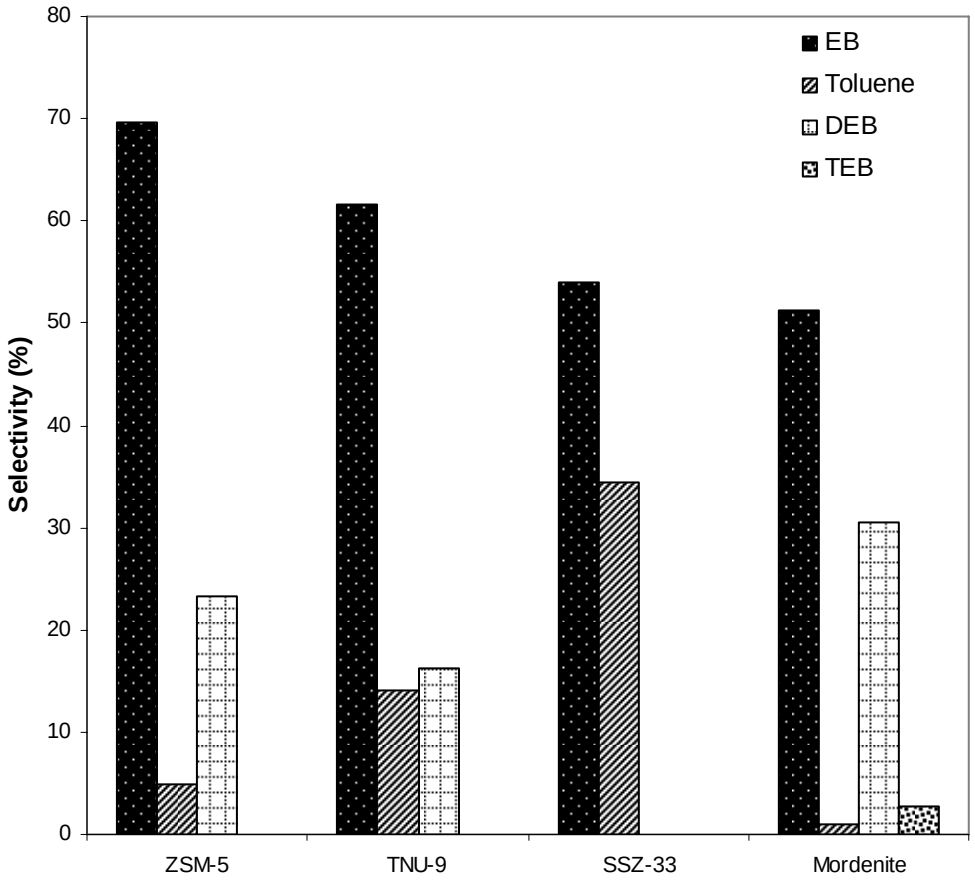

Figure 4.27 Product selectivity of benzene ethylation over the different catalysts at 18% conversion

With respect to the ethylation products, it can be seen from Fig. 4.27 that TNU-9 behaves like the 10-ring ZSM-5 for EB and DEB selectivity, while SSZ-33 shows no selectivity towards DEB. The effect of benzene conversion on ethylbenzene selectivity at 275^0C over all zeolite based catalysts under study is given in Fig. 4.28. EB selectivity over SSZ-33, mordenite and TNU-9 based catalyst shows a high dependence on benzene conversion and was noticed to decrease as benzene conversion increases. Ethylbenzene selectivity over ZSM-5 based catalyst on the other hand, shows a moderate dependence on benzene conversion. The effect of total acid sites on toluene formation at constant conversion level of 20% at 300^0C over all the zeolite based catalysts under study is given in Fig. 4.29. The yield of toluene increased with increase in total acid sites. It was observed that a maximum toluene yield of about 10.32% was obtained at 300^0C over SSZ-33 based catalyst at 20% benzene conversion. Therefore, to reduce cracking of ethylbenzene in the ethylation reaction over all the zeolite based catalysts, the total acid sites needs to be balanced.

It is a well established fact that the formation of dialkylbenzenes provides vital knowledge on the structure and acidity of zeolite catalysts [85]. From product diffusion shape selectivity effects, it is expected that the p/o ratio of the DEB isomers would be higher in medium pore ZSM-5 based catalyst than in the large pore zeolite. Within the distribution of isomers in the DEB, ZSM-5 showed the highest p/o ratio of ~9.9 at constant conversion level of 18%, while the lowest was noticed over SSZ-33. In conclusion, according to the results presented above, ZSM-5 based catalyst shows a slightly higher selectivity towards the formation of EB than TNU-9 and a much higher EB selectivity than SSZ-33 and mordenite based catalyst.

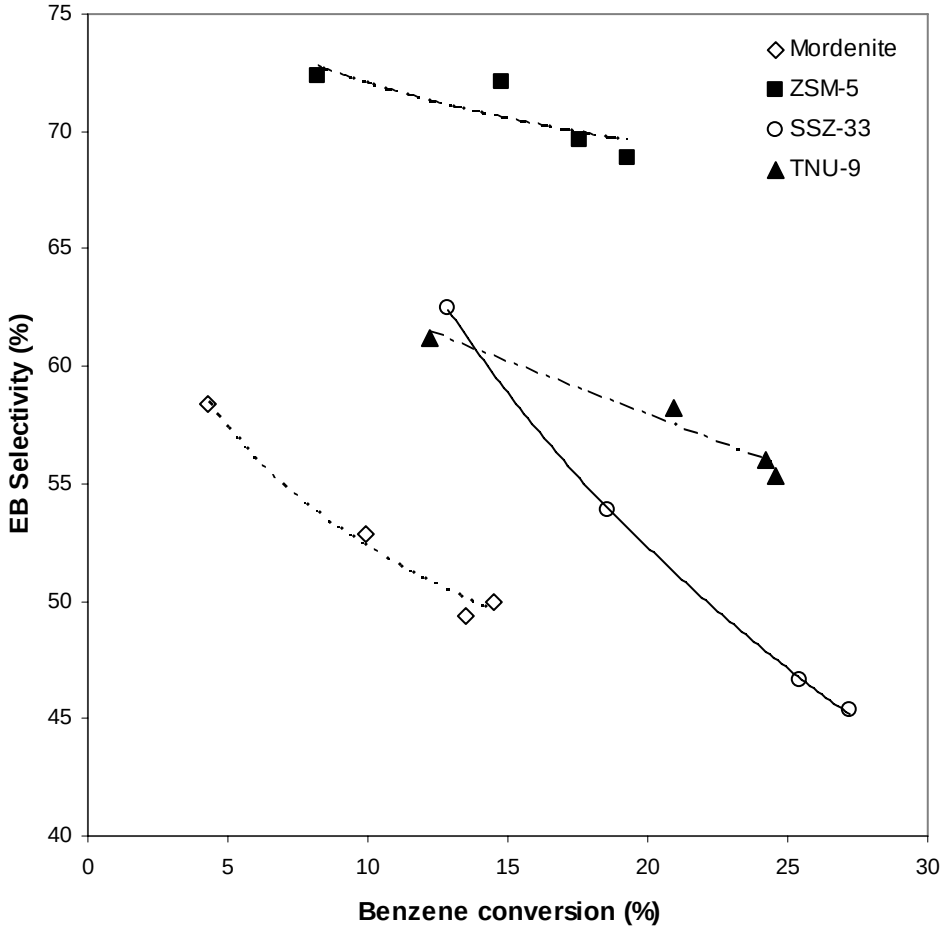

Figure 4.28 Effect of benzene conversion on ethylbenzene selectivity

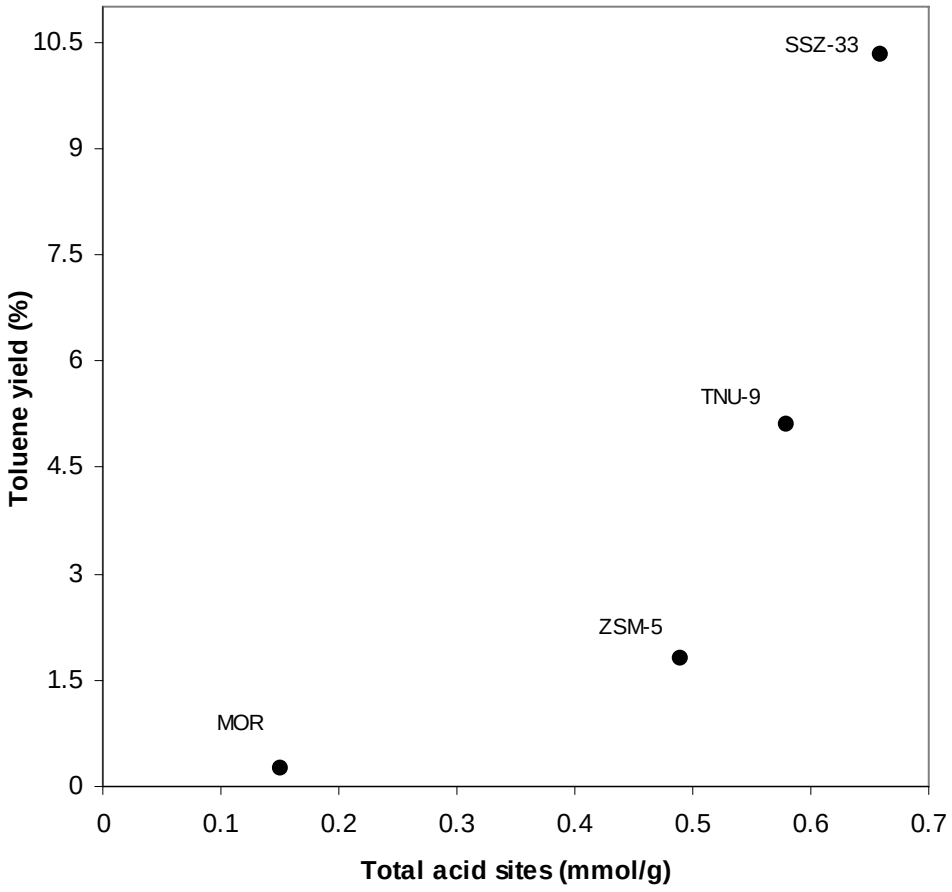

Figure 4.29 Effect of total acid sites on toluene formation at 300^0C at 20% benzene conversion

4.4.8 Kinetic Modeling

In this section, a comprehensive universal kinetic model for benzene ethylation over all the zeolite based-catalysts under study was developed. To develop a suitable kinetic model representing the overall ethylation of benzene with ethanol, we propose the reaction network shown in Scheme 3.

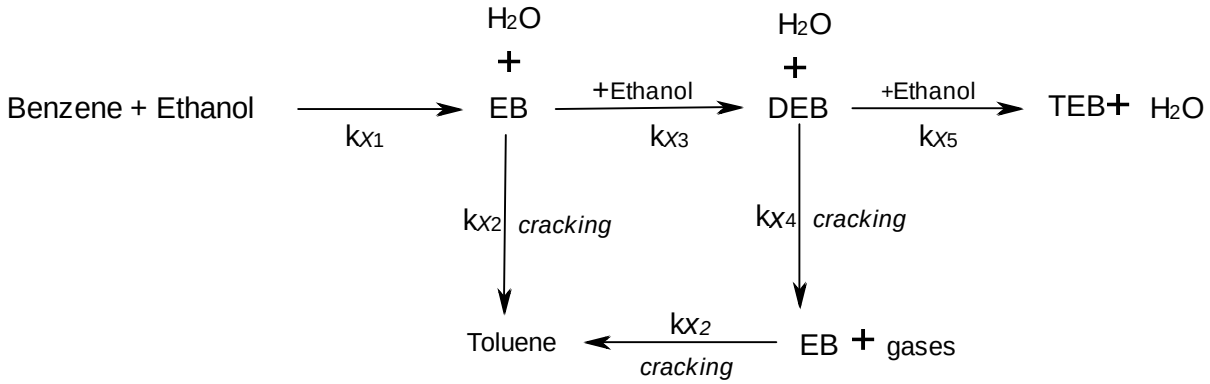

Scheme 3

4.4.8.1 Model development for ethylation reaction over mordenite based catalyst

Based on the product distribution observed in the ethylation reaction over mordenite based catalyst, a suitable kinetic model representing the ethylation reaction can be developed. Since toluene was not observed as one of the products in the ethylation reaction over mordenite based catalyst, the cracking of ethylbenzene as well as the cracking of diethylbenzene can therefore be neglected.

Therefore, k_{x2} and $k_{x4} \approx 0$, (where x = m in the case of mordenite). The following set of species balances and catalytic reactions can be written:

Rate of disappearance of benzene

$$-\frac{V}{W_C}\frac{dC_B}{dt} = \eta k_{m1} C_B C_E \varphi \tag{4.29}$$

Rate of formation of ethylbenzene

$$\frac{V}{W_C}\frac{dC_{EB}}{dt} = \left(\eta k_{m1} C_B C_E - \eta k_{m3} C_{EB} C_E\right)\varphi \tag{4.30}$$

Rate of diethylbenzene formation

$$\frac{V}{W_C}\frac{dC_{DEB}}{dt} = \left(\eta k_{m3} C_{EB} C_E - \eta k_{m5} C_{DEB} C_E\right)\varphi \tag{4.31}$$

Rate of triethylbenzene formation

$$\frac{V}{W_C}\frac{dC_{TEB}}{dt} = \eta k_{m5} C_{DEB} C_E \varphi \tag{4.32}$$

where C_B is the benzene concentration, C_{EB} is the concentration of ethylbenzene, C_{DEB} is the concentration of diethylbenzene, C_{TEB} is the concentration of triethylbenzene in the riser simulator, V is the volume of the riser (45 cm^3), W_C is the mass of the catalyst (0.81g of catalyst), t is the time (s), φ is the apparent deactivation function, η = an effectiveness factor and k is the rate constant (cm^3 /(g of catalyst .s)). By definition the molar concentration, C_x, of every species in the system can be related to its mass fraction, y_x (measurable from GC), by the following relation:

$$c_x = \frac{y_x W_{hc}}{V\ MW_x} \tag{4.33}$$

Where W_{hc} is the weight of feedstock injected into the reactor, MW_x is the molecular weight of specie x in the system, V is the volume of riser simulator.

Regarding catalyst deactivation, as deactivation functions can be expressed in terms of the catalyst time-on-stream [$\varphi = \exp(-\alpha t)$], deactivation can also be related to the progress of the reaction. The deactivation function based on time-on-stream was initially suggested by Voorhies, since then this model has been accepted and used extensively in the FCC literature.

A different approach for deactivation functions, based on coke concentration, was proposed by Froment [87]. As a result; a stoichiometric relationship can be established, as demonstrated by Al-Khattaf and de Lasa [67] between the amount of reactant and amount of coke produced. This allows for the use of a so-called "reactant conversion" model. This type of model has been reported to incorporate a sound mechanistic description of catalyst deactivation [68], allows for changes of chemical species without extra requirement of measuring the coke concentration [67]. For the reactant conversion model the deactivation function is

$$\varphi = \exp(-\lambda(1 - y_B)) \tag{4.34}$$

Where λ, is catalyst deactivation constant. Substituting Eqs.(4.33) and (4.34) into Eqs. (4.29) – (4.32), we have the following first order differential equations which are in terms of weight fractions of the species:

$$\frac{dy_B}{dt} = -\eta F_1 k_{m1} y_B y_E \frac{W_c}{V} \exp(-\lambda(1 - y_B)) \tag{4.35}$$

$$\frac{dy_{EB}}{dt} = \left[\eta F_2 k_{m1} y_B y_E - \eta F_1 k_{m3} y_{EB} y_E\right] \frac{W_c}{V} \exp(-\lambda(1 - y_B)) \tag{4.36}$$

$$\frac{dy_{DEB}}{dt} = \left[\eta F_3 k_{m3} y_{EB} y_E - \eta F_1 k_{m5} y_{DEB} y_E\right] \frac{W_c}{V} \exp(-\lambda(1 - y_B)) \tag{4.37}$$

$$\frac{dy_{TEB}}{dt} = \eta F_4 k_{m5} y_{DEB} y_E \frac{W_c}{V} \exp(-\lambda(1 - y_B)) \tag{4.38}$$

F_1, F_2, F_3 and F_4 are lumped constants given below.

$$F_1 = \frac{W_{hc}}{VMW_E}$$

$$F_2 = \frac{MW_{EB} W_{hc}}{VMW_B MW_E}$$

$$F_3 = \frac{MW_{DEB} W_{hc}}{VMW_{EB} MW_E}$$

$$F_4 = \frac{MW_{TEB} W_{hc}}{VMW_{DEB} MW_E}$$

It should be noted that the following assumptions were made in deriving the reaction network:

1. An irreversible reaction path is assumed for the ethylation reactions.

2. Catalysts deactivation is assumed to be a function of reactant conversion (RC). A single deactivation function is defined for all the reactions taking place.

3. Isothermal operating conditions can also be assumed given the design of the riser simulator unit and the relatively small amount of reacting species. This is justified by the negligible temperature change observed during the reactions.

4. A pseudo-first order reaction kinetic for all species involved in the reactions.

5. Negligible thermal conversion.

6. A single effectiveness factor was considered for benzene, ethylbenzene and triethylbenzene.

7. The effectiveness factor η was taken to be unity. This assumption was made based on the fact that p-xylene formed by catalytic reaction can easily escape via the pores of ZSM-5 [66] comparing mordenite with a larger pore opening; no diffusion restriction is expected in this reaction.

Equations (4.35) - (4.38) contain 7 parameters, $k_{m1,}$ $k_{m2,}$ $k_{m3,}$ $E_{m1,}$ $E_{m2,}$ E_{m3} and λ, which are to be determined by fitting into experimental data.

The temperature dependence of the rate constants was represented with the centered temperature form of the Arrhenius equation, i.e.

$$k_i = k_{oi} \exp\left[\frac{-E_i}{R}\left(\frac{1}{T}-\frac{1}{T_o}\right)\right] \qquad (4.39)$$

Since the experimental runs were done at 250, 275 and 300^0C, T_0 was calculated to be 275^0C. Where T_o is an average temperature introduced to reduce parameter interaction, k_{oi} is the rate constant for reaction i at T_o, W_c is the weight of catalyst and E_i is the activation energy for reaction i.

4.4.8.2 Model development for ethylation reaction over ZSM-5 based catalyst (Z-Catalyst).

A kinetic model development for benzene ethylation over ZSM-5 based catalyst using an activity decay model based on reactant conversion, which is based on Scheme 3, was developed for the ethylation reaction over ZSM-5. The slight increase in toluene formation noticed at elevated temperature which is probably due to cracking of ethylbenzene, was not accounted for in the kinetic model development.

Therefore, k_{x2} , k_{x4} and $k_{x5} \approx 0$, (where x = z in the case of ZSM-5 based catalyst). The following set of species balances and catalytic reactions can be written:

Rate of disappearance of benzene

$$-\frac{V}{W_C}\frac{dC_B}{dt} = \eta k_{z1} C_B C_E \varphi \tag{4.40}$$

Rate of formation of ethylbenzene

$$\frac{V}{W_C}\frac{dC_{EB}}{dt} = \left(\eta k_{z1} C_B C_E - \eta k_{z3} C_{EB} C_E\right)\varphi \tag{4.41}$$

Rate of formation of diethyl benzene

$$\frac{V}{W_C}\frac{dC_{DEB}}{dt} = \eta k_{z3} C_{EB} C_E \varphi \tag{4.42}$$

Substituting equations 5 and 6 into equations 12 – 14 results in the following first order differential equations which are in terms of weight fractions of the species:

$$\frac{dy_B}{dt} = -\eta H_1 k_{z1} y_B y_E \frac{W_c}{V} \exp(-\lambda(1 - y_B)) \tag{4.43}$$

$$\frac{dy_{EB}}{dt} = \left[\eta H_2 k_{z1} y_B y_E - \eta H_1 k_{z3} y_{EB} y_E\right]\frac{W_c}{V} \exp(-\lambda(1 - y_B)) \tag{4.44}$$

$$\frac{dy_{DEB}}{dt} = \eta H_3 k_{z3} y_{EB} y_E \frac{W_c}{V} \exp(-\lambda(1 - y_B)) \tag{4.45}$$

H_1, H_2 and H_3 are lumped constants given below.

$$H_1 = \frac{W_{hc}}{VMW_E}$$

$$H_2 = \frac{MW_{EB} W_{hc}}{VMW_B MW_E}$$

$$H_3 = \frac{MW_{DEB} W_{hc}}{VMW_{EB} MW_E}$$

Similar assumptions used in the kinetic model development for benzene ethylation over mordenite based catalyst, is also applicable in the ethylation of benzene with ethanol over ZSM-5 based catalyst. Equations (4.43) - (4.45) contain 5 parameters; k_{z1}, k_{z2}, E_{z1}, E_{z2} and λ, which are to be determined by fitting into experimental data.

4.4.8.3 Model development for ethylation reaction over SSZ-33 based catalyst.

In accordance with the products obtained in the ethylation reaction of benzene with ethanol over SSZ-33, a suitable kinetic model based on Scheme 3 was developed. Diethylbenzene was not accounted for in the model development due to the inconsistent and insignificant amount of DEB noticed in the ethylation reaction over SSZ-33, except at 250^0C, during which traces of DEB were observed.

Therefore, k_{x3}, k_{x4} and $k_{x5} \approx 0$ (due to absence of TEB), where x = s in the case of SSZ-33 based catalyst. The following set of species balances and catalytic reactions can be written:

Rate of disappearance of benzene

$$-\frac{V}{W_c}\frac{dC_B}{dt} = \eta k_{S1} C_B C_E \varphi \tag{4.46}$$

Rate of formation of ethylbenzene

$$\frac{V}{W_c}\frac{dC_{EB}}{dt} = \left(\eta k_{S1} C_B C_E - \eta k_{S2} C_{EB}\right)\varphi \tag{4.47}$$

Rate of formation of toluene

$$\frac{V}{W_c}\frac{dC_T}{dt} = \eta k_{S2} C_{EB} \varphi \tag{4.48}$$

Substituting equations 4.34 and 4.39 into equations 4.46–4.48 results in the following first order differential equations which are in terms of weight fractions of the species:

$$\frac{dy_B}{dt} = -\eta G_1 k_{S1} y_B y_E \frac{W_c}{V} \exp(-\lambda(1 - y_B)) \tag{4.49}$$

$$\frac{dy_{EB}}{dt} = \left[\eta G_2 k_{S1} y_B y_E - \eta k_{S2} y_{EB}\right]\frac{W_c}{V} \exp(-\lambda(1 - y_B)) \tag{4.50}$$

$$\frac{dy_T}{dt} = \eta G_3 k_{S2} y_{EB} \frac{W_c}{V} \exp(-\lambda(1 - y_B)) \tag{4.51}$$

G_1, G_2 and G_3 are lumped constants given below.

$$G_1 = \frac{W_{hc}}{VMW_E}$$

$$G_2 = \frac{MW_{EB} W_{hc}}{VMW_B MW_E}$$

$$G_3 = \frac{MW_T}{MW_{EB}}$$

The above proposed model equations were based on the simplified assumptions stated for both mordenite and ZSM-5 based catalysts, discussed earlier in section 4.4.8.1 Contained in equations 4.49-4.51 are five parameters to be determined by fitting into experimental data.

4.4.8.4 Model development for ethylation reaction over TNU-9 based catalyst.

Based on the product distribution presented, in which both ethylation and cracking reaction occur in the ethylation of benzene with ethanol over TNU-9 based catalyst, a kinetic model based on Scheme 3 was developed. Therefore, $k_{x5} \approx 0$ (due to absence of TEB). Where x = TNU in the case of TNU-9 based catalyst. The following set of species balances and catalytic reactions can be written:

Rate of disappearance of benzene

$$-\frac{V}{W_c}\frac{dC_B}{dt} = \eta k_{TNU-1} C_B C_E \varphi \tag{4.52}$$

Rate of formation of ethylbenzene

$$\frac{V}{W_c}\frac{dC_{EB}}{dt} = \left(\eta k_{TNU-1} C_B C_E - \left(\eta k_{TNU-2} C_{EB} + \eta k_{TNU-3} C_{EB} C_E\right)\right)\varphi \tag{4.53}$$

Rate of formation of toluene

$$\frac{V}{W_c}\frac{dC_T}{dt} = \eta k_{TNU-2} C_{EB} \varphi \tag{4.54}$$

Rate of diethylbenzene formation

$$\frac{V}{W_c}\frac{dC_{DEB}}{dt} = \left(\eta k_{TNU-3} C_{EB} C_E - \eta k_{TNU-4} C_{DEB}\right)\rho \tag{4.55}$$

Substituting equations 4.34 and 4.39 into equations 4.52-4.52 gives the following first order differential equations which are in terms of weight fractions of the species:

$$\frac{dy_B}{dt} = -\eta S_1 k_{TNU-1} y_B y_E \frac{W_c}{V}\exp(-\lambda(1-y_B)) \tag{4.56}$$

$$\frac{dy_{EB}}{dt} = \left[\eta S_2 k_{TNU-1} y_B y_E - \left(\eta k_{TNU-2} y_{EB} + \eta S_1 k_{TNU-3} y_{EB} y_E\right)\right]\frac{W_c}{V}\exp(-\lambda(1-y_B)) \tag{4.57}$$

$$\frac{dy_T}{dt} = \eta S_3 k_{TNU-2} y_{EB} \frac{W_c}{V}\exp(-\lambda(1-y_B)) \tag{4.58}$$

$$\frac{dy_{DEB}}{dt} = \left(\eta S_4 k_{TNU-3} y_{EB} y_E - \eta k_{TNU-4} y_{DEB}\right)\frac{W_c}{V}\exp(-\lambda(1-y_B)) \tag{4.59}$$

S_1, S_2, S_3 and S_4 are lumped constants given below.

$$S_1 = \frac{W_{hc}}{VMW_E}$$

$$S_2 = \frac{MW_{EB} W_{hc}}{VMW_B MW_E}$$

$$S_3 = \frac{MW_T}{MW_{EB}}$$

$$S_4 = \frac{MW_{DEB} W_{hc}}{VMW_{EB} MW_E}$$

Similar assumptions used in the kinetic model development for benzene ethylation over mordenite, SSZ-33 and ZSM-5 based catalyst, is also applicable to the model

development for ethylation of benzene with ethanol over TNU-9 based catalyst. Equations (4.56) - (4.59) contain 9 parameters; k_{TNU-1}- $k_{TNU-4,}$ E_{TNU-1}- E_{TNU-4} and λ, which are to be determined by fitting into experimental data.

4.4.8.5 Discussion of Kinetic Modeling Results.

The kinetic parameters k_{0i}, E_i, and λ for the ethylation reaction were obtained using nonlinear regression (MATLAB package). The values of the model parameters along with their corresponding 95% confidence limits (CLs) are shown in Tables 4.26, 4.30, 4.33 and 4.36 (RC model), while the resulting cross-correlation matrices are also given in Tables 4.27-4.29 for mordenite based catalyst: Tables 4.31 and 4.32 for ZSM-5 based catalyst, Tables 4.34 and 4.35 for SSZ-33 based catalyst and Tables 4.37-4.40 for TNU-9 based catalyst.

Table 4.26 Estimated kinetic parameters for mordenite catalyst based on reactant conversion (RC-model)

Parameters	k_{m1}	k_{m2}	k_{m3}	λ
E_i (kJ/ mol)	59.87	16.08	16.63	3.03
95% CL	3.61	6.54	9.61	1.12
k_{0i} X 10^3 (m3/ (kg of cat. s))	0.0065	0.0574	0.0712	
95% CL x 10^3	0.0030	0.0259	0.0345	

Table 4.27 Correlation matrix for benzene ethylation over mordenite based catalyst

	k_{m1}	E_{m1}	λ
k_{m1}	1.0000	0.5846	0.8903
E_{m1}	0.5846	1.0000	-0.5951
λ	0.8903	-0.5951	1.0000

Table 4.28 Correlation matrix for ethylbenzene ethylation over mordenite based catalyst

	k_{m2}	E_{m2}	λ
k_{m2}	1.0000	0.3145	0.7968
E_{m2}	0.3145	1.0000	-0.3560
λ	0.7968	-0.3560	1.0000

Table 4.29 Correlation matrix for diethylbenzene ethylation over mordenite based catalyst

	k_{m3}	E_{m3}	λ
k_{m3}	1.0000	-0.1222	0.6900
E_{m3}	-0.1222	1.0000	0.1822
λ	0.6900	0.1822	1.0000

Based on the correlation matrices of the regression analysis presented in Tables 4.27-4.29 for ethylation of benzene over mordenite, it shows the very low correlations between k_{m1}-k_{m3} and E_{m1}-E_{m3} and E_{m1}-E_{m3} and λ and the moderate correlation between k_{m1}-k_{m3} and λ. Similarly, Tables 4.31, 4.32, 4.34 and 4.35 report the very low correlations between k_{z1}, k_{z2}, k_{s1}, k_{s2} and E_{z1}, E_{z2}, E_{s1}, E_{s2} respectively, and E_{z1}, E_{z2}, E_{s1}, E_{s2} and λ. It can be observed that in the cross-correlation matrices presented in this study, most of the coefficients remain in the low level with only a few exceptions.

Table 4.30 Estimated kinetic parameters for ZSM-5 catalyst based on reactant conversion (RC-model)

Parameters	k_{Z1}	k_{Z2}	λ
E_i (kJ/ mol)	17.12	8.90	2.28
95% CL	2.64	5.80	0.98
k_{0i} X 10^3 (m3/ (kg of cat. s))	0.0132	0.0310	
95% CL X 10^3	0.0069	0.0164	

Table 4.31 Correlation matrix for benzene ethylation over ZSM-5 based catalyst

	k_{Z1}	E_{Z1}	λ
k_{Z1}	1.0000	0.2295	0.7937
E_{Z1}	0.2295	1.0000	0.2332
λ	0.7937	0.2332	1.0000

Table 4.32 Correlation matrix for ethylbenzene ethylation over ZSM-5 based catalyst

	k_{Z2}	E_{Z2}	λ
k_{Z2}	1.0000	-0.1668	0.8922
E_{Z2}	-0.1668	1.0000	0.4619
λ	0.8922	0.4619	1.0000

Table 4.33 Estimated kinetic parameters for SSZ-33 catalyst based on reactant conversion (RC-model)

Parameters	k_{S1}	k_{S2}	λ
E_i (kJ/ mol)	12.29	67.97	2.94
95% CL	4.72	10.57	0.75
k_{0i} X 10^3 (m3/ (kg of cat. s))	0.0569	3.0000	
95% CL X 10^3	0.0193	0.6512	

Table 4.34 Correlation matrix for benzene ethylation over SSZ-33 based catalyst

	k_{S1}	E_{S1}	λ
k_{S1}	1.0000	0.2228	0.7944
E_{S1}	0.2228	1.0000	0.2030
Λ	0.7944	0.2030	1.0000

Table 4.35 Correlation matrix for ethylbenzene cracking over SSZ-33 based catalyst

	k_{S2}	E_{S2}	λ
k_{S2}	1.0000	0.3107	0.6963
E_{S2}	0.3107	1.0000	-0.1320
λ	0.6963	-0.1320	1.0000

Table 4.36 Estimated kinetic parameters for TNU-9 catalyst based on reactant conversion (RC-model)

Parameters	k_{TNU-1}	k_{TNU-2}	k_{TNU-3}	k_{TNU-4}	λ
E_i (kJ/ mol)	10.44	15.02	24.51	12.82	2.44
95% CL	2.71	1.36	5.79	3.52	0.93
k_{0i} X 10^4 (m^3/ (kg of cat. s))	0.116	2.700	0.362	16.67	
95% CL x 10^3	0.067	0.060	0.022	8.13	

Table 4.37 Correlation matrix for benzene ethylation over TNU-9 based catalyst

	k_{TNU-1}	E_{TNU-1}	λ
k_{TNU-1}	1.0000	0.1033	0.8937
E_{TNU-1}	0.1033	1.0000	-0.1019
λ	0.8937	-0.1019	1.0000

Table 4.38 Correlation matrix for ethylbenzene cracking over TNU-9 based catalyst

	k_{TNU-2}	E_{TNU-2}	λ
k_{TNU-2}	1.0000	0.2219	0.7839
E_{TNU-2}	0.2219	1.0000	-0.1467
λ	0.7839	-0.1467	1.0000

Table 4.39 Correlation matrix for ethylbenzene ethylation over TNU-9 based catalyst

	k_{TNU-3}	E_{TNU-3}	λ
k_{TNU-3}	1.0000	-0.1153	0.7761
E_{TNU-3}	-0.1153	1.0000	0.1607
λ	0.7761	0.1607	1.0000

Table 4.40 Correlation matrix for diethylbenzene cracking over TNU-9 based catalyst

	k_{TNU-4}	E_{TNU-4}	λ
k_{TNU-4}	1.0000	0.3262	0.6074
E_{TNU-4}	0.3262	1.0000	-0.1725
λ	0.6074	-0.1725	1.0000

Comparing the energies of activation for benzene ethylation over mordenite (59.87 kJ/mol), ZSM-5 (17.12 kJ/mol), SSZ-33 (12.29 kJ/mol) and TNU-9 based catalyst (10.44 kJ/mol), it can be inferred that the high energy of activation noticed over mordenite based catalyst as compared with all other catalysts used in this study is anticipated, since in mordenite based catalyst, the cross channels are sufficiently small and with respect to hydrocarbons, the structure is effectively one-dimensional and may be regarded as an array of parallel, noninterconnecting channels [88].

Comparing this to the three-dimensional pore structure of ZSM-5 [89], containing interconnected channels of 10-ring parallel to [100] (5.1 X 5.5 Å) and to [010] (5.3 X 5.6 Å), which permits complete access from one pore to all others in the structure, thereby permitting the entering of feed molecules as well as moving out of the product molecules, a much lower apparent energy of activation is expected over ZSM-5 as compared with mordenite based catalyst.

Considering SSZ-33 based catalyst [90], which contains 12 and 10 ring interconnected channels of 6.4 X 7.0 Å, 5.9 X 7.0 Å (12-ring parallel to [001] and [100], respectively, and 4.5 X 5.1 Å (10 MR parallel to [010]), a lower apparent activation energy for benzene ethylation is expected, as compared with the medium pore (10-ring) ZSM-5 zeolite. It can be observed that over mordenite and ZSM-5 based catalysts, benzene ethylation was found to be higher than the apparent activation energy needed to form DEB, as a result of ethylbenzene ethylation. The difference in apparent activation energy for benzene ethylation (59.87 and 17.12kJ/mol) and ethylbenzene ethylation (16.08 and 8.90kJ/mol) noticed over both catalysts is not unusual, since alkylation

reactions of long substituted benzene generally occurs with greater ease compared to their shorter substituted counterparts [69].

It is evident from Table 4.24 that the increase in temperature leads to a larger fraction of cracking products, which clearly validate the higher apparent activation energy noticed for EB cracking (67.97 kJ/mol) over SSZ-33 based catalyst, as compared with the apparent energy of activation obtained for benzene ethylation (12.29 kJ/mol) over the same catalyst. Sridevi et al. [63] and Barman et al. [17] reported an apparent energy of activation of 60.03 kJ/mol and 56 kJ/mol for ethylation of benzene over $AlCl_3$ impregnated 13X zeolite and cerium exchange NaX zeolite, respectively. These values are in agreement, or have the same order with the value obtained in this present study for benzene ethylation over mordenite based catalyst.

Graphical comparisons between experimental and model predictions for the reactant conversion model (RC) based on the optimized parameters for mordenite and ZSM-5 is shown in Figs. 4.24 and 4.25, respectively. It can be seen that the model predictions compared very well with the experimental data.

CHAPTER 5

CONCLUSION AND RECOMMENDATIONS

5.1 CONCLUSIONS

A novel fluidized bed process for the production of ethylbenzene through benzene ethylation over zeolite based catalysts was successfully investigated. The study was carried out using five fluidizable catalysts based on ZSM-5, Y, SSZ-33, TNU-9 and mordenite based catalyst. Unlike previous studies which lay much emphasis on catalysis design, this work brings into consideration a new perspective which is aimed at improving the overall efficiency of the process by studying the effects of fluidization and the use of short contact times on benzene ethylation. As expected, fluidization led to a more uniform product distribution in comparison to fixed bed processes where temperature gradients in the reactor can negatively affect the product quality. It was also found that significant benzene conversion was achieved using short contact times (0-15sec.) owing to fluidization. Further more, the use of short contact times was advantageously employed to suppress undersirable side reactions which normally lead ethylbenzene cracking and high rate of catalyst decativation through coking.

P/O ratios much higher than the equilibrium value was achieved at substantial levels of benzene conversion even when the poor shape selective Y zeolite was used. The result of this study therefore shows that even a non-optimized catalyst can perform exceptional well in the alkylation of benzene with ethanol using a fluidized bed.

Over the ZSM-5 based catalyst, it was possible to achieve a benzene conversion of up to 16.95% which gave an ethylbenzene selectivity and diethylbenzene selectivity of 60.41% and 37.40% respectively at 400^0C at a reaction time of 15s for 1:1

(benzene/ethanol) molar ratio. The conversion of benzene shows a significant decline with increasing feed mole ratio of benzene to ethanol from 1:1 to 3:1.

Over the Y zeolite based catalyst, acidity plays a major role in benzene conversion. Significant benzene conversion was achieved over USY-2 catalyst as compared to the negligible benzene conversion observed over USY-1 catalyst even at high temperatures. Toluene was found in considerable amount in the ethylation of benzene with ethanol over USY-2 catalyst. It is worth mentioning that toluene was not observed over USY-1 catalyst at all conversion levels.

The zeolite structure in combination with the reaction temperature determine the types of reactions that occur. SSZ-33 based catalyst produced the highest benzene conversion as compared to its conversion over ZSM-5, TNU-9 and mordenite based catalyst. But, ethylbenzene selectivity was found to be highest in the ethylation reaction over ZSM-5 based catalyst as compared to its ethylation over all other zeolite catalysts. Considerable amount of toluene was obtained in the ethylation over SSZ-33 based catalyst, while negligible amount was noticed over mordenite based catalyst. It can be concluded that acidity plays a major role in toluene formation over these zeolites.

5.2 RECOMMENDATIONS

(1) In the light of the excellent results of this study, it is recommended that a similar study should be carried out with other important alkylation reactions.

(2) The catalysts used in this study did not undergo any of the conventional catalyst modifications aimed at enhancing para-diethylbenzene selectivity during benzene ethylation. A combination of catalyst modification and use of short contact time will hopefully improve the results of the study even better.

APPENDIX

Table A3.1: Retention time of different compounds in the GC

GC conditions

Flow rate of carrier gas (Helium) : 20ml/min

Oven Temperature: programmed from 40^0C to 250^0C in 25mins

Compounds	Retention time (min)
Gaseous hydrocarbons	3.019-3.45
Benzene	8.607
Ethanol	8.337
Ethylbenzene	13.114
1,2 Diethylbenzene	16.919
1,3 Diethylbenzene	16.452
1,4 Diethylbenzene	16.616
Para-xylene	13.304
Meta-xylene	13.459
Ortho-xylene	14.487
1,3,5 Trimethylbenzene	15.572

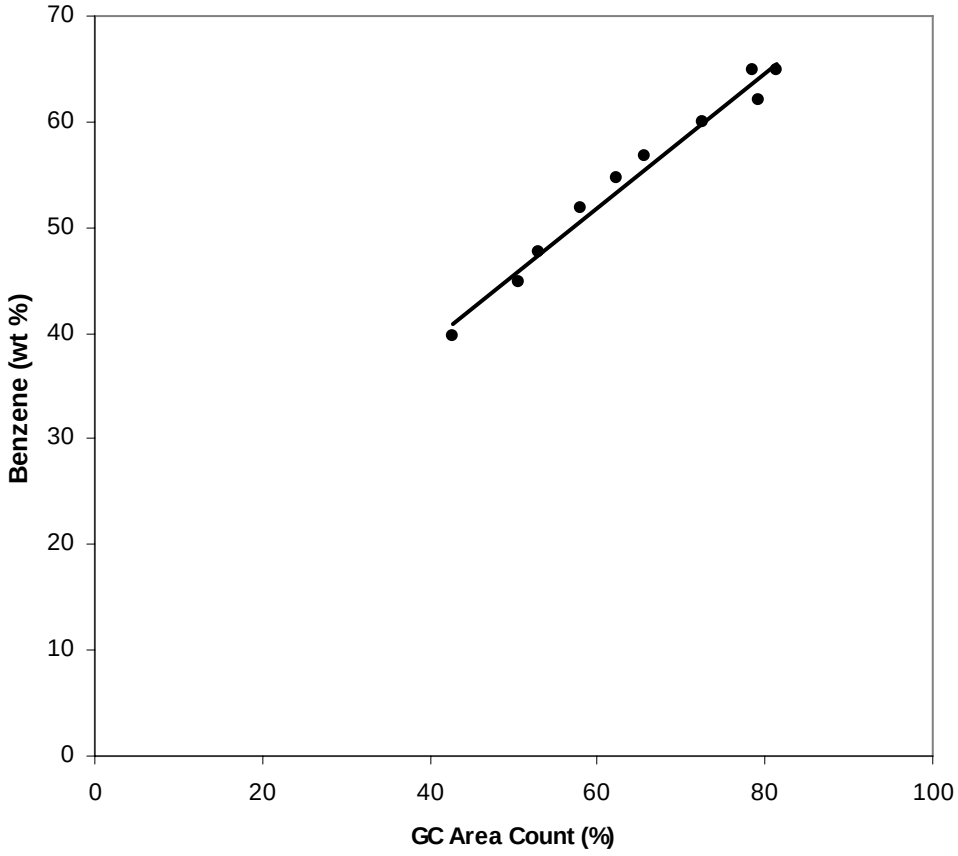

Figure A 3.1. Benzene calibration curve

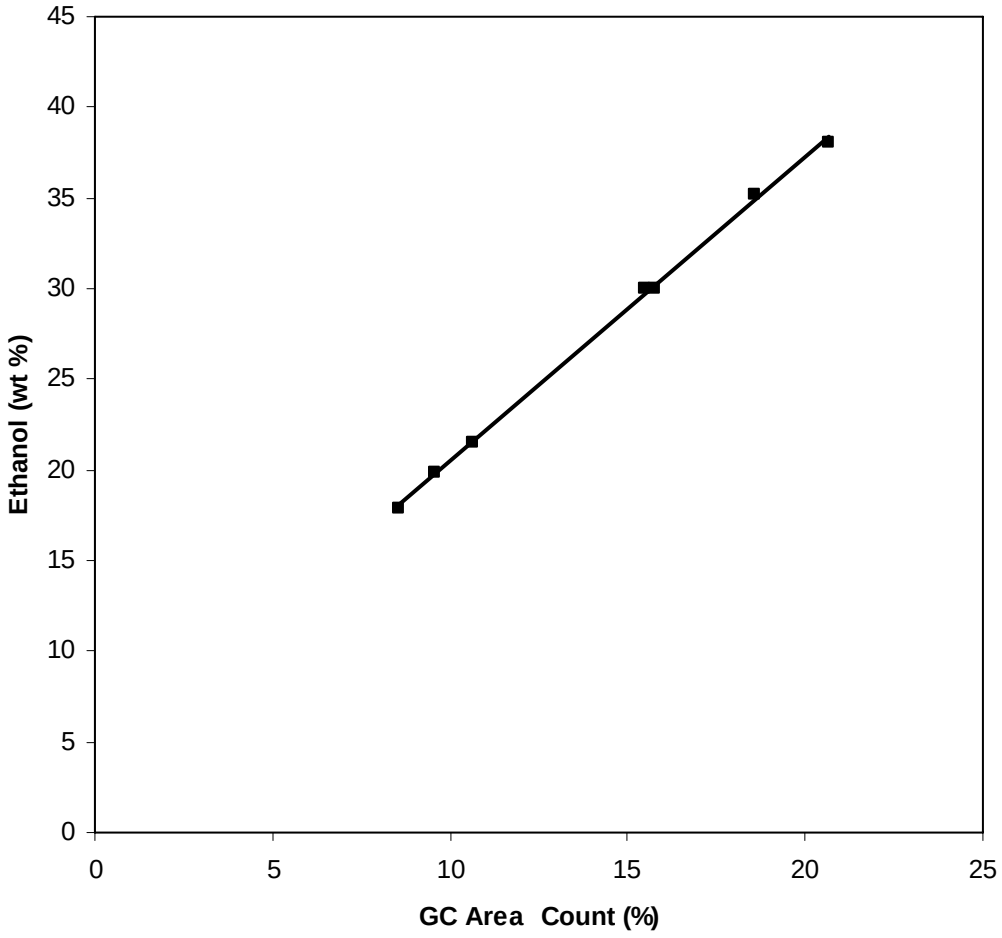

Figure A 3.2. Ethanol calibration curve

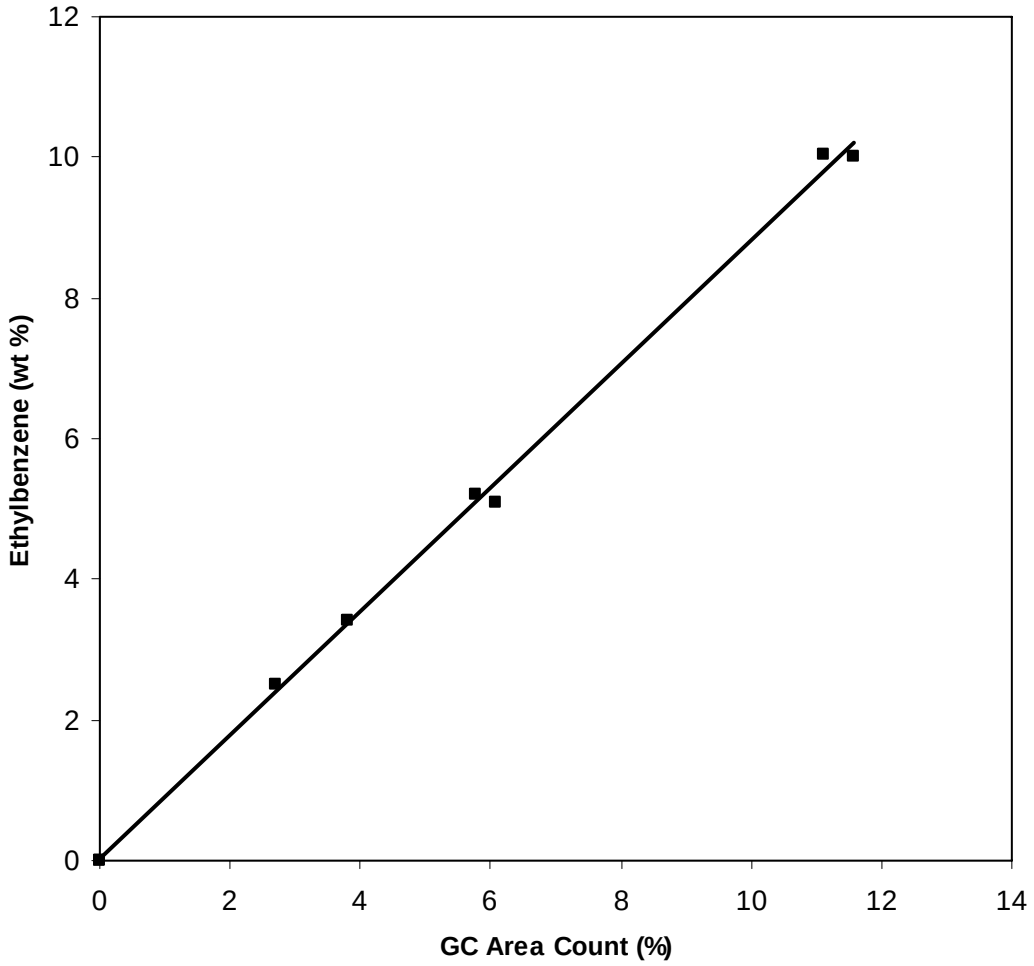

Figure A 3.3. Ethylbenzene calibration curve

NOMENCLATURE

Ci concentration of specie i in the riser simulator (mol/m^3)

CL confidence limit

E_i apparent activation energy of ith reaction (kJ/mol)

E_D activation energy for benzene diffusion (kJ/mol)

E_{in} activation energy for benzene ethylation (kJ/mol)

k_i apparent rate constant for the ith reaction (m^3/ kg_{cat}. s)

k_1 rate constant of reaction 1 (m^3/ kg_{cat}. s)

k_2 rate constant of reaction 2 (m^3/ kg_{cat}. s)

k_3 rate constant of reaction 3 (m^3/ kg_{cat}. s)

k_4 rate constant of reaction 4 (m^3/ kg_{cat}. s)

k_0 Pre-exponential factor in Arrhenius equation defined at an average temperature [m^3/ (kg_{cat}.s), units based on first order reaction

MWi molecular weight of specie i

R universal gas constant (kJ/(kmol K))

t reaction time (s)

T reaction temperature (K)

T_0 average temperature of the experiment (350^0C)

V volume of the riser (45 cm^3)

Wc mass of the catalysts (0.81 g cat)

Whc total mass of hydrocarbons injected in the riser (0.162 g)

y_i mass fraction of ith component (wt %)

Subscripts

0 at time t = 0

1 for reaction (1)

2 for reaction (2)

3 for reaction (3)

4 for reaction (4)

cat catalyst

i for ith component

Chemical species

W water

E Ethanol

B Benzene

EB Ethylbenzene

DEB Diethylbenzene

T Toluene

Greek letter

α apparent deactivation constant (s^{-1}) (TOS Model)

REFERENCES

[1] Sanghamitra Barman, Narayan C. Pradhan and Jayanta K.Basu, Kinetics of Alkylation of benzene with ethyl alcohol catalyzed by Ce-exchanged NaX zeolite. Indian Chem. Engr. Section A, Vol. 48, No. 1, January-March **2006**.

[2] L. Sun, X. Guo, M. Liu, X. Wang, ethylation of coking benzene over nanoscale HZSM-5 zeolites: Effect of hydrothermal treatment, calcinations and La_2O_2 modification. Appl. Catal. A Gen.355 (**2009**) 184-191.

[3] Weikamp, J., Puppe, L., Shape selective catalysis in zeolites. Catalysis and Zeolites- Fundamentals and Applications; Springer, Berlin, **1999**.

[4] Perego, C.; Ingallina, P., Recent advances in the industrial alkylation of aromatics: new catalysts and new processes. Catal. Today **2002**, 73, 3.

[5] U .Sridevi, B. K. Bhaskar Rao, Narayan C. Pradhan. Kinetics of alkylation of benzene with ethanol on $AlCl_3$ – impregnated 13X zeolites. Chem. Eng. J. 83, **2001**, 185-189.

[6] M. Raimondo, G. Perez, A. De Stefanis, A.A.G. Tomilinson, O. Ursini, PLS vs zeolites as sorbents and catalysts 4. Effects of acidity and porosity on alkylation of benzene by primary alcohols. Appl. Catal. A 164 (**1997**) 119.

[7] V.R. Vijayaraghavan, K.J.A. Raj, Ethylation of benzene with ethanol over substituted large pore aluminophosphate-based molecular sieves. J. Mol. Catal. A 207 (**2004**) 41.

[8] N.N. Binitha, S. Sugunan, Preparation, characterization and catalytic activity of Titania pillared montmorillonite clays Micropor. Mesopor. Mater. 93 (**2006**) 82.

[9] Chen, N. Y.; Garwood, W. E., Industrial application of shape-selective catalysis. Catal. Rev. Sci. Eng. **1986,** 28, 185.

[10] Corma, A., Inorganic solid acids and their use in acid-catalyzed hydrocarbon reactions Chem. Rev. **1995**, 95, 559.

[11] Cejka, J.; Wichterlova, B., Acid-catalyzed synthesis of mono-and dialkylbenzenes over zeolites: Active sites, zeolite Topology and reaction mechanisms. Catal. Rev. **2002,** 44, 375-421.

[12] Corma, A., Water-resistant solid Lewis acid catalysts: Meerwein-Ponndorf-Verley and Oppenauer reactions catalyzed by tin-beta zeolite. J. Catal. **2003**, 216, 298.

[13] N. Giordano, L. Pino, S. Cavallaro, P. Vitarelli, B. S. Rao, Alkylation of toluene with methanol on zeolites. The role of electronegativity on the chain or ring alkylation. Zeolites 7 (**1987**) 131.

[14] T. Yashima, K. Sato, T. Hayasaka, N. Hara, Alkylation on synthetic zeolites, III. Alkyalation of toluene with methanol and formaldehyde on alkali cation exchange zeolites, J. Catal, 26 (**1972)** 303-312.

[15] J. Engelhardt, J. Szanyi, J. Valyon, Alkylation of toluene with methanol on commercial X-zeolite in different alkali cation forms. J. Catal 107 (**1987**) 296.

[16] A. M. Brownstein, in: W.R Moser (Ed.), Catalysis of Organic Reactions, vol. 5, Marcel Dekker, **1981**, p.3.

[17] J. M. Serra, A. Corma, D. Farrusseng, L. Baumes, C. Mirodatos, C. Flego, C. Perego, Styrele from toluene by combinatorial catalysis. Catal. Today*,* 81, 3 (**2003**) 425.

[18] H. Vinek, M. Derewinski, G. Mirth, J.A. Lercher, Alkylation of toluene with methanol over alkali exchange ZSM-5. Appl. Catal. 68 (**1991**) 277.

[19] K.H. Chandawar, S. B. Kulkarni, P. Ratnaswamy, Alkylation of benzene with ethanol over ZSM-5 zeolites. Appl. Catal. A 4 **(1982**) 287.

[20] Pierre Levesque and Le H. Dao, Alkylation of benzene using an aqueous solution of ethanol. Appl. Catal, 53, 1**989,** 157-167.

[21] Junhua Gao, Lidong Zhang, Jinxian Hu, Wenhuai Li, Jianguo Wang, Effect of zinc salt on the synthesis of ZSM-5 for alkylation of benzene with ethanol. Catalysis Communications 10 (**2009**) 1615-1619.

[22] K. Joseph Antony Raj, E.J. Padma Malar, V.R. Vijayaraghavan , Shape-selective reaction with AEL and AFI type molecular sieves alkylation of benzene, toluene and ethylbenzene with ethanol, 2-propanol, methanol and t- butanol. J.Mol Catal A, Chem 243, **2006,** 99-105.

[23] T. Odedairo, S. Al-Khattaf, Chem. Eng. J. 157 **(2010)** 204-215.

[24] Anderson, J.R.; Foger, K.; Mole, T.; Rajyadhyaksha, R.A.; Sanders, J. V. Reactions on ZSM-5-type zeolite Catalysts. *J. Catal*. **1979**, 58,114-130.

[25] Anderson, J.R.; Mole, T.; Christov, V. Mechanism of Some Conversions over ZSM-5 Catalysts, *J. Catal*. **1980,** 61, 477- 484.

[26] Bhat, Y.S.; Halgeri, A.B.; Prasada Rao, T.S.R. Kinetics of Toluene Alkylation with Methanol on HZSM-8 zeolite Catalysts, *Ind. Eng. Chem. Res*. **1998**, 28, 894-899.

[27] Chandavar, K. H.; Kulkarni, S. B.; Ratnaswamy, P. Alkylation of Benzene with Ethyl Alcohol over ZSM-5 zeolites, *Appl. Catal*. **1982**, 4, 287-295.

[28] Lee, B.; Wang, I. Kinetic Analysis of Ethylation of Toluene on HZSM-5, *Ind. Eng. Chem. Prod. Res. Dev*. **1985**, 24, 201-208.

[29] Fraenkel, D.; Levy, M. Comparative study of Shape- selective Toluene Alkylation over HZSM-5, *J. Catal*. **1989**, 118, 10-21.

[30] Wang, B.; Lee, C.W.; Cai, T.; Park, S. Benzene alkylation with 1-Dodecene over Y-zeolite. *Bull. Korean Chem. Soc*. **2001**, Vol 22, No.9.

[31] Yuan, X.D.; Park, J.N.; Wang, J.; Lee, C.W.; Park, S.E. Alkylation of benzene with 1-dodecene over USY zeolite catalyst: Effect of pre-treatment and reaction conditions. *Korean J. Chem. Eng*. **2002**, 19, 607-610.

[32] Nociar, A.; Hudec, P.; Jakubik, T.; Smieskova, A.; Zidek, Z. Alkylation of benzene by linear α-olefins C_{16} over dealuminated Y-zeolites and mordenites. *Petroleum & Coal*. **2003,** Vol. 45, 3-4.

[33] Deshmukh, A.R.A.S.; Gumaste, V.K.; Bhawal, B.M. Alkylation of benzene with long chain (C8-C18) linear primary alcohols over Y-zeolite. *Catal. Letters*. **2000**, 64, 247-250.

[34] Namuangruk, S.; Pantu, P.; Limtrakul, J. Alkylation of benzene with ethylene over faujasite zeolite investigated by the ONIOM method. *J. Catal.* **2004**, 225, 523-530.

[35] T. Odedairo, S. Al-Khattaf, Ind. Eng. Chem. Res. 49 (**2010**) 1642-1651.

[36] Wanger P, Nakagawa Y ,Lee GS, Davis ME, Elomari S, Medurd RC, Zones SI (**2000**) J Am Chem Soc 122:263.

[37] A. Corma, F.J. L1opis, C. Martinez, G. Sastre, S. Valencia, J. Catal. 268 **(2009)** 9-17.

[38] J. Cejka, N. Zilkova, S.I. Zones, M. Bejblova, 18th Saudi Japan Symposium, Nov, **2008**

[39] Y.H. Ma, L.A. Savage, Xylene isomerization using zeolites in a gradientless reactor system. AICHE J. **1987**, 33, 1233.

[40] *de* Lasa, H. I. U.S.Patent 5, **1991**, 102,628.

[41] Breck, D. W. Zeolite Molecular sieves. Wiley: New York, **1974**, 771

[42] Van der Waal, J. C.; van Bekkum, H. J. Molecular sieves, and multifunctional microporous materials in organic synthesis. Jour. Porous Mater. **1998**, 5, 289-303.

[43] Weitkamp, J. Zeolites and Catalysis. Solid State Ion. **2000**, 131,175

[44] Wanger P, Nakagawa Y ,Lee GS, Davis ME, Elomari S, Medurd RC, Zones SI (**2000**) J Am Chem Soc 122:263.

[45] Lawton, S. L.; Leonowicz, M. E.; Patridge, R. D.; Chu, P.; Rubin, M.K. Twelve ring pockets on the external surface of MCM-22 crystals. Micropor. Mesopor. Mater. **1998**, 23, 109-117

[46] Gramm, F, Baerlocher Ch, McCusker, LB, Warrender SS, Wright PA, Han, B, Hong SB, Liu Z, Ohsuna T, Terasaki, O, **2006**. Nature 444, 79

[47] Weisz, P. B.; Frilette, V. J. Intracrystalline and molecular-shape-selective catalysis by zeolite salts. J. Phys. Chem. **1960**, 64, 342

[48] Wichterlova, B.; Cejka, J. Mechanism of n-propyl toluene formation in C3 alkylation of toluene: the effect of zeolite structural type. J. Catal. **1994**, 146, 523-529

[49] Wichterlova, B.; Cejka, J,; Zilkova, N. Selective synthesis of cumene and p-cymene over Al and Fe silicates with large and medium pore structures. Micropor. Mater. **1996**, 6, 405-414

[50] Niwa, M.; Kato, S.; Hattori, T.; Murakami, Y.J. Fine control of the pore-opening size of the zeolite mordenite by chemical vapor deposition of silicon alkoxide. Chem. Soc., Faraday Trans. 1 **1984**, 80, 3135.

[51] J. R. Anderson, T. Mole, V. Christov, J. Catal. 61, **1980,** 477

[52] Y. Du, H. Wang, S. Chen, J. Mol. Catal. A 179, **2002**, 253

[53] T.F. Degnan Jr., C. M. Smith, C.R. Venkat, Appl. Catal. A 221, **2001**, 283

[54] T. Tsai, S. Liu, I. Wang Disproportionation and Transalkylation of alkylbenzenes over zeolite catalysts. Appl. Catal. A: Gen. 181 **(1999)** 355-398.

[55] D.H. Olson, W.O. Haag, Catalytic materials, in: T.E. Whyte et al. (Eds.), ACS Symposium Series 248, Am. Chem. Soc., Washington, DC, **1984**, p. 275

[56] M. Guisnet, P. Magnoux, Coking & Deactivation of zeolites. Influence of pores structure. Appl. Catal. A: Gen. 54, **(1989)** 1.

[57] M. Guisnet, P. Magnoux, Organic Chemistry of coke formation. Appl. Catal. A: Gen. 212, **(2001)** 83-96.

[58] A. Marcilla, A. Gomez-Siurana, F.J. Valdes, Influence of temperature on the composition of the coke obtained in the catalytic cracking of low density polyethylene in the presence of USY and HZSM-5 zeolites. Microporous & Mesoporous Mat. 109 **(2008)** 420-428.

[59] B. Rajesh, M. Palanichamy, V. Kazansky, V. Murugesan, Ethylbenzene with ethanol over substituted medium pore aluminophosphate-based molecular sieves. J. Mol. Catal. A **2002**, 187, 259.

[60] E. Klemm, J. Wang, G. Emig, A study of shape selectivity in ethylation/disproportionation of ethylbenzene on ZSM-5 zeolites using a continuum and a Monte Carlo method. Chem. Eng. Sci. **1997**, Vol. 52, 18, 3173-3182.

[61] A. B. Halgeri, Shape Selective Alkylation over Pore Engineered Zeolite Catalysts-IPCL Approach from Concept to Commercialization. Bull Catal. Soc. India. **2003**, 2, 184.

[62] M. Guisnet and P. Magnoux. In: E.G. Deraoune, F. Lemas, C. Naccache and F. Ramoa Ribeiro Editors, Zeolite Microporous Solids: Synthesis, Structure and Reactivity NATO ASI Ser., Ser. C 352 Kluwer Academic Publishing **(1992),** p. 457.

[63] Voorhies, A.,. Carbon formation in catalytic cracking. Industrial Engineering and Chemical Research 37, **1945,** 318-322.

[64] S.M. Waziri, S. Al-Khattaf, Kinetics of ethylbenzene ethylation with ethanol over ZSM-5 based catalyst in a riser simulator. Industrial and Engineering Chemistry and Research, **2009,** 48, 8341-8348.

[65] A.K. Agarwal, M.L. Brisk, Sequential experimental design for precise parameter estimation. 1. Use of reparameterization. Ind. Eng. Chem. Process Des. Dev. 24 **(1985)** 203.

[66] J. Wei, A mathematical theory of enhanced para-xylene selectivity in molecular-sieve catalysts. J. Catal. **1982**, 76, 433-439.

[67] S. Al-Khattaf, H.I. de Lasa, Catalytic cracking of cumene in a riser simulator: A catalyst activity decay model. Ind. Eng. Chem. Res. **2001**, 40, 5398-5404.

[68] J.A. Atias, G. Tonetto, H. de Lasa, Catalytic conversion of 1,2,4-Yrimethylbenzene in a CREC riser simulator. A heterogeneous model with adsorption and reaction phenomena. Ind. Eng. Chem. Res. **2003**, 42, 4162-4173.

[69] Kaeding, W. W. Shape- Selective Reactions with zeolite Catalysts: V. Alkylation or Disproportionation of ethylbenzene to produce p-Diethylbenzene. J. Catal. **1995**, 95,512.

[70] Al-Khattaf, S.; Tukur, N. M; Al-Amer, A.; Al-Mubaiyedh, U.A. Catalytic Transformation of C_7- C_9 Methyl Benzenes over USY-Based FCC Zeolite Catalyst. Appl. Catal. A. **2006,** 305, 21.

[71] Li, Y.; Xue, B.; Yang, Y. Synthesis of ethylbenzene by alkylation of benzene with diethyl oxalate over HZSM-5. *Fuel Proc. Tech*. **2009** in press.

[72] Li, Y.; Xue, B.; He, X. Catalytic synthesis of ethylbenzene by alkylation of benzene with diethyl carbonate over HZSM-5. *Catal. Comm.* 10 **2009**, 702-707

[73] Lin, C.C.; Park, S.W.; Hatcher, W.J. *Ind. Eng. Chem. Process. Des. Dev*. **1983**, 22.

[74] Siffert, S.; Gaillard, L.; Su, B.L. Alkylation of benzene by propene on a series of beta zeolites: toward a better understanding of the mechanisms. *J. Mol. Catal***. 2000**, 10, 267-279.

[75] Corma, A. Inorganic solid acids and their use in acid-catalyzed hydrocarbon reactions *Chem. Rev*. **1995**, 95, 559.

[76] Chen, N. Y.; Garwood, W. E. Industrial application of shape-selective catalysis. *Catal. Rev. Sci. Eng*. **1986**, 28, 185-264.

[77] Bolton, A. P. Hydrocracking, isomerization and other industrial processes, in Rabo, J. A, Ed., *Zeolite Chemistry and Catalysis*. ACS Monograph **1976**, vol. 171, 714.

[78] Levenspiel, O. "Chemical Reaction Engineering" Third Edition, *John Wiley & Sons.* **1999**.

[79] Atias, J.A.; Tonetto, G.; de Lasa, H. Catalytic conversion of 1,2,4-Trimethylbenzene in a CREC Riser Simulator. A heterogeneous model with adsorption and reaction phenomena. *Ind. Eng. Chem. Res*. **2003**, 42, 42, 4162-4173.

[80] C.A. Emeis, J. Catal. 141 **(1993)** 347-354.

[81] B. Gil, S.I. Zones, S.J. Hwang, M. Bejblova, J. Cejka, J. of Physical Chemistry Vol. 112 Issue 8 **(2008)** 2997-3007.

[82] S.H. Lee, D.K. Lee, C.H. Shin, Y.K. Park, P.A. Wright, W.M. Lee, S.B. Hong, J. Catal. 215 (2003) 151

[83] S. B. Hong, Catal. Surv. Asia 12 **(2008)** 131.

[84] T. Tsai, S. Liu, I. Wang, Appl. Catal. A 181 **(1999)** 355.

[85] N. Zilkova, M. Bejblova, B. Gil, S. I. Zones, A.W. Burton, C.Y. Chen, Z. Musilova-Pavlackova, G. Kosova, J. Cejka, J. Catal. 266 (**2009)** 79-91

[86] S. Al-Khattaf, Z. Musilova-Pavlackova, M.A. Ali, J. Cejka, Top. Catal. 52 **(2009)** 140

[87] G.F. Froment, K.B. Bischoff, Chemical Reactor Analysis and Design, 2nd ed., John Wiley & Sons: New York **1979**; p288.

[88] C. N. Satterfield, Hetero. Catal. In Industrial Practice, 2nd ed., **1991**.

[89] H.V. Koningsveld, H.V. Bekkum, J.C. Jansen, Acta Crystallogr. B 43 **(1987)** 127.

[90] F.J. L1opis, G. Sastre, A. Corma, J. Catal. 227 **(2004)** 227-241.

VITAE

NAME:	**Taiwo Ayodeji Odedairo**
NATIONALITY:	**Nigerian**
DATE OF BIRTH:	**November 16, 1980**
PLACE OF BIRTH:	**Ibadan, Nigeria**
EDUCATION:	**B.Sc. Chemical Engineering** **Obafemi Awolowo University, Ile Ife,** **2006** **M.S. Chemical Engineering** **King Fahd University of Petroleum & Minerals,** **Dhahran, Saudi Arabia, April, 2010**
EMAIL ADDRESS:	**tarish221@yahoo.com**
PRESENT ADDRESS:	**Building 903, room 111** **KFUPM, Dhahran Saudi Arabia**
PERMANENT ADDRESS:	**Plot 1 & 2 Ogundiran Layout** **N.N.P.C. pipe line Apata Ibadan** **Oyo State, Nigeria.**